Göttingen, HASCO2014

July 21st, 2014

QCD and jets: experiment

Juan Terrón (Universidad Autónoma de Madrid, Spain)

- **Outline**
  - → Jets and Jet Algorithms
  - → Jets in e^+e^- collisions
  - → Structure Functions
  - → Jets in Neutral Current DIS
  - → Jets in Photoproduction

Jets

What is a jet?

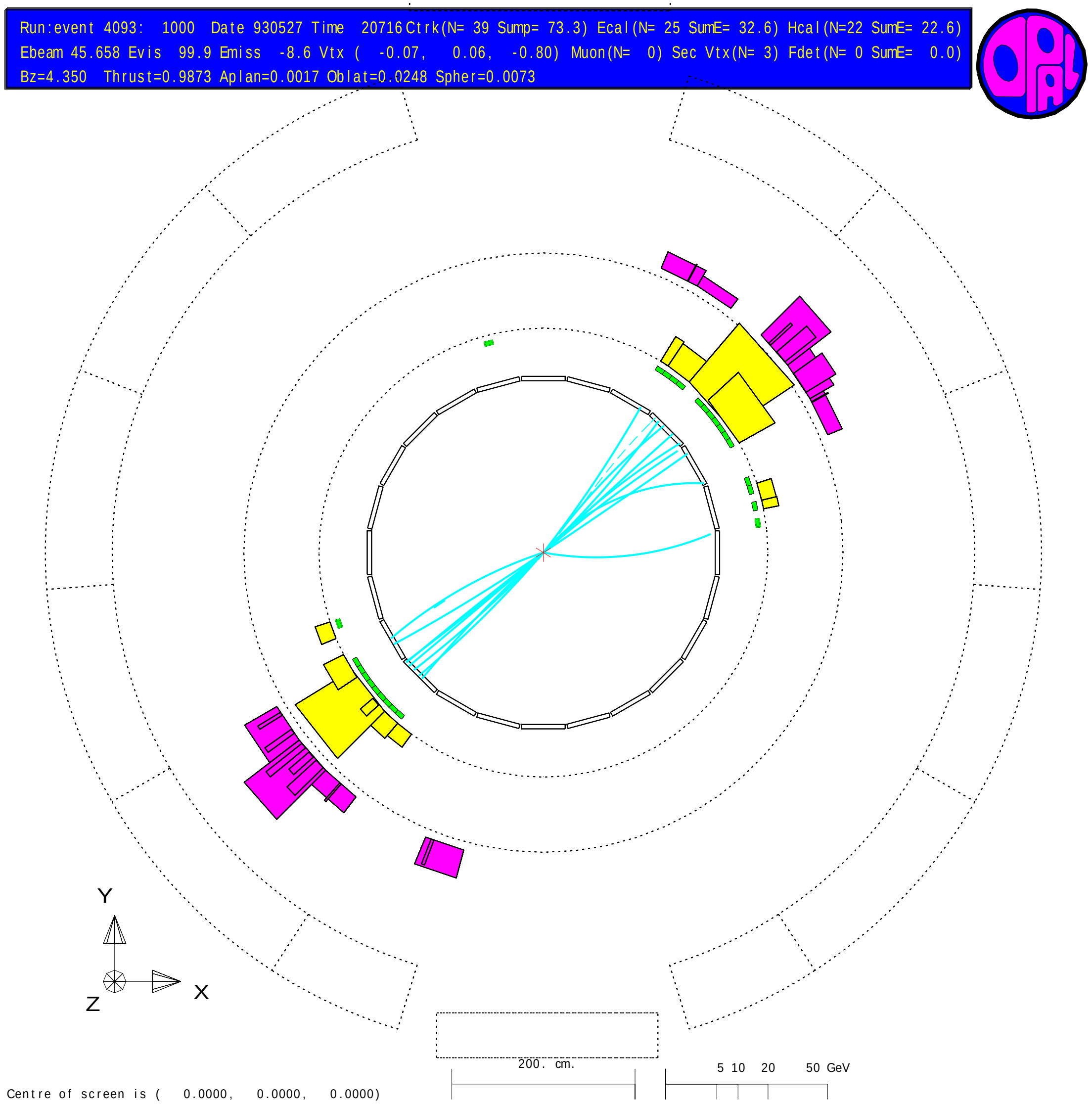

$e^+e^- \rightarrow \text{jet} + \text{jet}$ (e^+e^- **annihilation**)

What is a jet (II)?

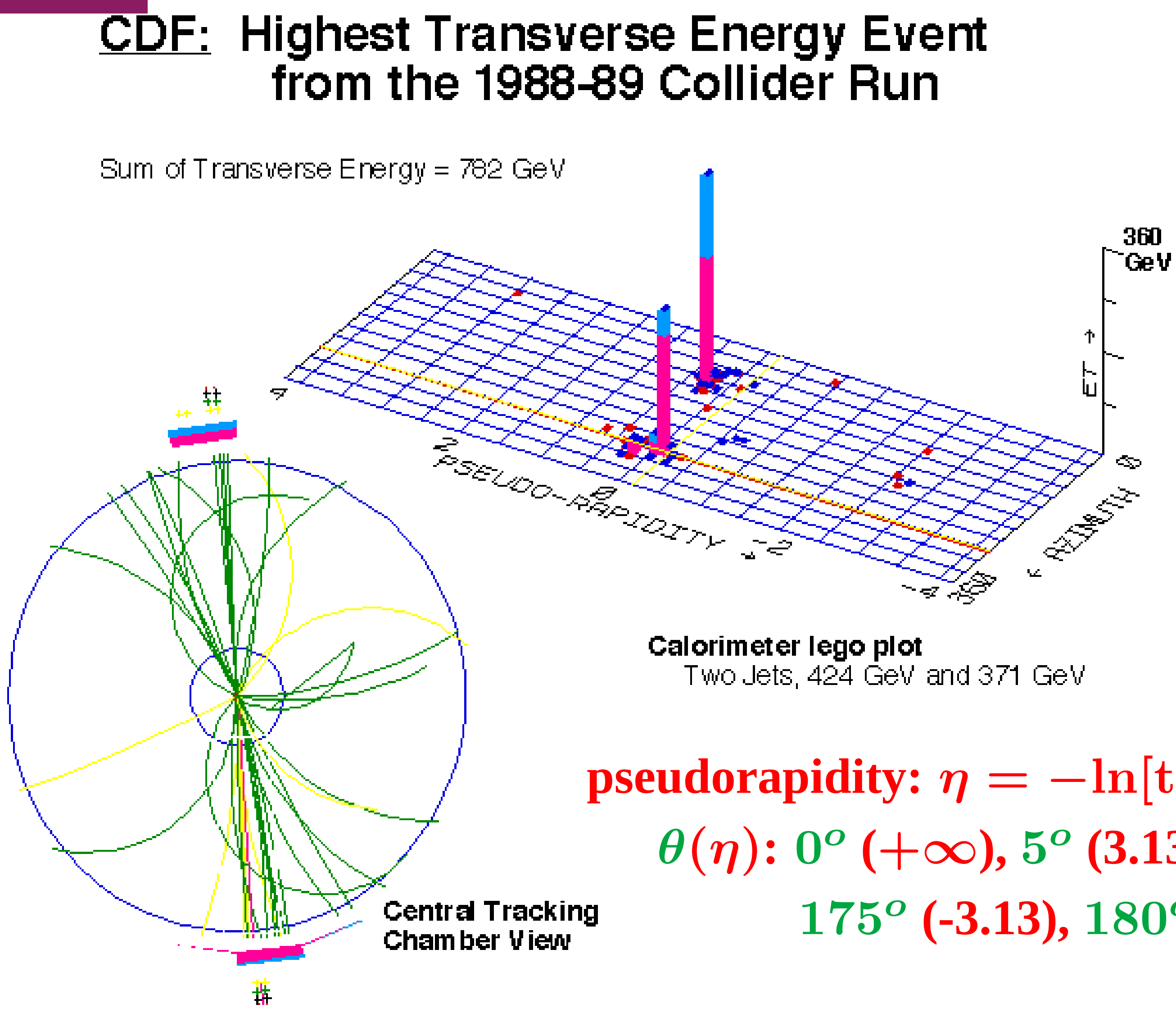

pseudorapidity: $\eta = -\ln[\tan(\theta/2)]$

$\theta(\eta)$: 0^o **(**$+\infty$**)**, 5^o **(3.13)**, 90^o **(0)**

175^o **(-3.13)**, 180^o **(**$-\infty$**)**

$p\bar{p} \rightarrow \text{jet} + \text{jet} + \text{Anything}$ **(**$p\bar{p}$ **collision)**

What is a jet (III)?

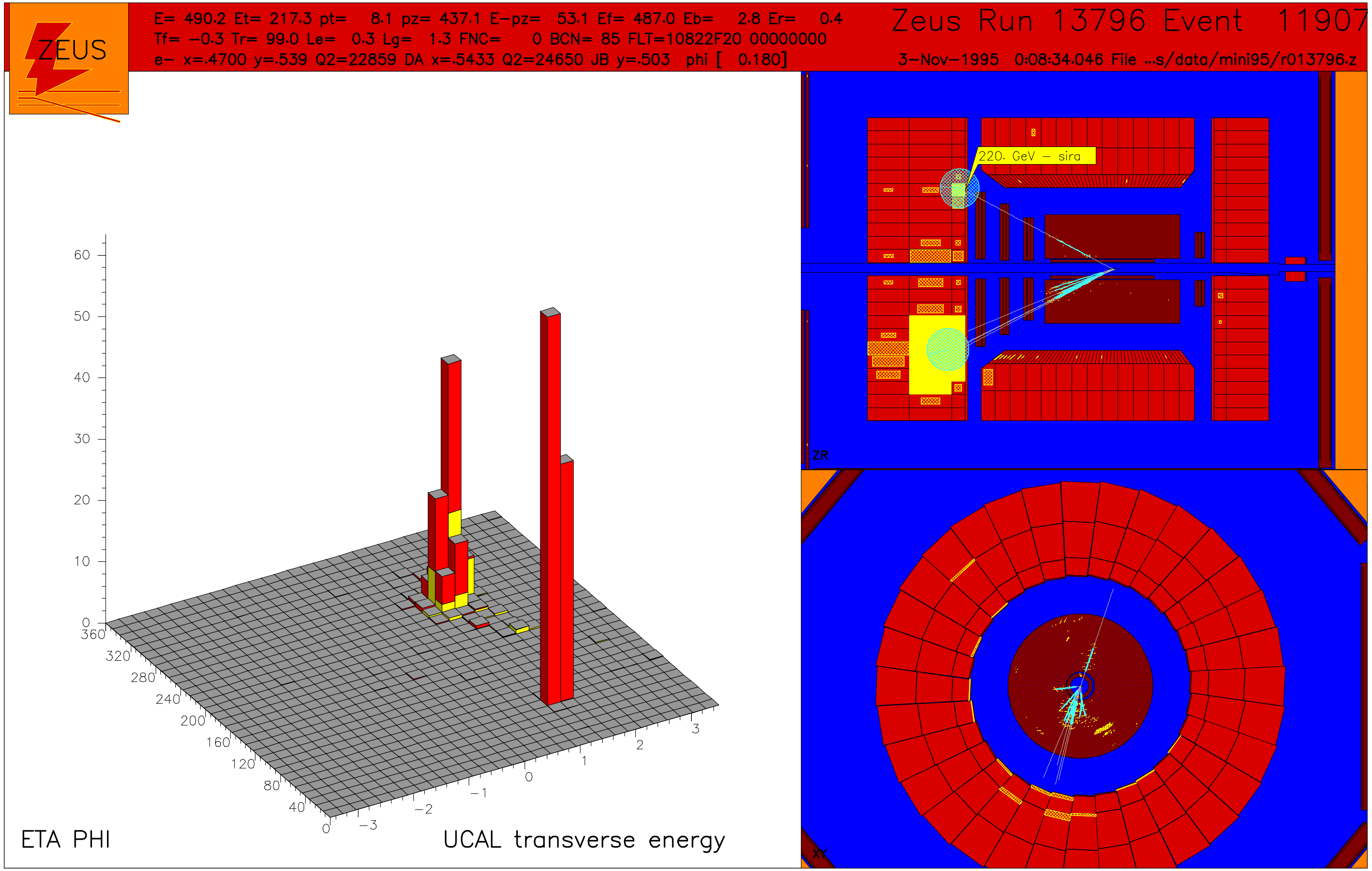

$ep \rightarrow e\ + \text{jet}\ + \text{Anything}$ **(NC DIS)**

What is a jet (IV)?

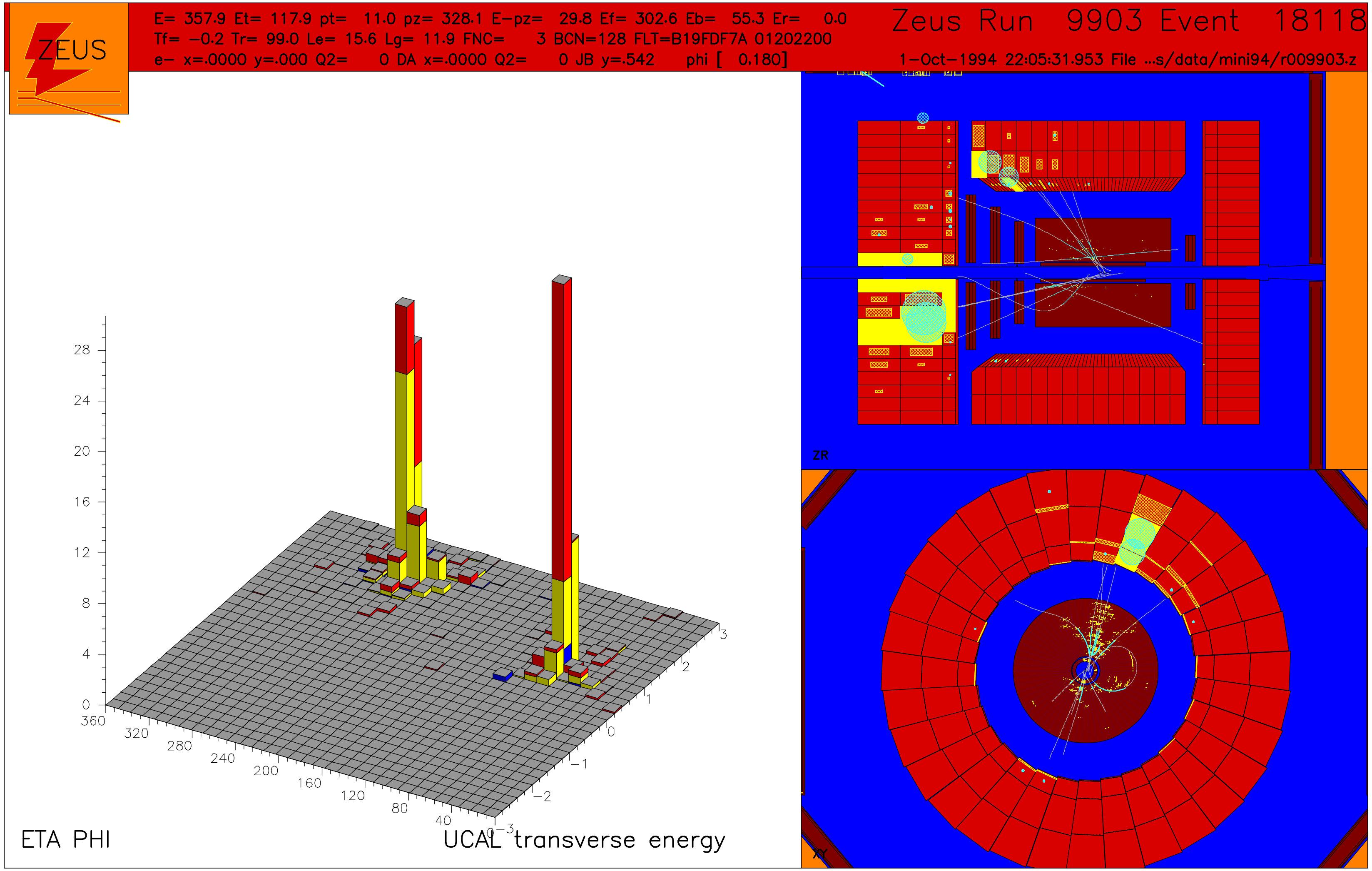

$ep \to \text{jet} + \text{jet} + \text{Anything}$ **(photoproduction)**

What is a jet (V)?

$$pp \to \text{jet} + \text{jet} + \text{Anything}$$

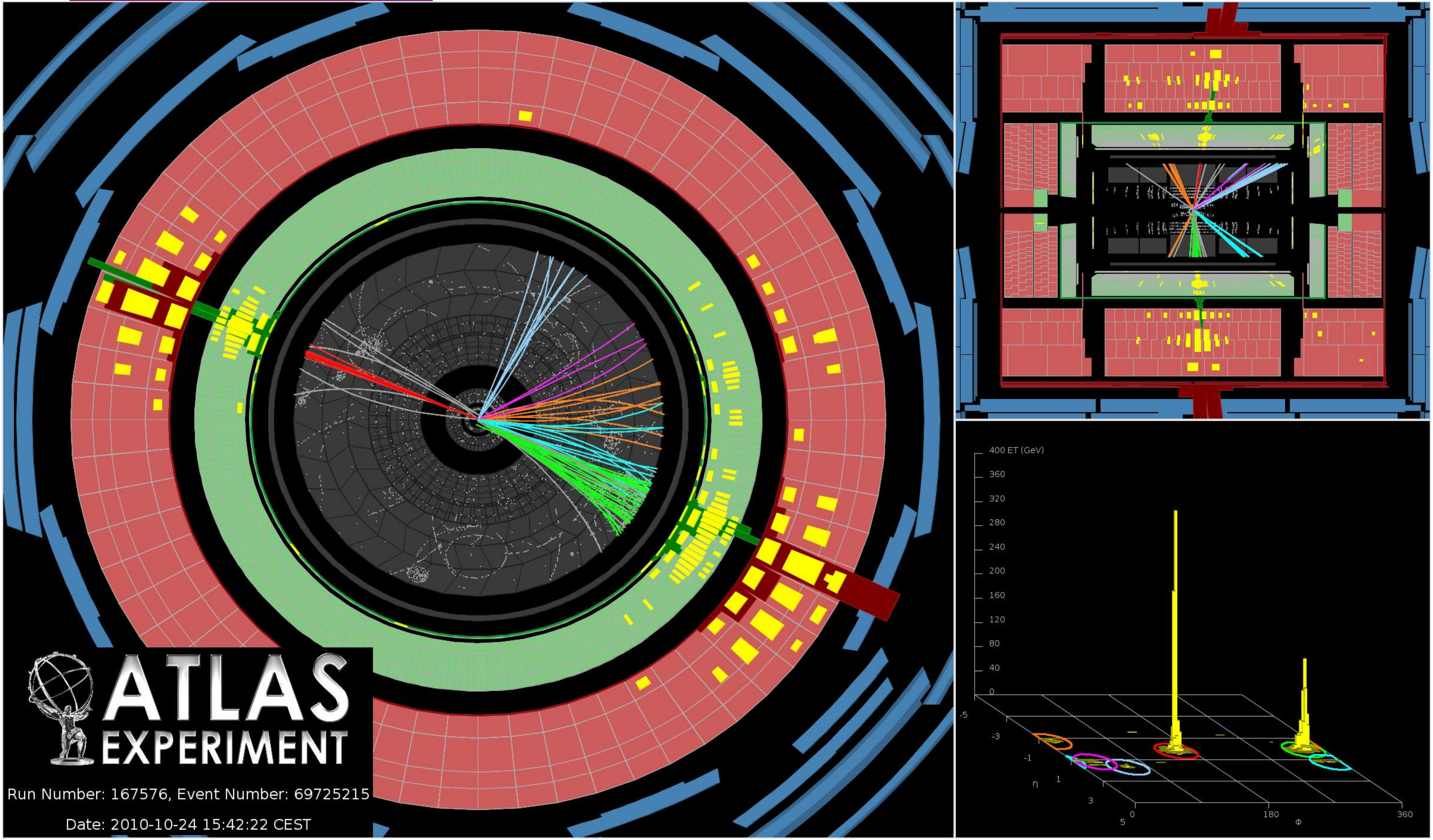

What is a jet (VI)?

$$pp \to \text{jet} + \text{jet} + \text{Anything}$$

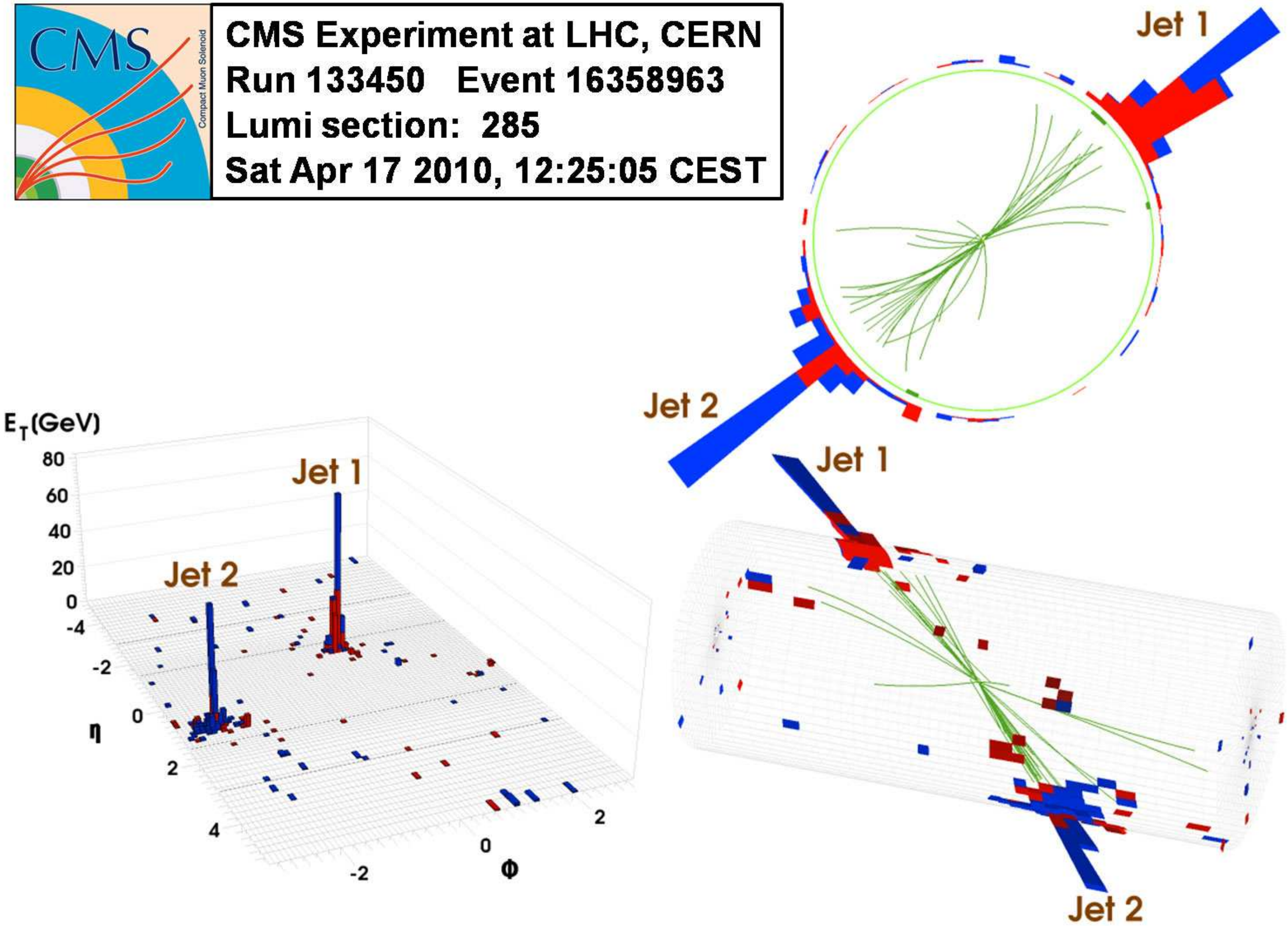

Some good reasons to study jets

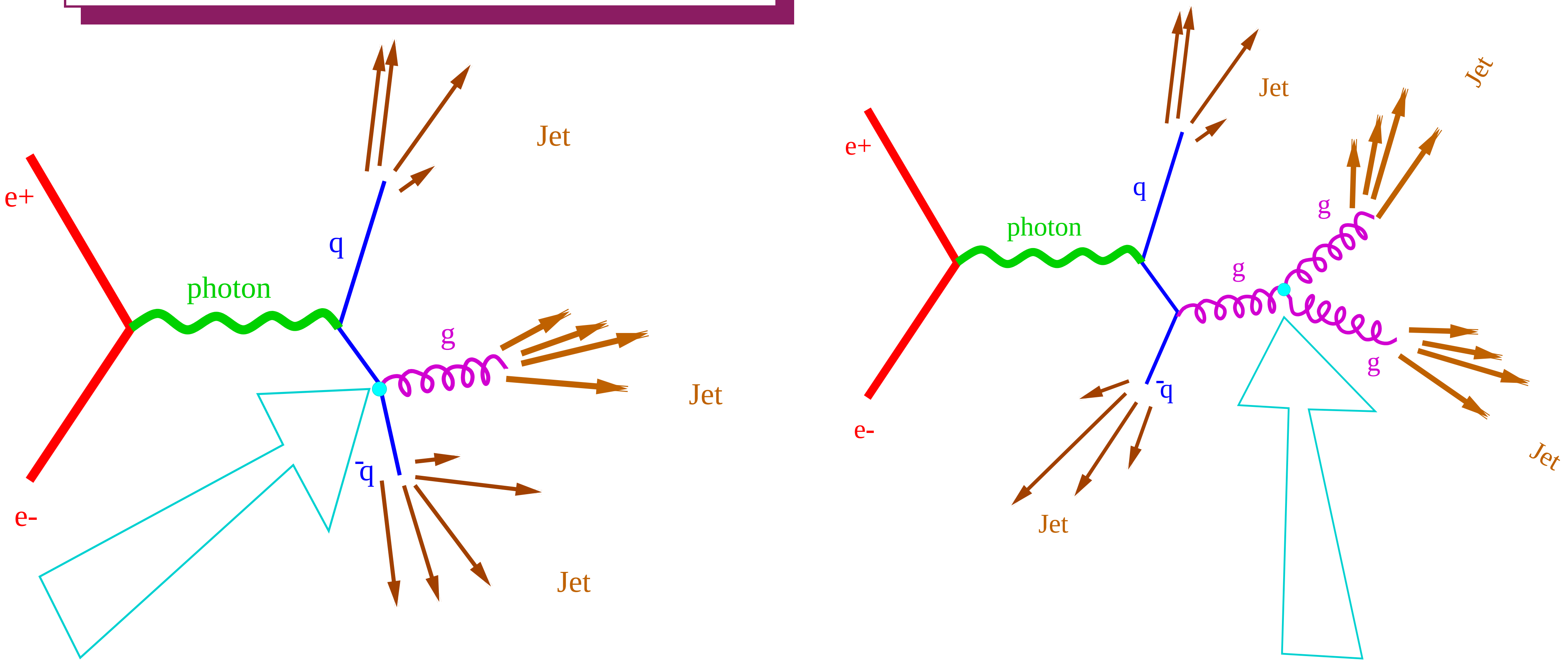

- **Studies of the strong interactions:**

$\longrightarrow$ **measurements of the strong coupling constant (α_S)**

$\longrightarrow$ **colour dynamics (e.g. the self-coupling of the gluon)**

Some good reasons to study jets (II)

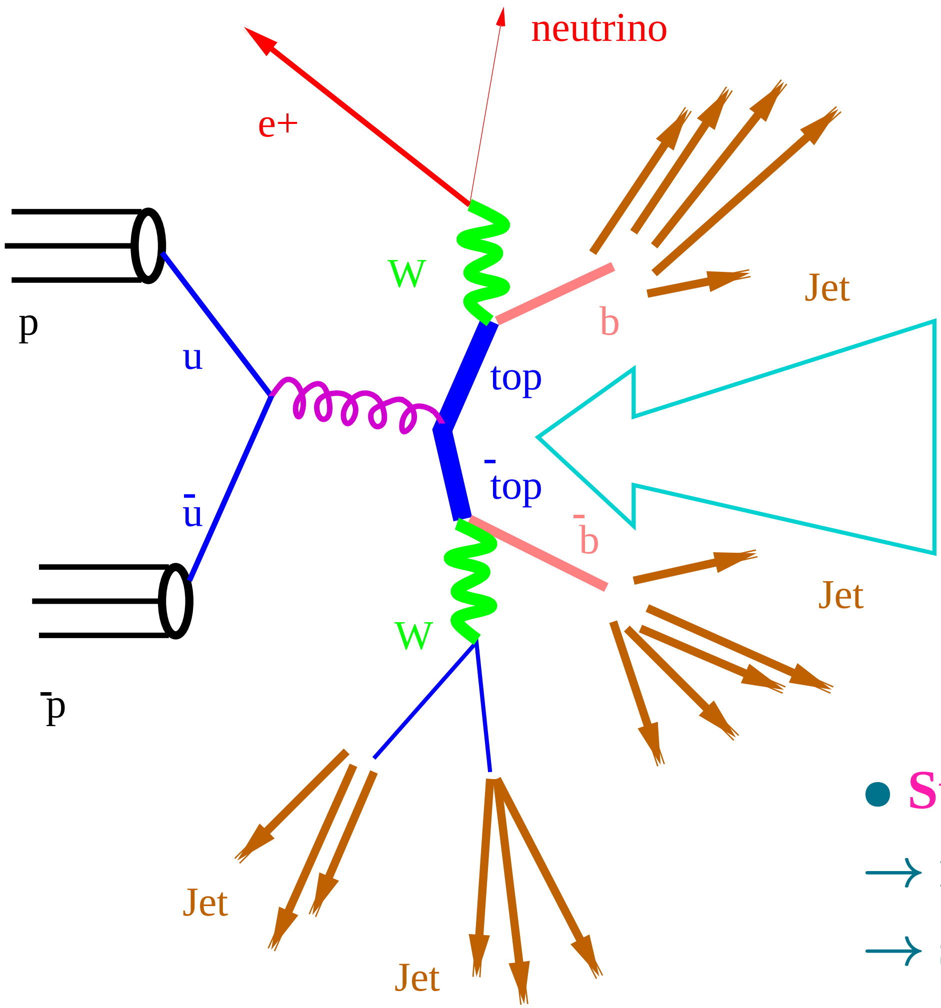

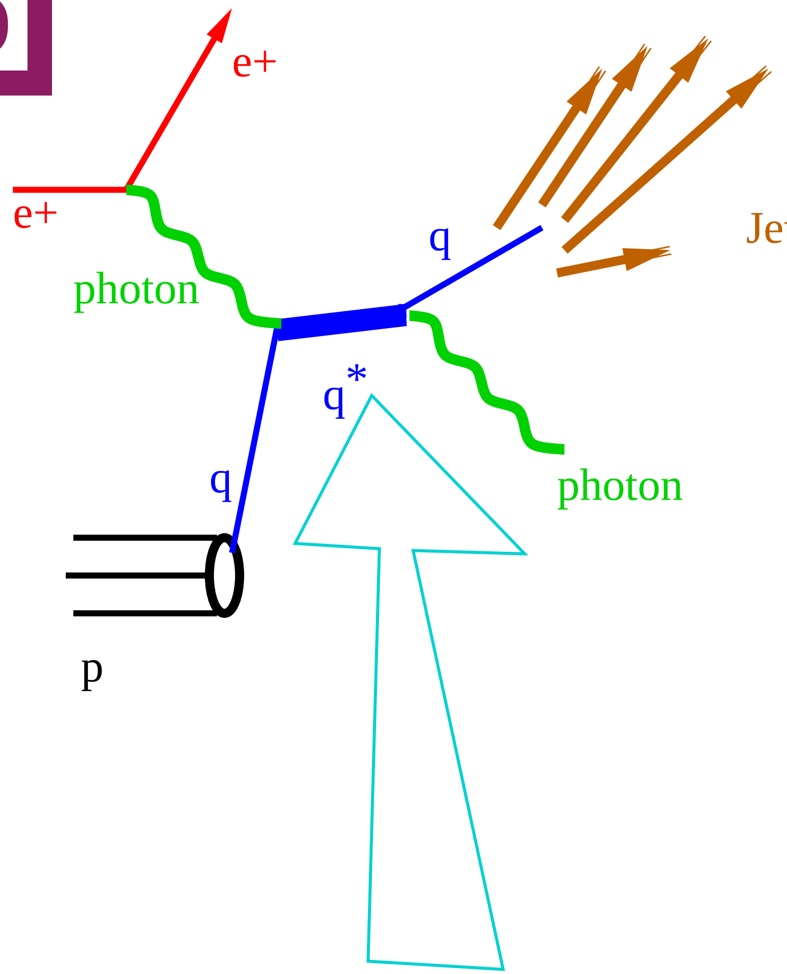

- **Study of and search for new heavy particles:**

→ measurements of top quark production

→ search for excited quarks

Some good reasons to study jets (III)

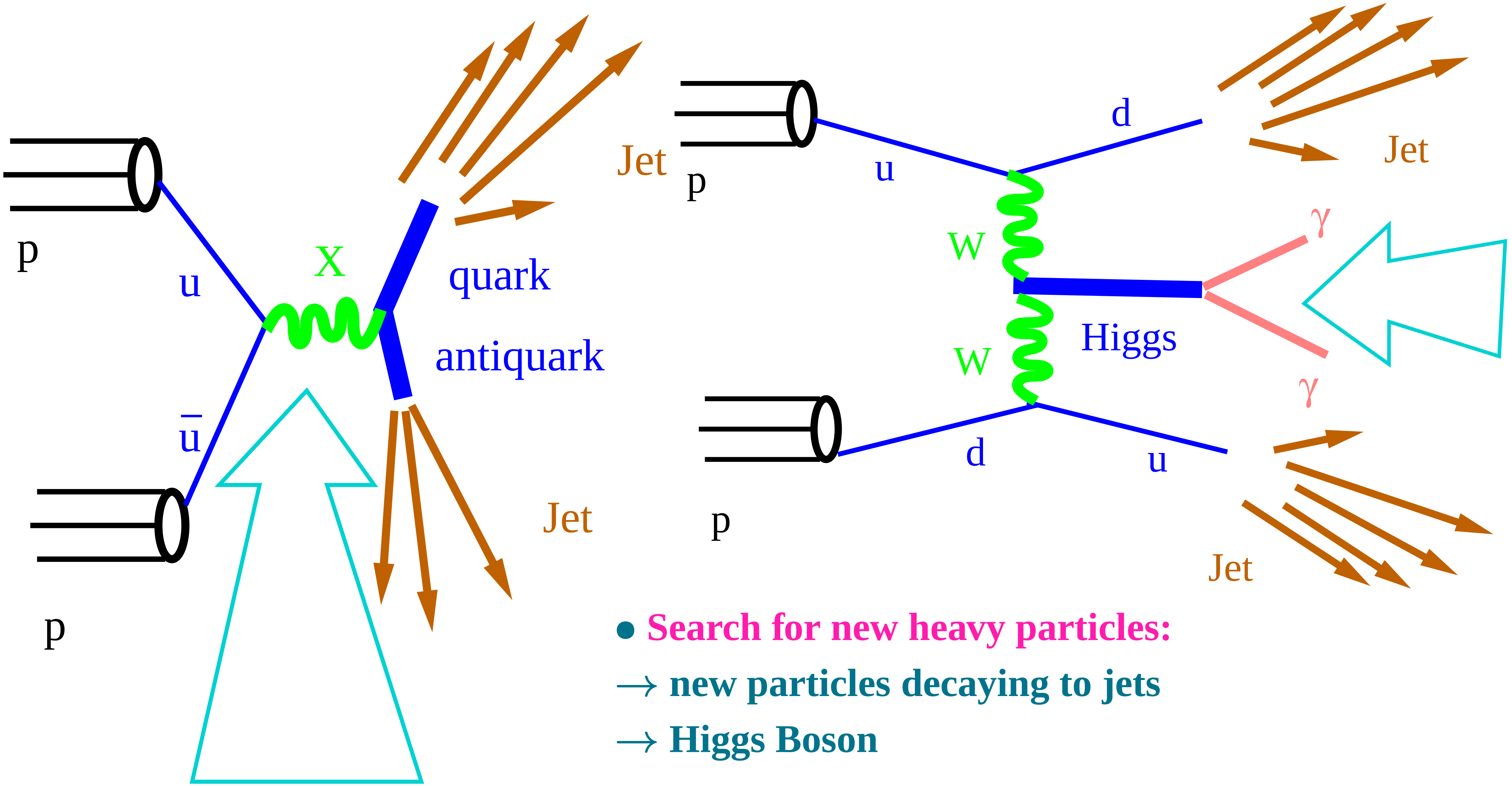

- **Search for new heavy particles:**

$\longrightarrow$ **new particles decaying to jets**

$\longrightarrow$ **Higgs Boson**

Jet Algorithms

How to find jets?

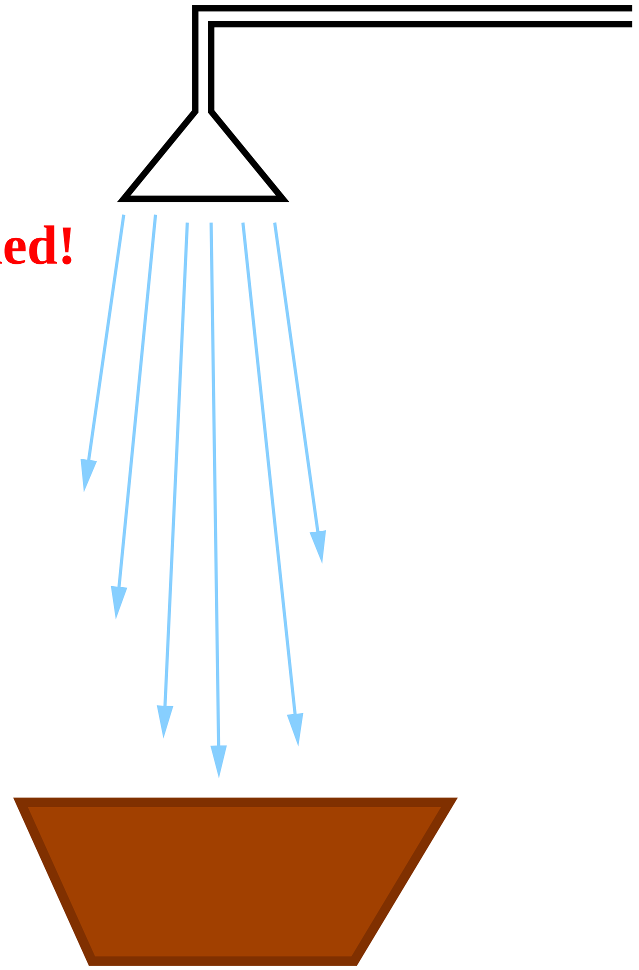

- **To reconstruct the final-state quarks and gluons**

  $\rightarrow$ **Something more sophisticated than a bucket is needed!**

  $\Rightarrow$ $\boxed{\textbf{JET ALGORITHM}}$

  $\rightarrow$ **MEASURABLE!**

  $\rightarrow$ **CALCULABLE!**

  $\rightarrow$ **ACCURATE!**

- **Jet algorithm:**

  $\rightarrow$ **Reference frame**

  $\rightarrow$ **Variables of the hadron**

  $\rightarrow$ **Combining hadrons**

Variables for Jet Search in e^+e^- annihilations

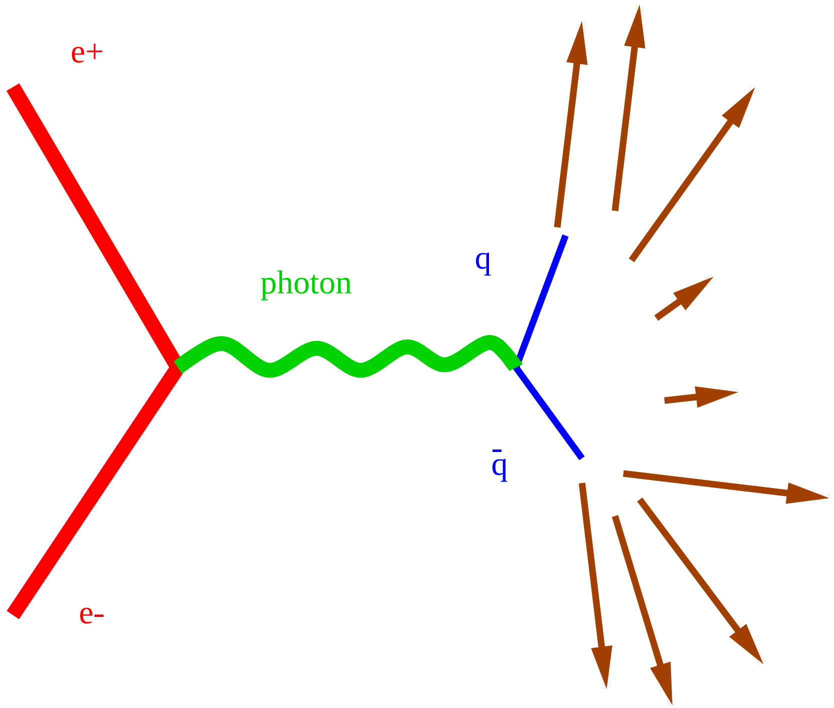

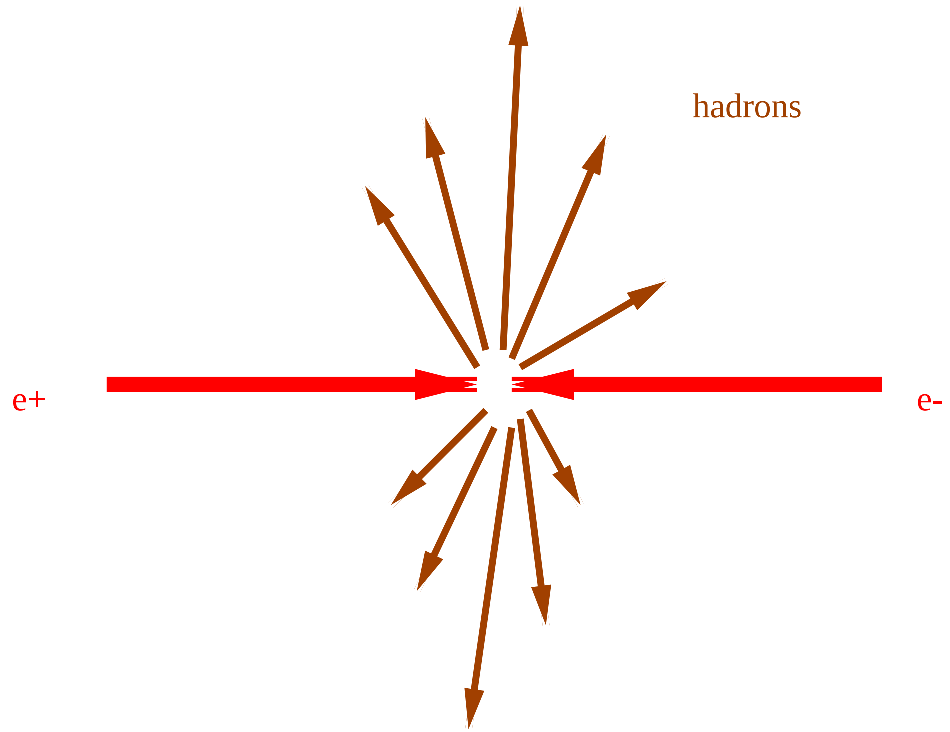

- e^+e^- **annihilations in the centre-of-mass system**
- **Invariance under rotations** $\Rightarrow$ **Energies and angles**

$\Rightarrow$ Input to the jet algorithm: $\boldsymbol{E_i}$, $\boldsymbol{\theta_i}$ and $\boldsymbol{\phi_i}$ for every hadron $\boldsymbol{i}$

$\Rightarrow$ "distance" between hadrons $\boldsymbol{i}$ and $\boldsymbol{j}$: their angular separation $\boldsymbol{\theta_{ij}}$

Combining the hadrons to build up jets: cluster algorithms

- Hadrons are combined iteratively according to their "distance"
- Usually a binary decision
- Two-step procedure:
  - $\longrightarrow$ decision about combining hadrons i and j based on d_{ij}
  - $\longrightarrow$ momentum of the combined pseudo-particle (ij) (recombination procedure)

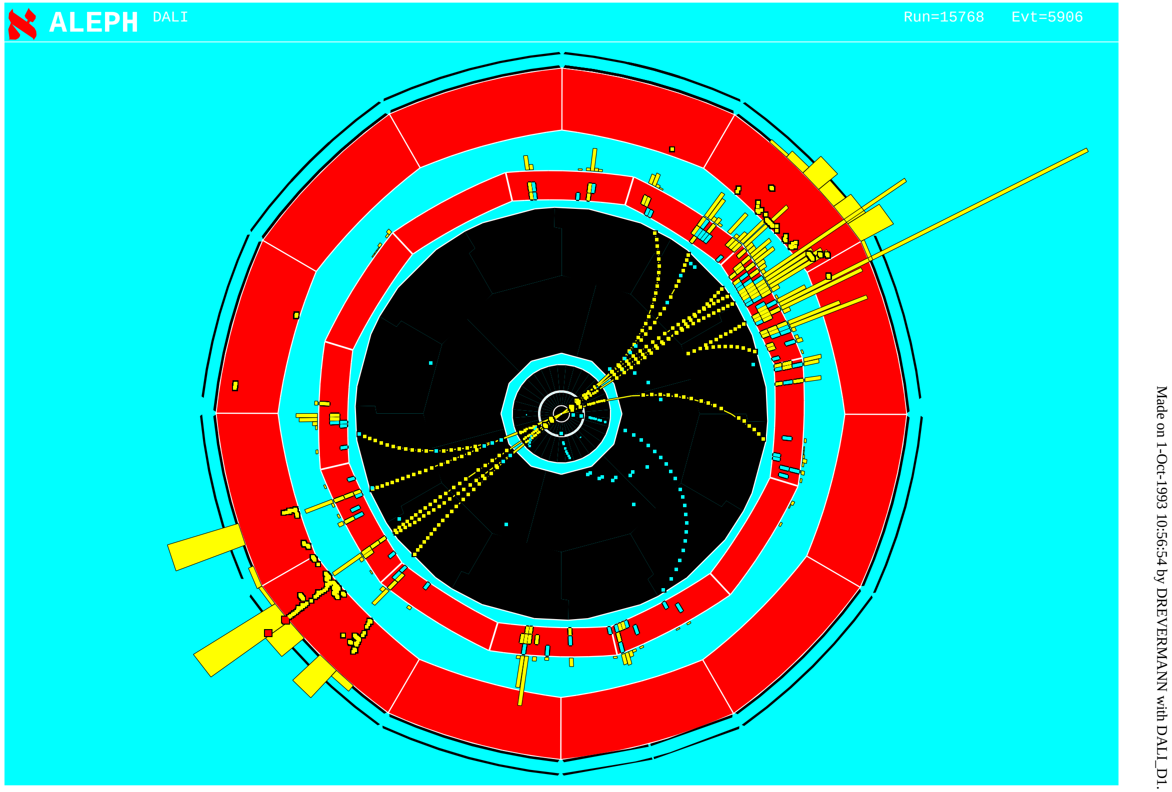

- They have a long and successful history in e^+e^- annihilations
- The JADE algorithm has been the standard
  - $\longrightarrow$ distance definition: $d_{ij}^2 = 2E_iE_j(1-\cos\theta_{ij})$
  - $\longrightarrow$ recombination procedure: $p_{(ij)} \equiv p_i + p_j$

Combining the hadrons to build up jets: cone algorithms

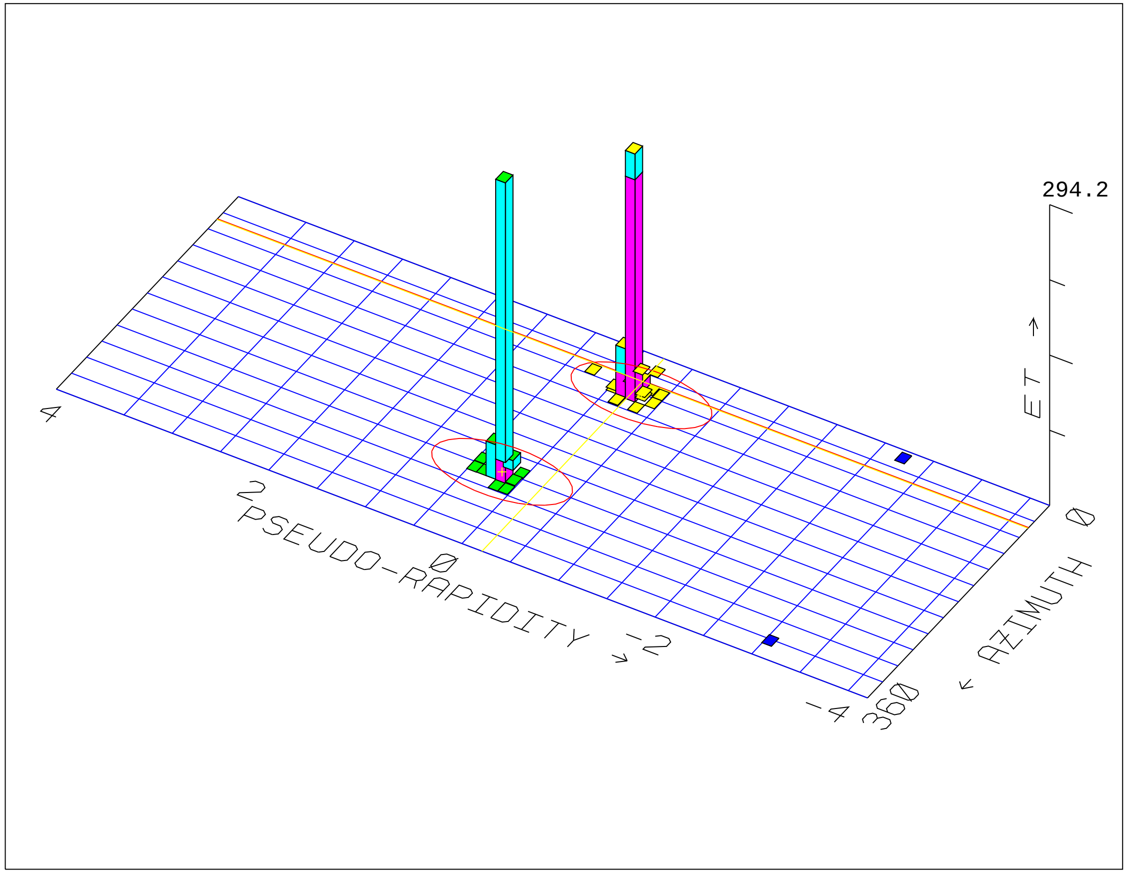

- Maximizing the total transverse energy of the hadrons within a cone of fixed size
- Three-step procedure:
  - $\longrightarrow$ constructing the seeds (starting positions for the cone)
  - $\longrightarrow$ moving the cone around until a stable position is found
  - $\longrightarrow$ dealing with overlapping cones (to merge or not to merge)
- They have been applied mainly to $p\bar{p}$ collisions
- The iterative cone algorithm has been the standard
  - $\longrightarrow$ distance definition: $d_{iJ} \equiv \sqrt{(\eta_i - \eta_J)^2 + (\phi_i - \phi_J)^2}$
  - $\longrightarrow$ cone axis: $\eta_J \equiv \frac{1}{E_T} \sum_i E_{T,i} \cdot \eta_i, \quad \phi_J \equiv \frac{1}{E_T} \sum_i E_{T,i} \cdot \phi_i, \quad E_T = \sum_i E_{t,i}$

Requirements on a jet algorithm

MEASURABLE, CALCULABLE, ACCURATE

→ **Simple to use in experimental analyses and theoretical calculations**

→ **Insensitive to the presence of soft particles or particle (strong) decays**

→ **infrared and collinear safe, so that it can be calculated order-by-order in perturbative QCD**

→ **Close correspondence with the final state quarks and gluons**

→ **small hadronisation corrections**

→ **Suppression of beam remnant jet contributions**

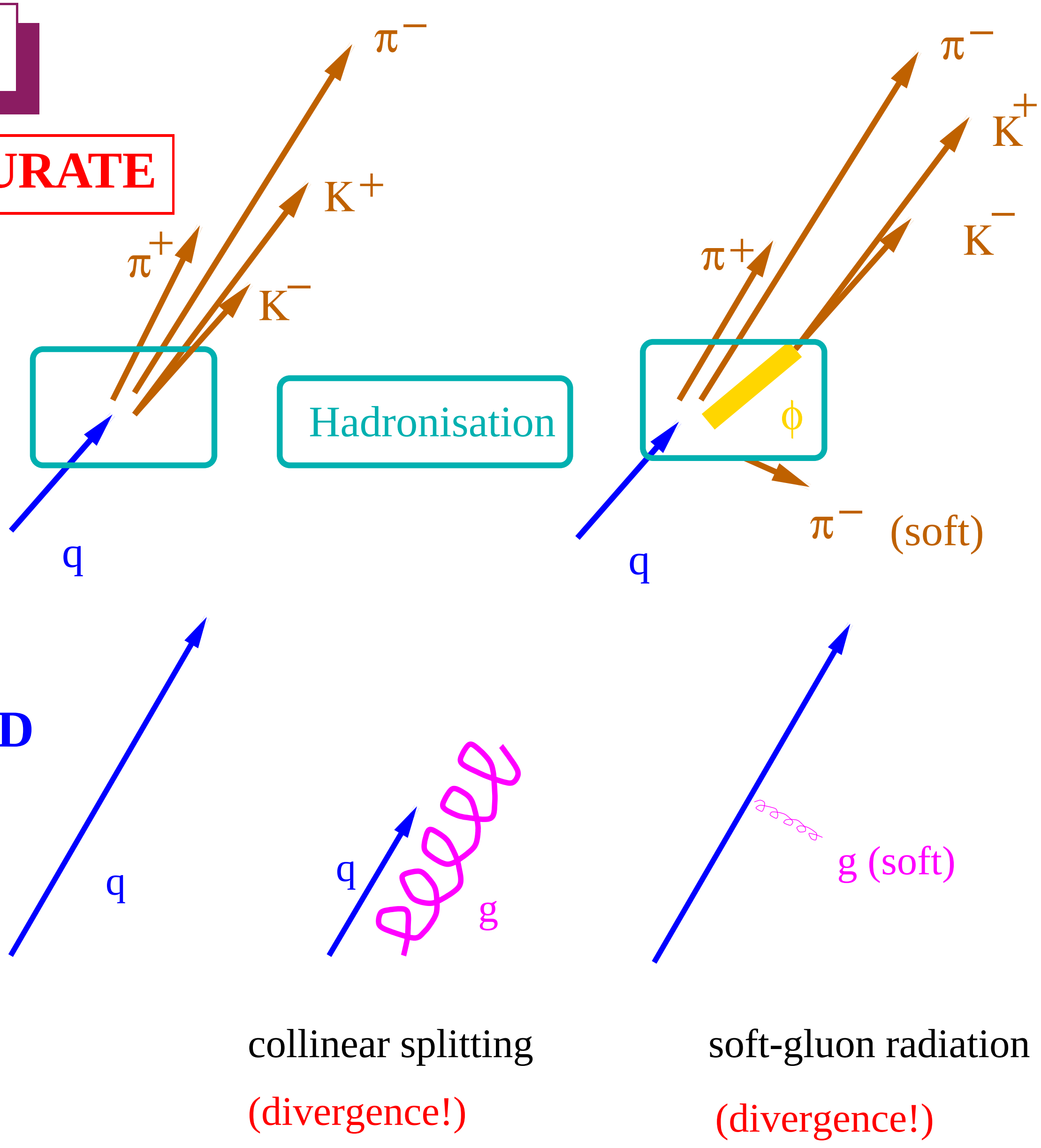

Fulfilling the requirements

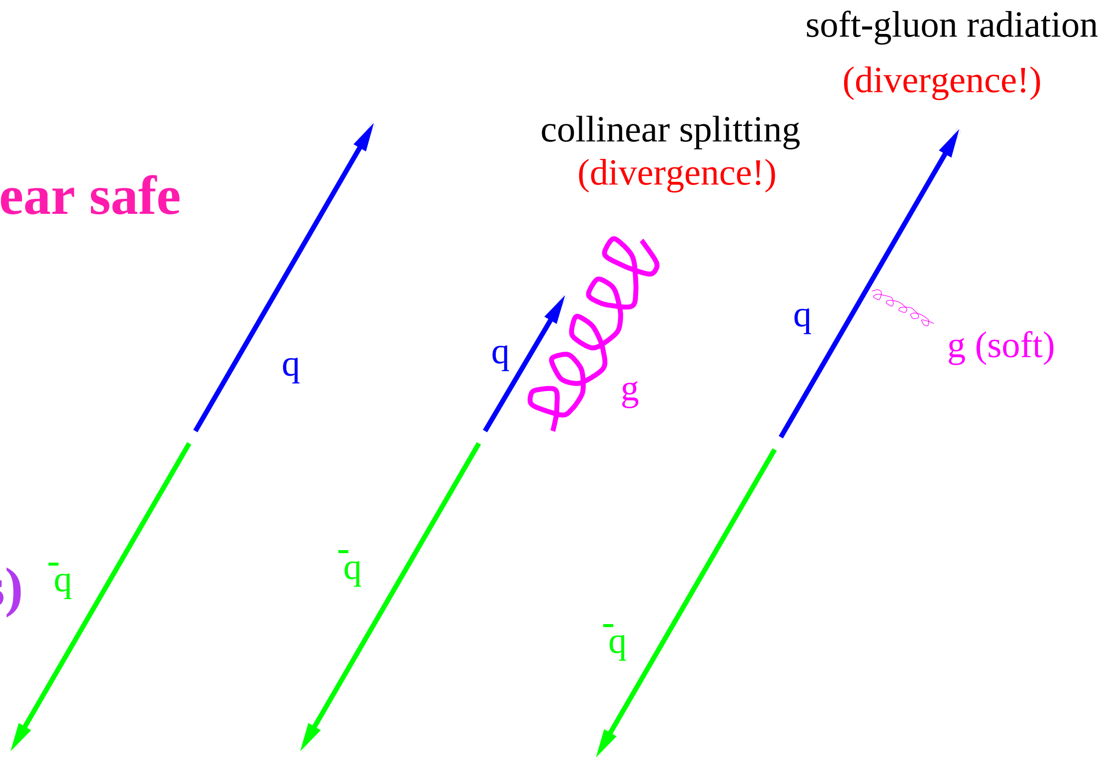

- **The JADE algorithm is infrared and collinear safe**

$\longrightarrow$ **First situation: two particles (partons) with equal and opposite momenta**

$$d^2_{12} = 4E_1(\bar{q})E_2(q) = s_{cm}$$

For $d^2_{cut} < s_{cm} \Rightarrow$ Two jets

$\longrightarrow$ **Second situation: three particles (partons)**

the two collinear partons will be combined

$$d^2_{2'3'} = 2E'_2(q)E'_3(g)(1 - \cos 0) = 0 \;!!$$

$p_{(2'3')} = p'_2 + p'_3 = p_2$ **!! (it wouldn't be the case if the p were added quadratically)**

$d^2_{1(2'3')} = 4E_1(\bar{q})E_{(2'3')}(qg) = s_{cm}$ **and for $d^2_{cut} < s_{cm} \Rightarrow$ Two jets**

$\longrightarrow$ **Third situation: the soft gluon will be combined with the closest (in angle) quark**

e.g. $d^2_{2'3'} = 2E'_2(q)E'_3(g)(1 - \cos\theta_{2'3'}) < 2E_1(\bar{q})E'_3(g)(1 - \cos\theta_{13'})$

$p_{(2'3')} = p'_2 + p'_3 = p_2$!!

$d^2_{1(2'3')} = 4E_1(\bar{q})E_{(2'3')}(qg) = s_{cm}$ **and for $d^2_{cut} < s_{cm} \Rightarrow$ Two jets**

- **The final result is the same in each configuration!**

Fulfilling the requirements (II)

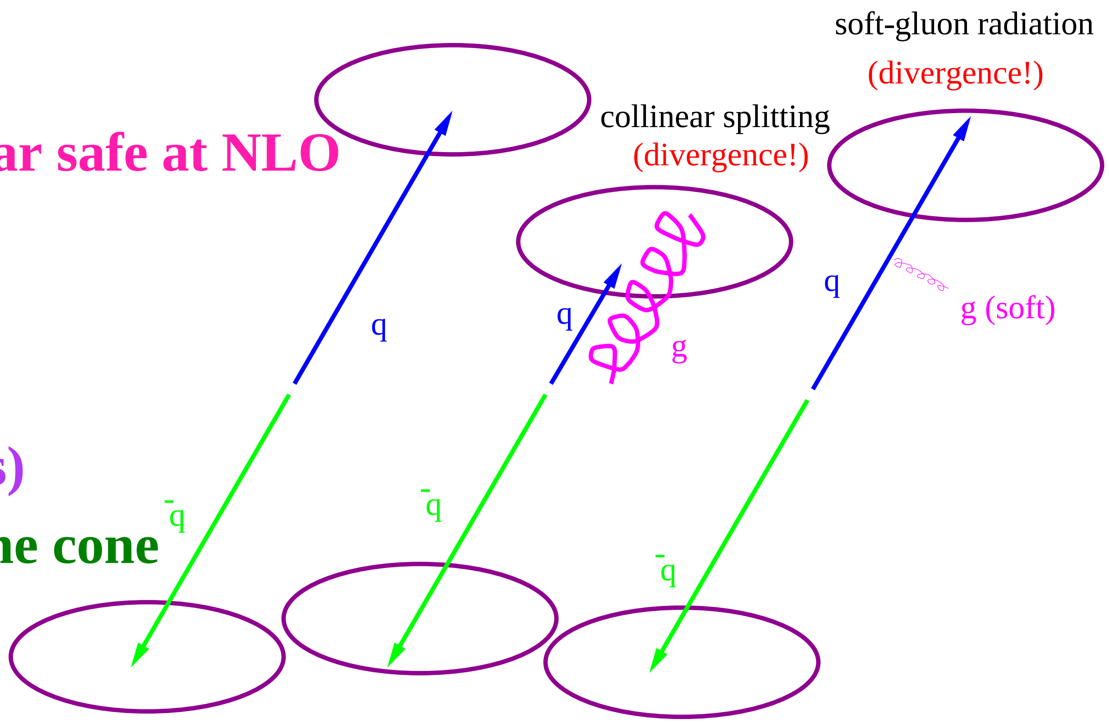

- The cone algorithm is infrared and collinear safe at NLO

→ First situation: two particles (partons) with equal and opposite momenta

Each of them defines a cone ⇒ Two jets

→ Second situation: three particles (partons)

the two collinear partons will lie in the same cone

⇒ Two jets

→ Third situation: if the soft gluon is far from the other partons ($\sqrt{\Delta\eta^2 + \Delta\phi^2} > R$) it won't be lumped with any of them

⇒ Two jets

The jet axes and transverse energies will differ from the the values found in the 1st or 2nd situation by a quantity that $\to 0$ as $E(g) \to 0$!

- The final result is the same in each configuration!

Jets in e^+e^- collisions

Observation of jets in e^+e^- collisions

- First evidence for jets arising from quarks in $e^+e^- \to q\bar{q}$ events was obtained at the SPEAR e^+e^- collider in 1975
- Since jets could not be discerned simply by looking at the pattern of outgoing tracks, a method to define the jet axis was devised: the direction in which the sum of the squares of the momenta transverse to the axis was minimal:

$\to S = \frac{3\sum_i p_{\perp\,i}^2}{2\sum_i p_i^2}$ (sphericity) $\to$ jet-like event: $S = 0$ $\to$ isotropic event: $S \approx 1$

- $p_{\perp\,i}$: momentum of the ith particle perpendicular to the sphericity axis
- QCD predicts that as the cms energy increases, the events should become more jet-like so the sphericity should decrease
- Comparison to isotropic phase-space (PS) and jet models:
  - $\to$ both models are consistent with the data for $\sqrt{s} = 3.0$ GeV
  - $\to$ for $\sqrt{s} = 6.2$ and 7.4 GeV, the data are peaked toward low S and have significantly lower mean S than the PS model and agree with the jet model

SPEAR data

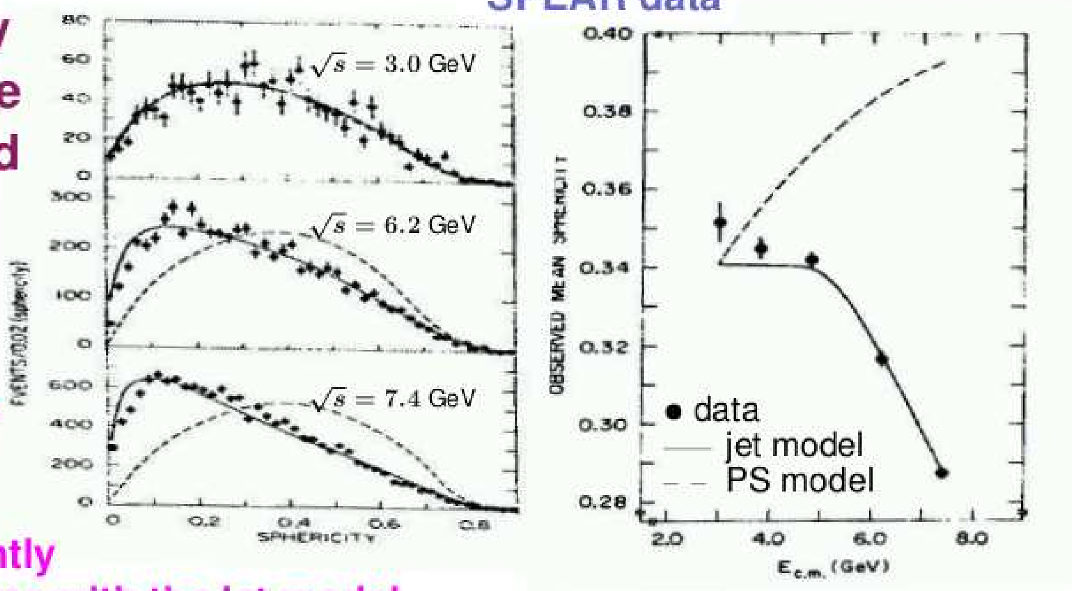

Observation of jets in e^+e^- collisions

- The quark spin can also be inferred from the angular distribution of the thrust axis in hadronic Z decays $\longrightarrow$ the angular distribution has the form

$$\frac{d\sigma}{d\cos\theta_{\rm th}} \propto 1 + \alpha\cos^2\theta_{\rm th}$$

where $\theta_{\rm th}$: polar angle of thrust axis

$\longrightarrow$ spin-$1/2$ quarks: $\alpha = +1$
$\longrightarrow$ spin-0 quarks: $\alpha = -1$

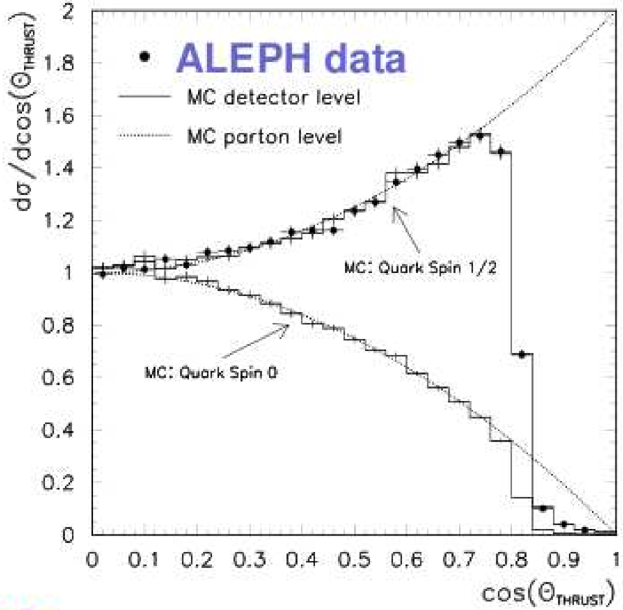

- Comparison to the predictions

  $\longrightarrow$ the spin-0 curve is clearly incompatible the data
  $\longrightarrow$ the spin-$1/2$ curve is in excellent agreement with the measurements
  $\Rightarrow$ Confirmation that quarks are fermions with spin $1/2$

Observation of gluon jets in e^+e^- collisions

- In e^+e^-, gluons first appear as the $\mathcal{O}(\alpha_s)$ correction to the $e^+e^- \to q\bar{q}$ process
- First observation of three-jet events in $e^+e^- \to q\bar{q}g$ at the PETRA e^+e^- collider in 1979 $\to$ direct evidence for the existence of gluons by looking for deviations from the quark-parton model predictions

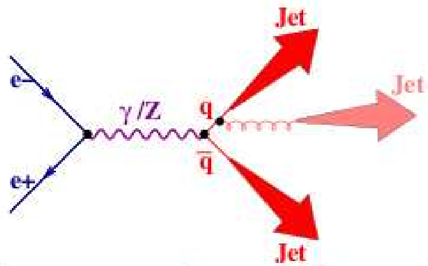

$e^+e^- \to \text{jet} + \text{jet} + \text{jet}$

- The quark-parton model for the process $e^+e^- \to q\bar{q}$ predicts back-to-back jets of hadrons with typical transverse momentum of ~ 0.3 GeV
- In QCD,
  - $\longrightarrow$ gluons will be radiated from the quarks and so the jets will no longer be back-to-back
  - $\longrightarrow$ the p_T distribution of the final-state hadrons will broaden with increasing energy
  - $\longrightarrow$ the $q\bar{q}g$ state must be coplanar since the momenta should sum 0 by momentum conservation
    - $\longrightarrow$ the final-state hadrons will have small transverse momentum wrt the plane and large transverse momentum in the plane
  - $\longrightarrow$ if the gluon is radiated with a large transverse momentum, the events will have a three-jet topology

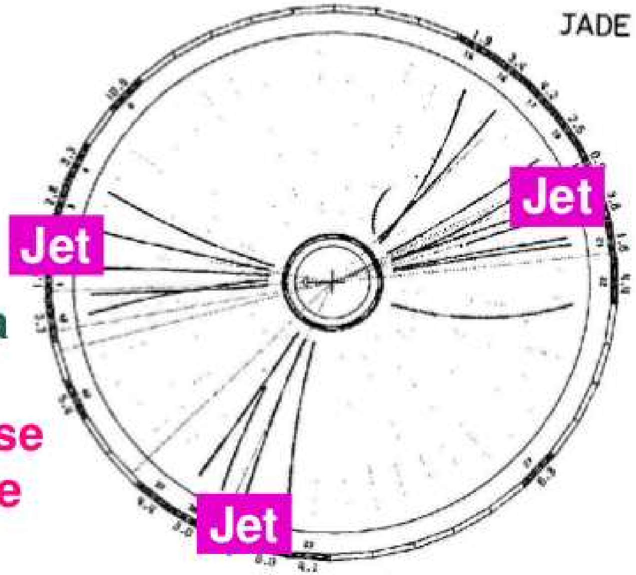

Observation of gluon jets in e^+e^- collisions

- Two methods were used to determine the jet axis from the final-state hadrons:
  $\longrightarrow$ minimising $\sum p_T^2$ (sphericity axis)
  $\longrightarrow$ maximising $\sum |p_{||}|$ (thrust axis)
- Normalised transverse momentum distribution $\sigma^{-1} d\sigma/dp_T^2$ evaluated wrt the sphericity axis as a function of p_T^2 at $\sqrt{s} = 13 - 17$ and $24.7 - 31.6$ GeV:
  $\longrightarrow$ the data at both energies are in reasonable agreement for $p_T^2 < 0.2$ GeV^2
  $\longrightarrow$ the high-energy data are well above the low energy data for $p_T^2 > 0.2$ GeV^2

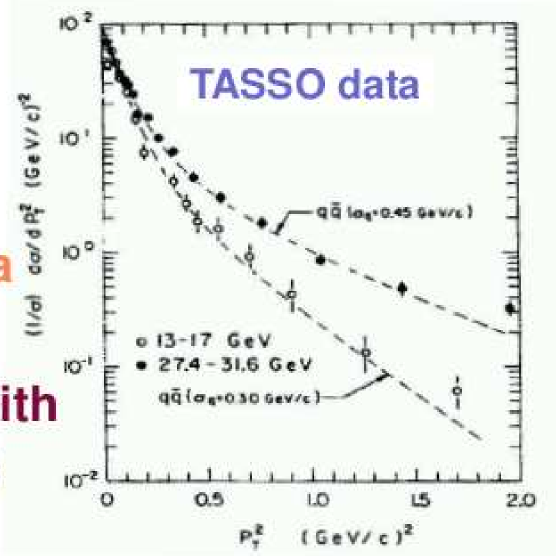

- The low-energy data have been fitted for $p_T^2 < 1.0$ GeV^2 with the jet model: the value of the parameter σ_q (it determines the width of the p_T distribution) obtained was 0.30 GeV
- For the high-energy data, $\sigma_q = 0.45$ GeV in contradiction with the quark-parton model which assumes the quark to fragment into hadrons with an energy-independent p_T distribution
- QCD predicts the p_T to increase with the energy due to gluon bremsstrahlung

Observation of gluon jets in e^+e^- collisions

$$\langle p_T^2 \rangle_{\rm out} = \frac{1}{N} \sum_{j=1}^{N} (\vec{p}_j \cdot \vec{n}_1)^2$$ (momentum component normal to the event plane)

$$\langle p_T^2 \rangle_{\rm in} = \frac{1}{N} \sum_{j=1}^{N} (\vec{p}_j \cdot \vec{n}_2)^2$$ (momentum component in the event plane perpendicular to the jet axis)

where $\vec{n}_3$: direction of sphericity axis, $\vec{n}_1$: direction which maximises $\sum p_T^2$, $\vec{n}_2$: direction orthogonal to $\vec{n}_1$ and $\vec{n}_3$

$\rightarrow$ $\vec{n}_2 - \vec{n}_3$: event plane

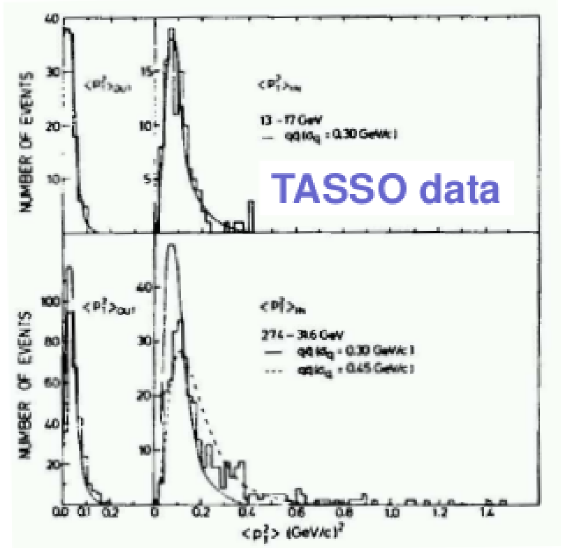

$\longrightarrow$ the data show only little increase in $\langle p_T^2 \rangle_{\rm out}$ between the low-energy and the high-energy data

$\longrightarrow$ the distribution of $\langle p_T^2 \rangle_{\rm in}$ becomes much wider at high energies and a long tail is observed

- **Comparison to the jet-model predictions:**
  - $\longrightarrow$ hadrons resulting from pure $q\bar{q}$ events will be on average distributed uniformly around the jet axis
  - $\longrightarrow$ fair agreement with the $q\bar{q}$ model is found both for $\langle p_T^2 \rangle_{\rm in}$ and $\langle p_T^2 \rangle_{\rm out}$ for the low-energy data
  - $\longrightarrow$ at high energy, there is a fair agreement between $\langle p_T^2 \rangle_{\rm out}$ and the $q\bar{q}$ model with $\sigma_q = 0.3$ GeV
  - $\longrightarrow$ the long tail in $\langle p_T^2 \rangle_{\rm in}$ is not reproduced by the model $\longrightarrow$ this discrepancy cannot be removed by increasing σ_q

$\Rightarrow$ the data include a number of planar events not reproduced by the $q\bar{q}$ model
$\longrightarrow$ evidence for $q\bar{q}g$ events

Jet rates in e^+e^- collisions

- The topology of hadronic events in e^+e^- collisions is modified by the effects of gluon radiation, giving rise to events which differ from the collimated two-jet topology coming from the fragmentation of $q\bar{q}$ events
- Since the amount of gluon radiation is directly proportional to α_s, the study of the topology of hadronic decays in e^+e^- provides a determination of $\alpha_s(M_Z)$
- The strategy consists of finding variables which characterize the "three-jetness" of the events $\longrightarrow$ the variables have to be infrared and collinear safe to be able to perform reliable calculations: jet rates as a function of the resolution parameter $y_{\rm cut}$
- Comparison to Monte Carlo predictions:
  $\longrightarrow$ the predictions show in general a good agreement with the data
- The three-jet rate (R_3) at $y_{\rm cut} = 0.08$ as a function of $\sqrt{s}$ shows the running of α_s directly

OPAL data

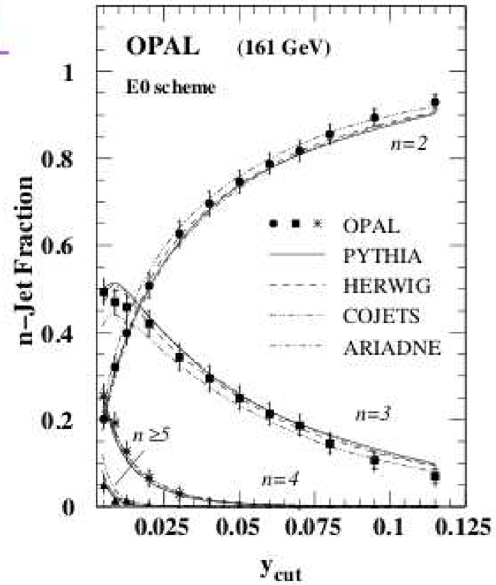

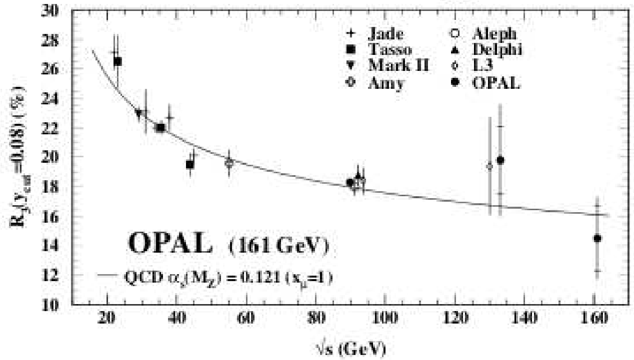

Theoretical Uncertainties

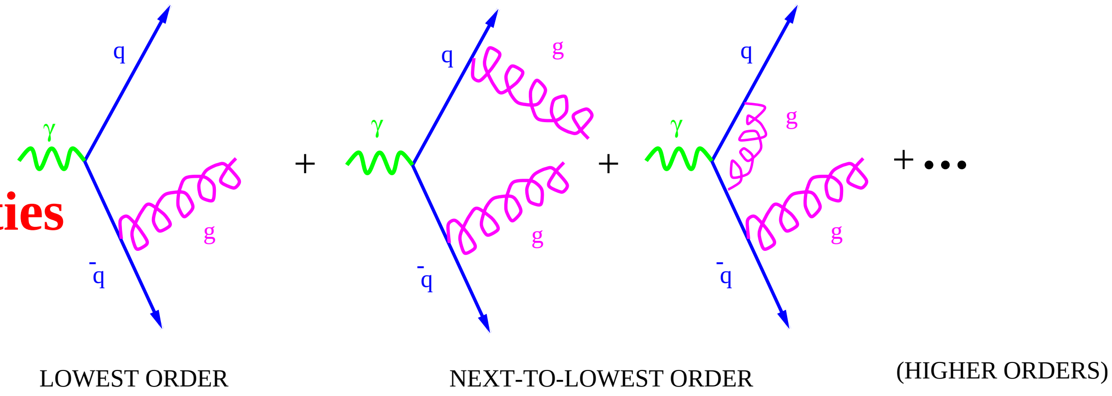

- **Being collinear and infrared safe**

does NOT mean small theoretical uncertainties

- **Perturbative QCD calculations are performed to a certain order in α_S**

$\rightarrow$ **the size of higher-order contributions constrains the accuracy with which (e.g.) α_S can be experimentally determined**

- **The size of the higher-order contributions DEPENDS on the jet algorithm**

- **How can higher-order effects be estimated without computing them?**

$\rightarrow$ **by investigating the renormalisation-scale dependence (μ_R)**

$$A = A_1 \cdot \alpha_S(\mu_R) + A_2 \cdot \alpha_S^2(\mu_R) + \ldots\text{(higher orders)}$$

At all orders A does NOT depend on μ_R

$\Rightarrow$ **The size of the "…" is such that it cancels the μ_R variation of the first two terms**

Theoretical Uncertainties (II)

- NLO calculations for three-jet production in e^+e^-: $\rightarrow$ variation with μ_R to asses the size of higher-order contributions

$\rightarrow$ Performance of various jet algorithms: variation of the observable f_3 over the range $0.1 < \mu_R/M_Z < 1.0$

  - JADE algorithm: 15%
  - Durham algorithm: 8%
  - Geneva algorithm: 3%

- The Durham and Geneva jet algorithms were specifically designed for the purpose of reducing the higher-order contributions upon identifying the limitations of the JADE algorithm

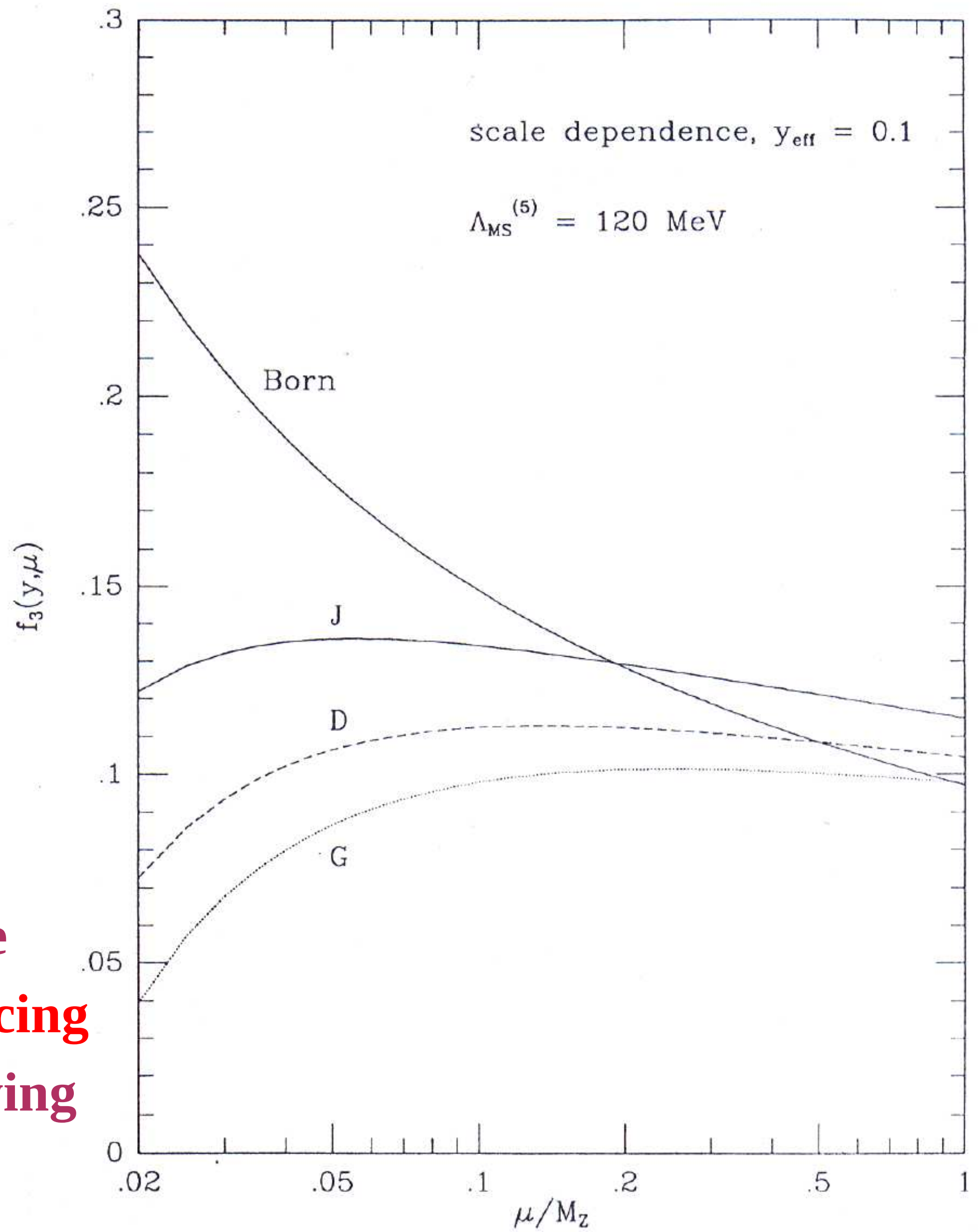

Improving the jet algorithm

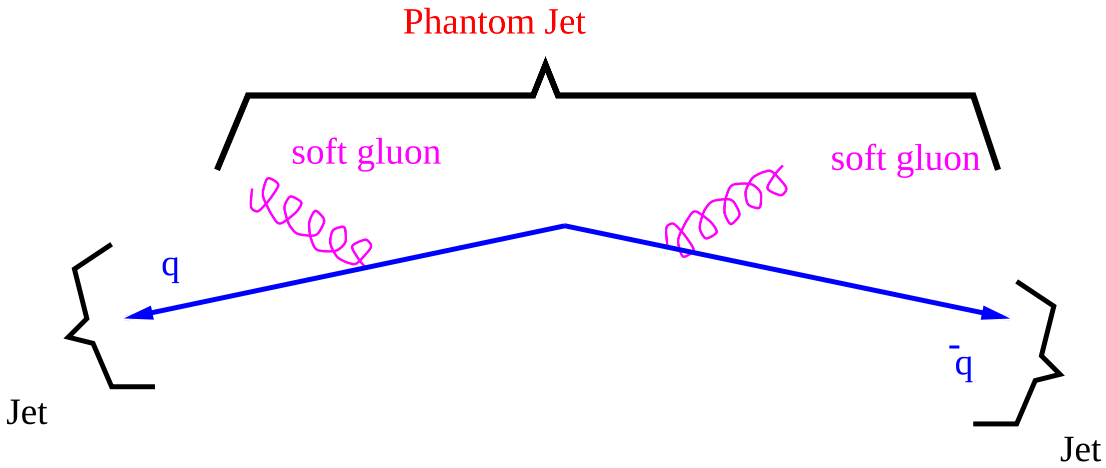

- **The limitation of the JADE algorithm:**
  - $\rightarrow$ **soft gluons are copiously radiated**
  - $\rightarrow$ **but soft gluons far apart can be combined into and a "phantom" jet**
- **This peculiar behaviour arises from the definition of "distance" in the JADE algorithm:**

$\boxed{d_{ij}^2 = 2E_iE_j(1-\cos\theta_{ij})}$ $\Rightarrow$ **two soft gluons can be very close "$d_{gg} \ll d_{gq}$"**

- **An improved definition of the distance:**

$$\boxed{d_{ij}^2 = 2 \cdot min(E_i^2, E_j^2) \cdot (1-\cos\theta_{ij})}$$

which amounts to replacing the invariant mass
$\rightarrow$ **by the minimum relative k_T of the pair**

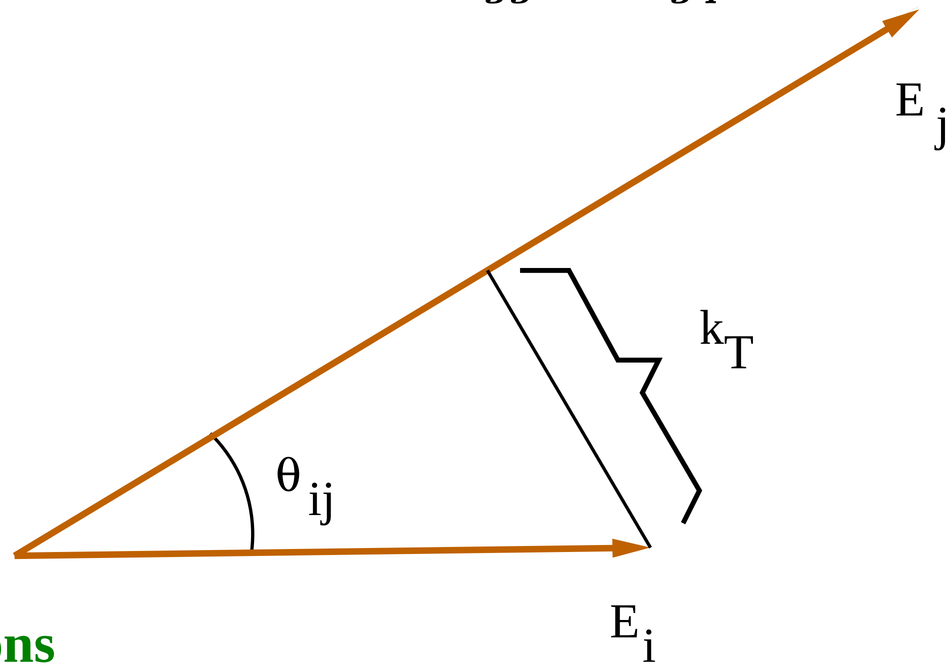

$\Rightarrow$ **Durham (or k_T) algorithm**
$\rightarrow$ **it also allows the resummation of contributions from multiple-soft-gluon emissions**

Hadronisation Effects

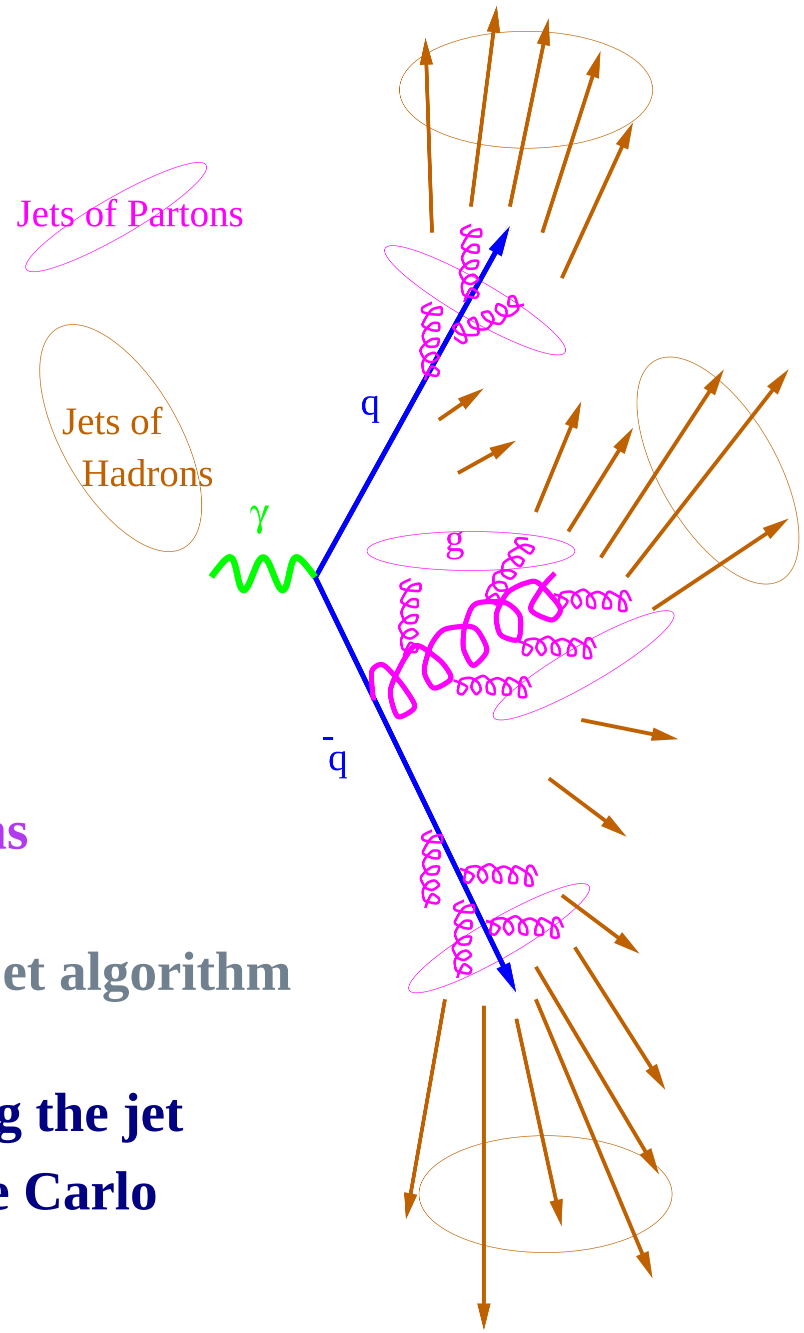

- **Being collinear and infrared safe**
  does NOT mean small hadronisation uncertainties
- **Parton-to-Hadron (hadronisation) effects are non-perturbative and are estimated with Monte Carlo simulations that include**
  - **$\rightarrow$ q and g radiation in the parton-shower approach**
  - **$\rightarrow$ fragmentation of the final-state partons into hadrons**
- **The size of the hadronisation effects DEPENDS on the jet algorithm**
- **They are estimated by comparing the results of applying the jet algorithm to the parton and hadron levels of the Monte Carlo simulated events**

Hadronisation Effects (II)

- **Jet rates in e^+e^- annihilations as functions of the resolution parameter y_{cut}**
- **Comparison of hadron and parton level calculations using Monte Carlo simulations**
- **The size of the hadronisation effects depends upon**
  - **$\rightarrow$ the distance definition**
  - **$\rightarrow$ the recombination procedure**
- **The hadronisation effects are LARGEST for**
  - **$\rightarrow$ the JADE algorithm with the E scheme $(p_{ij} = p_i + p_j)$**
  - **$\rightarrow$ the Geneva algorithm**
- **The hadronisation effects are SMALLEST for**
  - **$\rightarrow$ the JADE algorithm with the $E0$ scheme $(E_{ij} = E_i + E_j, \quad \vec{p}_{ij} = \frac{E_{ij}}{|\vec{p}_i+\vec{p}_j|}(\vec{p}_i + \vec{p}_j|))$**
  - **$\rightarrow$ the Durham algorithm**

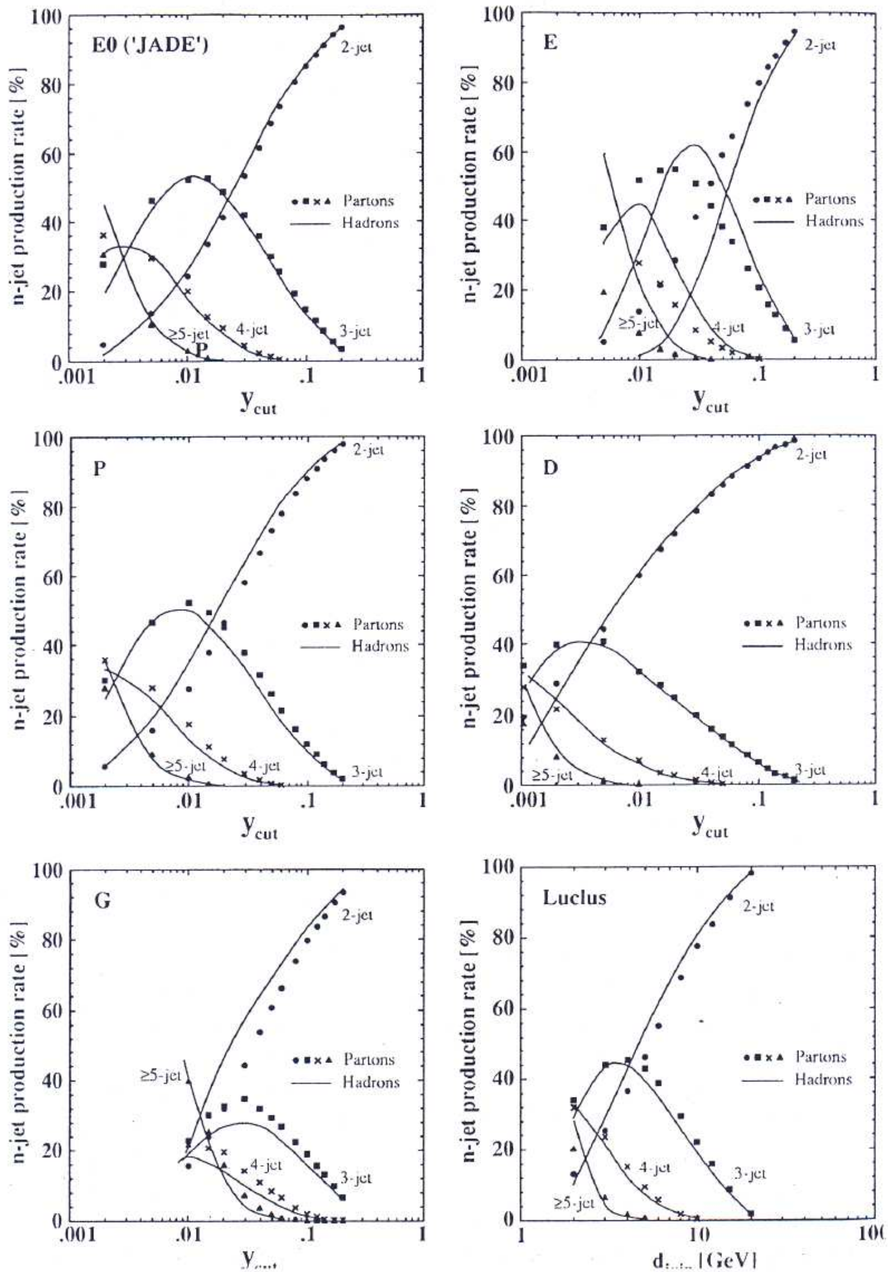

Importance of the details of the jet algorithms

- The "details" of a jet algorithm are RELEVANT for
  - $\longrightarrow$ precise comparisons between DATA and THEORY to make accurate determinations of the fundamental parameters (e.g. $\alpha_S(M_Z)$)
  - $\longrightarrow$ precise identification and reconstruction of new heavy particles
- The decision on which algorithm to choose must be based on the size of the uncertainties
  - $\longrightarrow$ higher-order contributions
  - $\longrightarrow$ hadronisation corrections
  - $\longrightarrow$ hadronisation uncertainties
  - $\longrightarrow$ experimental uncertainties

Determination of $\alpha_s(M_Z)$ in e^+e^- collisions

- The QCD prediction for the differential two-jet rate as a function of the two-jet resolution parameter y_3 is given by

$$\frac{1}{\sigma}\frac{d\sigma}{dy_3} = \frac{\alpha_s(\mu)}{2\pi}A(y_3) + \left(\frac{\alpha_s(\mu)}{2\pi}\right)^2 \cdot \left[B(y_3) + 2\pi b_0 \ln\left(\frac{\mu^2}{s}\right) \cdot A(y_3)\right]$$

where $A(y_3)$ and $B(y_3)$ contain the full information of the second order matrix elements, μ: renormalisation scale

- Since the predictions correspond to a partonic final state with at most four partons $\longrightarrow$ need to apply hadronisation corrections
- A value of $\alpha_s(M_Z)$ of

$$\alpha_s(M_Z) = 0.121 \pm 0.002\ (\text{stat})\ \pm 0.003\ (\text{exp.})\ \pm 0.007\ (\text{th.})$$

was obtained by fitting the measured differential two-jet rate distribution using the second order QCD prediction corrected for hadronisation effects

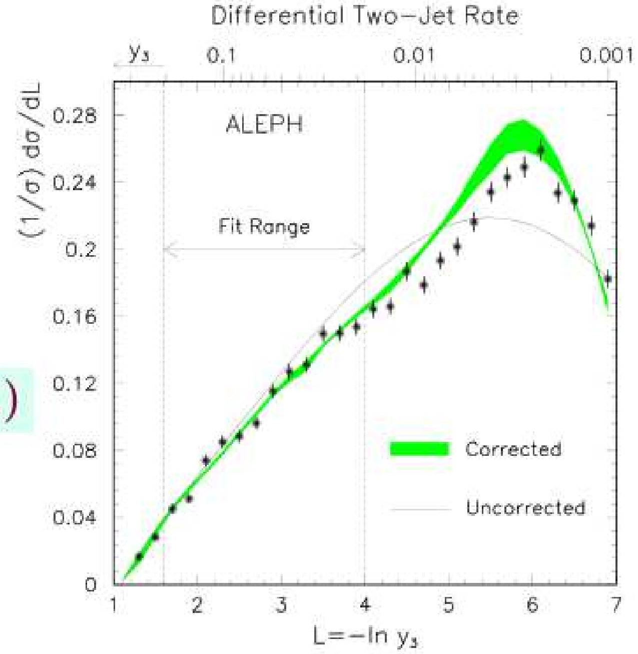

ALEPH data

Determination of the spin of the gluon in e^+e^- collisions

- A study of three-jet events in e^+e^- collisions gives insight into the dynamics of perturbative QCD $\longrightarrow$ three-jet events arise from hard non-collinear gluon radiation
- For massless jets, there are only four independent variables: two angular variables and two of the energy fractions, $x_i = 2E_i/\sqrt{s}$ since $x_1 + x_2 + x_3 = 2$ by energy conservation ($x_1 > x_2 > x_3$)
- The LO cross section for the process $e^+e^- \to q\bar{q}g$ with vector gluon (spin 1) is

$$\frac{1}{\sigma_0}\frac{d^2\sigma^V}{dx_1 dx_2} = \frac{2\alpha_s}{3\pi}\left[\frac{x_1^2 + x_2^2}{(1-x_1)(1-x_2)} + \text{permut}\right]$$

and for scalar gluon (spin 0),

$$\frac{1}{\sigma_0}\frac{d^2\sigma^S}{dx_1 dx_2} = \frac{2\tilde{\alpha}_s}{3\pi}\left[\frac{x_3^2}{(1-x_1)(1-x_2)} + \text{permut}\right]$$

where $\tilde{\alpha}_s$: effective coupling in a theory with scalar gluons

TASSO data

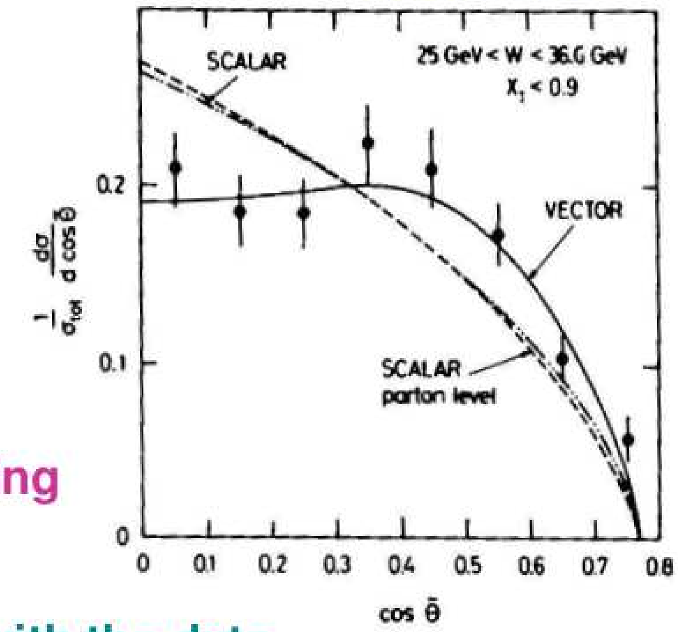

- The spin of the gluon can be determined by comparing the data and predictions for the variable

$$|\cos\tilde{\theta}| = \frac{x_2 - x_3}{x_1} \quad \text{(Ellis-Karliner angle)}$$

$\longrightarrow$ the scalar gluon model is in clear disagreement with the data
$\longrightarrow$ the vector gluon model provides a very good description of the data

Triple-gluon vertex

- QCD is based on the $SU(3)$ non-abelian group which induces the self-coupling of the gauge bosons whereas QED is based on the abelian $U(1)$ group (no self-coupling)

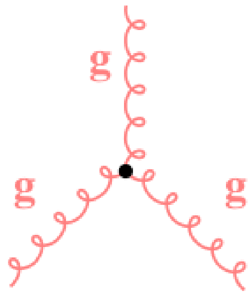

→ Due to the presence of the gluon self-coupling, the effects of the triple-gluon vertex should be observed

→ The events should contain at least four jets in the final state

- Events with at least four jets are needed since the diagrams that contain the triple-gluon vertex are

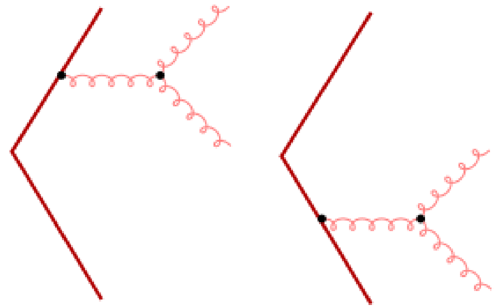

- The diagrams

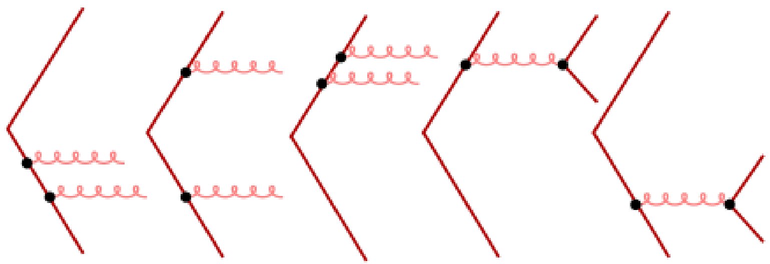

also contribute to the four-jet cross section, but they are present in abelian theories as well

Four-jet events in e^+e^-: triple-gluon vertex

- Four-jet events have been observed at the e^+e^- collider LEP

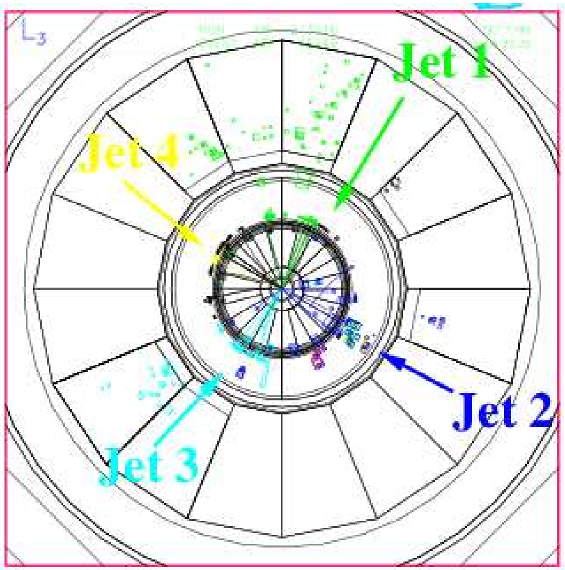

$\longrightarrow$ **QCD prediction confirmed by data!**

- The four-jet cross sections for $e^+e^- \to q\bar{q}gg$ and $e^+e^- \to q\bar{q}q\bar{q}$ can be expressed as

$$\frac{1}{\sigma_0} d\sigma_{q\bar{q}gg}(y_{ij}) = \left(\frac{\alpha_s C_F}{\pi}\right)^2 \left[A(y_{ij}) + \left(1 - \frac{1}{2}\frac{C_A}{C_F}\right) B(y_{ij}) + \frac{C_A}{C_F} C(y_{ij})\right] dY_{ij}$$

$$\frac{1}{\sigma_0} d\sigma_{q\bar{q}q\bar{q}}(y_{ij}) = \left(\frac{\alpha_s C_F}{\pi}\right)^2 \left[N_F \frac{T_F}{C_F} D(y_{ij}) + \left(1 - \frac{1}{2}\frac{C_A}{C_F}\right) E(y_{ij})\right] dY_{ij}$$

where

$\longrightarrow$ $y_{ij} = (p_i + p_j)^\mu (p_i + p_j)_\mu / s$ is the normalised two-body invariant mass and i, j run over the four partons

$\longrightarrow$ C_A, C_F and T_F are the color factors

$\longrightarrow$ N_F is the number of active quark flavors

$\longrightarrow$ A, ..., E are group-independent kinematic functions

$\longrightarrow$ σ_0 is the Born cross section for the process $e^+e^- \to q\bar{q}$

$\longrightarrow$ dY_{ij} is the product of the differentials of any five of the six y_{ij} variables

Four-jet events in e^+e^-: triple-gluon vertex

- Variables have been devised to highlight the non- abelian character of QCD in contrast to abelian theories, eg the $SU(3)$ group of QCD could be replaced by the abelian $[U(1)]^3$ group
- These variables are
  - → Bengtsson-Zerwas angle χ_{BZ}, the angle between the planes determined by the two lowest and the two highest energy jets:

$$\cos \chi_{BZ} = \left| \frac{(\vec{p}_1 \times \vec{p}_2) \cdot (\vec{p}_3 \times \vec{p}_4)}{|\vec{p}_1 \times \vec{p}_2| \, |\vec{p}_3 \times \vec{p}_4|} \right|$$

  - → Nachtmann-Reiter angle θ^*_{NR}, the angle between the momentum vector differences of jets 1,2 and jets 3,4:

$$|\cos \theta^*_{NR}| = \left| \frac{(\vec{p}_1 - \vec{p}_2) \cdot (\vec{p}_3 - \vec{p}_4)}{|\vec{p}_1 - \vec{p}_2| \, |\vec{p}_3 - \vec{p}_4|} \right|$$

  - → α_{34}, the angle between the two lowest energy jets:

$$\cos \alpha_{34} = \frac{\vec{p}_3 \cdot \vec{p}_4}{|\vec{p}_3| \, |\vec{p}_4|}$$

Do the data favour an abelian or a non-abelian theory?

- These variables have been measured in four-jet events at LEP, eg

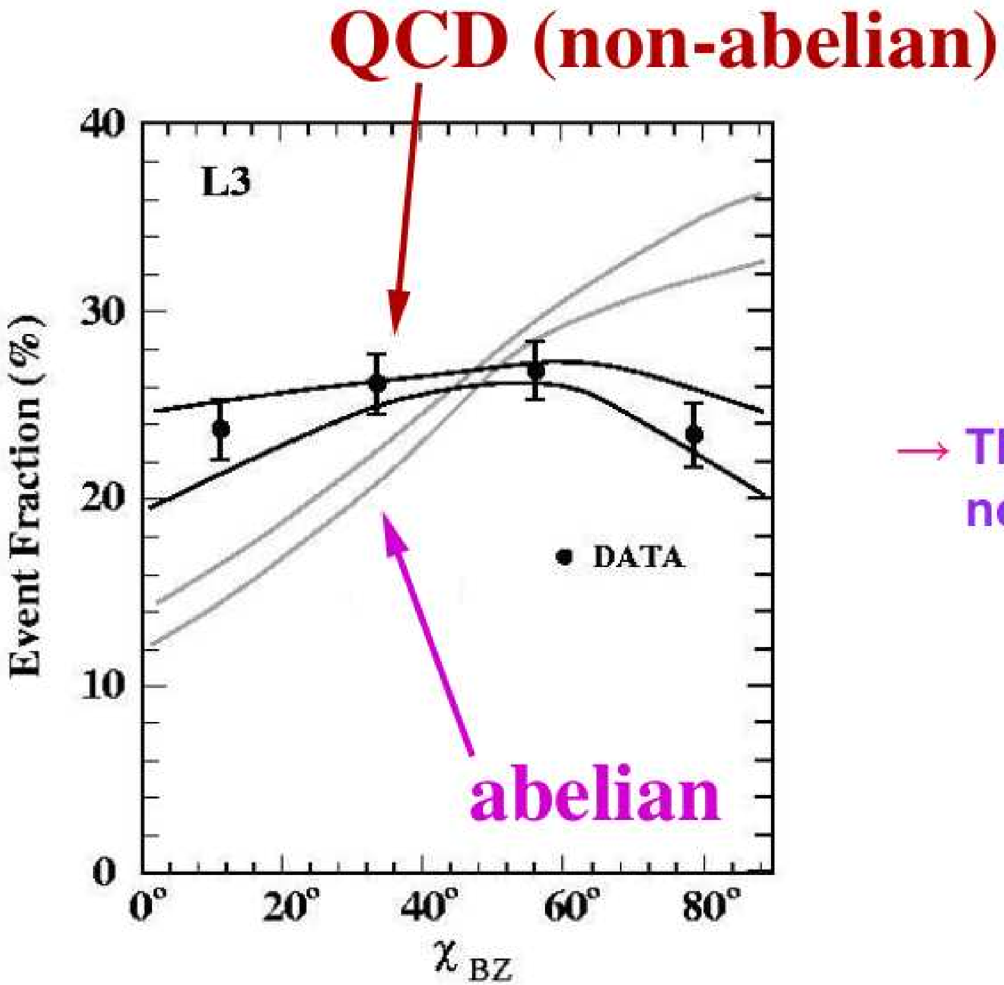

→ The data clearly favour a theory with non-abelian character: QCD

→ QCD prediction confirmed by data!

Four-jet events in e^+e^-: color factors

- A simultaneous measurement of the ratios C_A/C_F and T_F/C_F at e^+e^- colliders is possible through the study of angular correlations in four-jet events: the values are extracted from a fit of the theory to the data distributions on the angular variables

→ The results obtained are

$$C_A/C_F = 2.11 \pm 0.16\,(\text{stat}) \pm 0.28\,(\text{syst})$$
$$T_F/C_F = 0.40 \pm 0.11\,(\text{stat}) \pm 0.14\,(\text{syst})$$

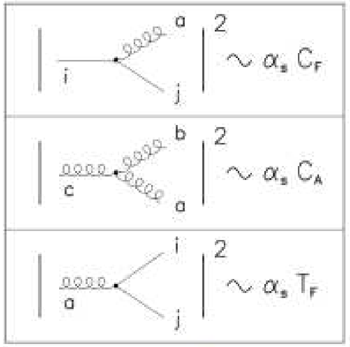

For $SU(N_C) \rightarrow C_A = N_C$

$$C_F = \frac{N_C^2-1}{2N_C}$$

$$T_F = 1/2$$

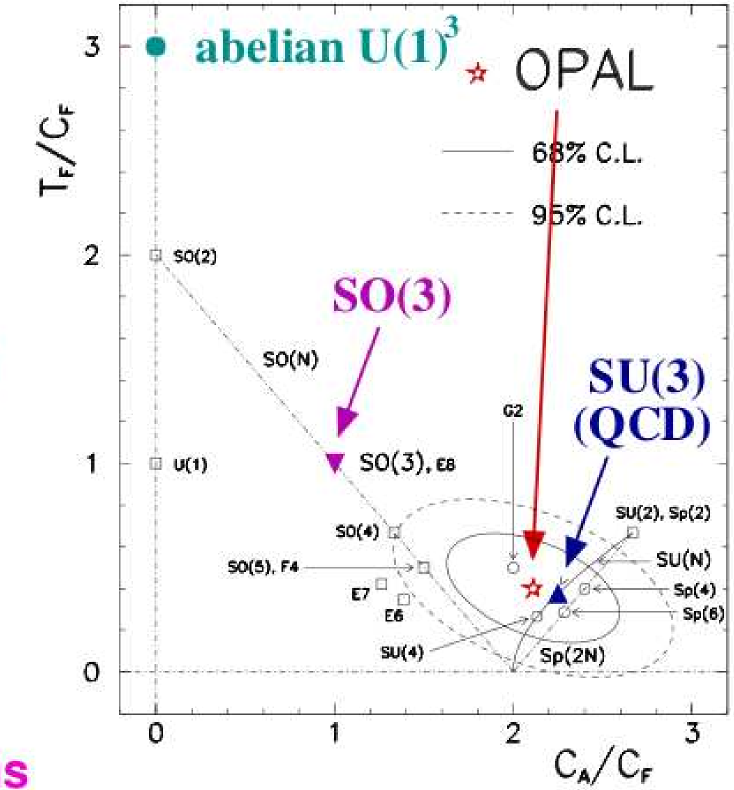

- The $U(1)^3$ and $SO(3)$ theories are clearly excluded by the measurements
- The results are in agreement with the predictions of the $SU(3)$ theory (QCD)

→ **QCD prediction confirmed by data!**

Measurements of α_s

Determinations of $\alpha_s(M_Z)$ in e^+e^- using measurements of event shapes and jet rates for which NNLO calculations are available

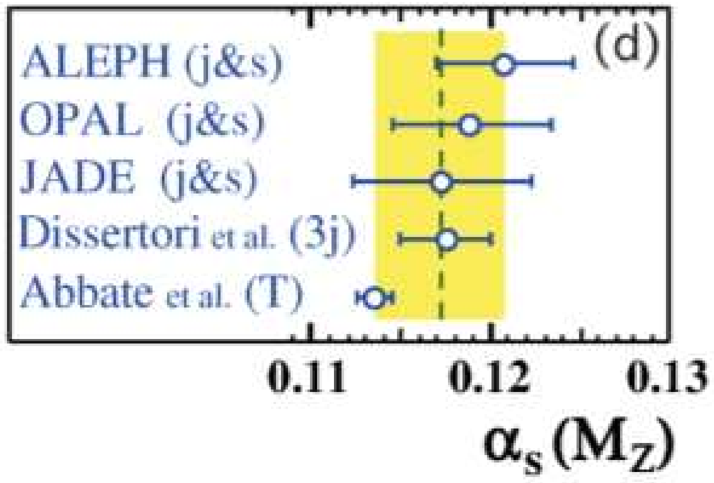

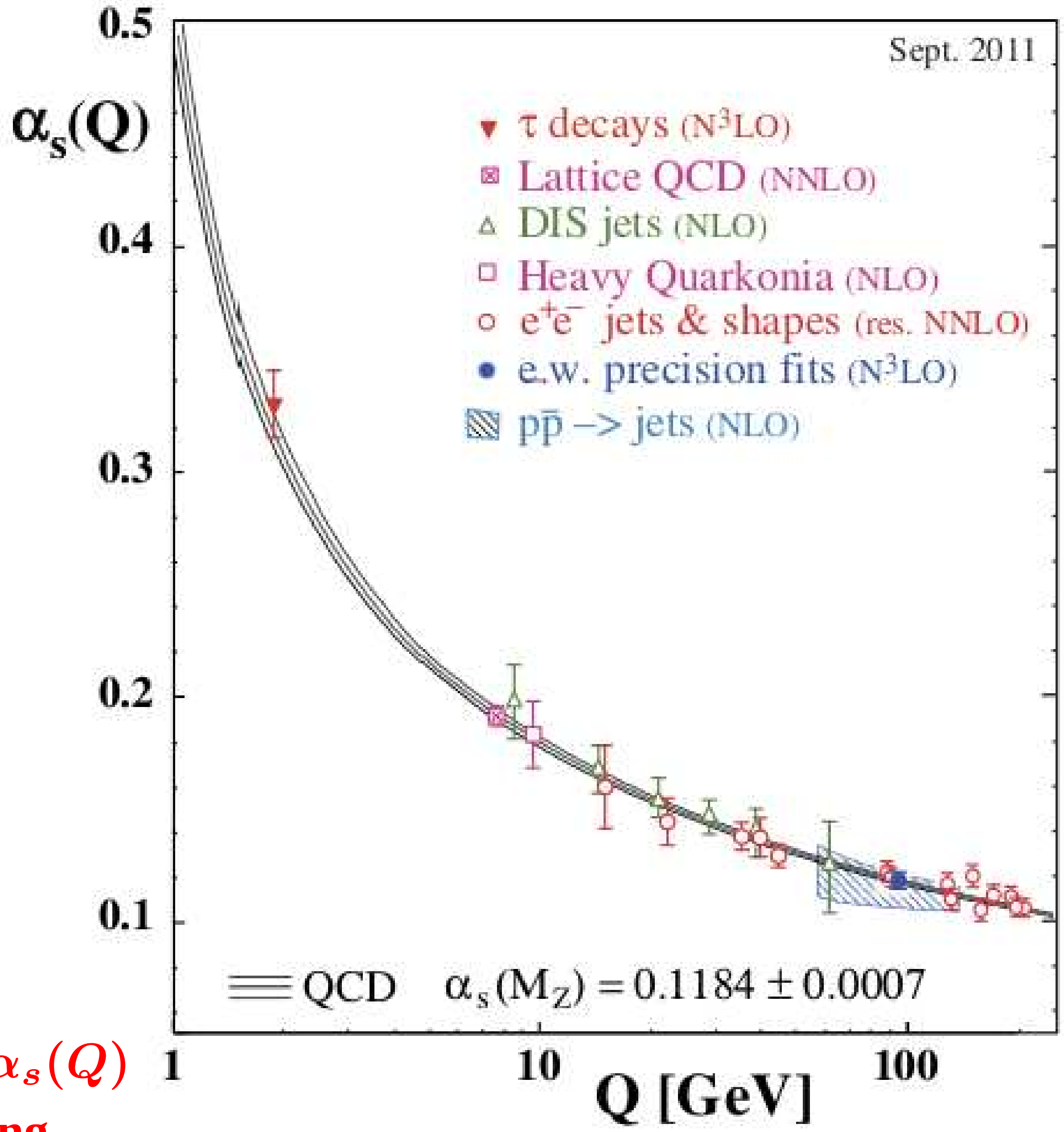

Determinations of $\alpha_s(Q)$ $\rightarrow$ test of the running

Structure Functions

Universality (and usefulness) of Proton PDFs

$$\sigma_{pp\to H(W,Z,\ldots)+X} = \sum_{a,b} \int_0^1 dx_1\, f_{a/p}(x_1,\mu_F^2) \int_0^1 dx_2\, f_{b/p}(x_2,\mu_F^2)\ \hat{\sigma}_{ab\to H(W,Z,\ldots)}$$

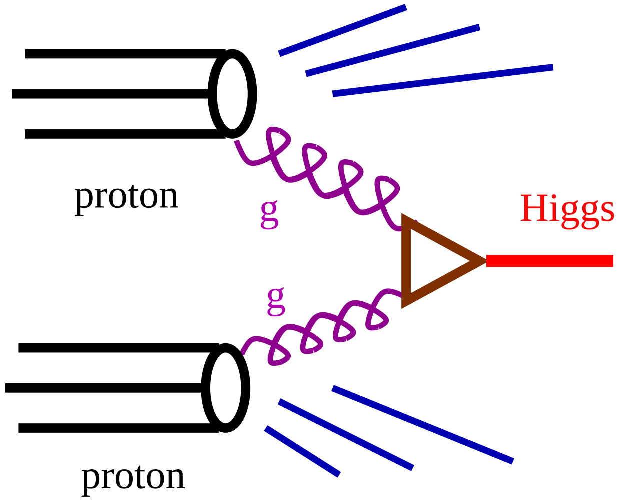

σ_H sensitive to gluon distribution at
$x \sim \frac{M_H}{\sqrt{s}} \sim 8\cdot 10^{-3}$ and $\mu_F^2 \sim M_H^2 \sim$ ~ 13000 GeV^2;
$\Delta\sigma_H^{PDF}/\sigma_H \sim \pm 3\%$ (for $M_H = 115$ GeV)

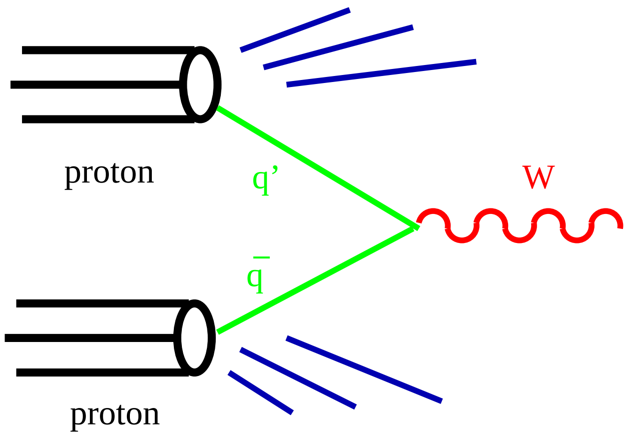

σ_W sensitive to sea distribution at
$x \sim \frac{M_W}{\sqrt{s}} \sim 6\cdot 10^{-3}$

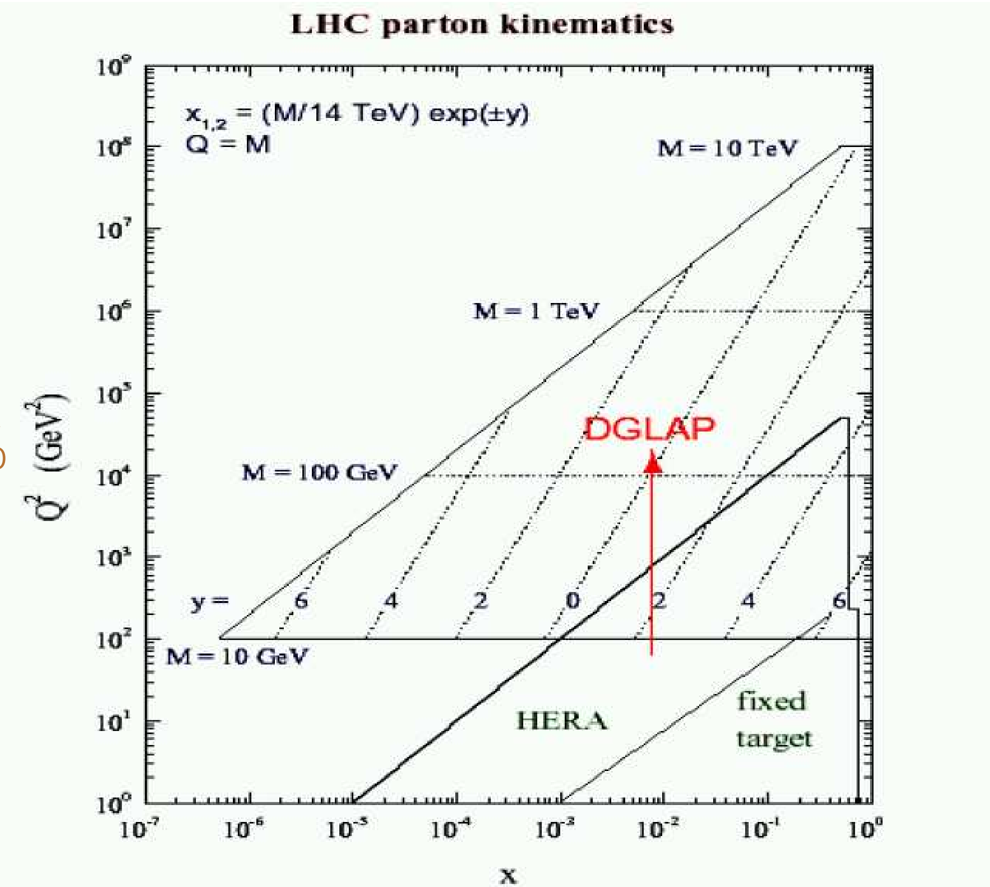

and $\mu_F^2 \sim M_W^2 \sim 6400$ GeV^2; $\Delta\sigma_W^{PDF}/\sigma_W \sim \pm 3\%$

Kinematics of Neutral Current Deep Inelastic Scattering

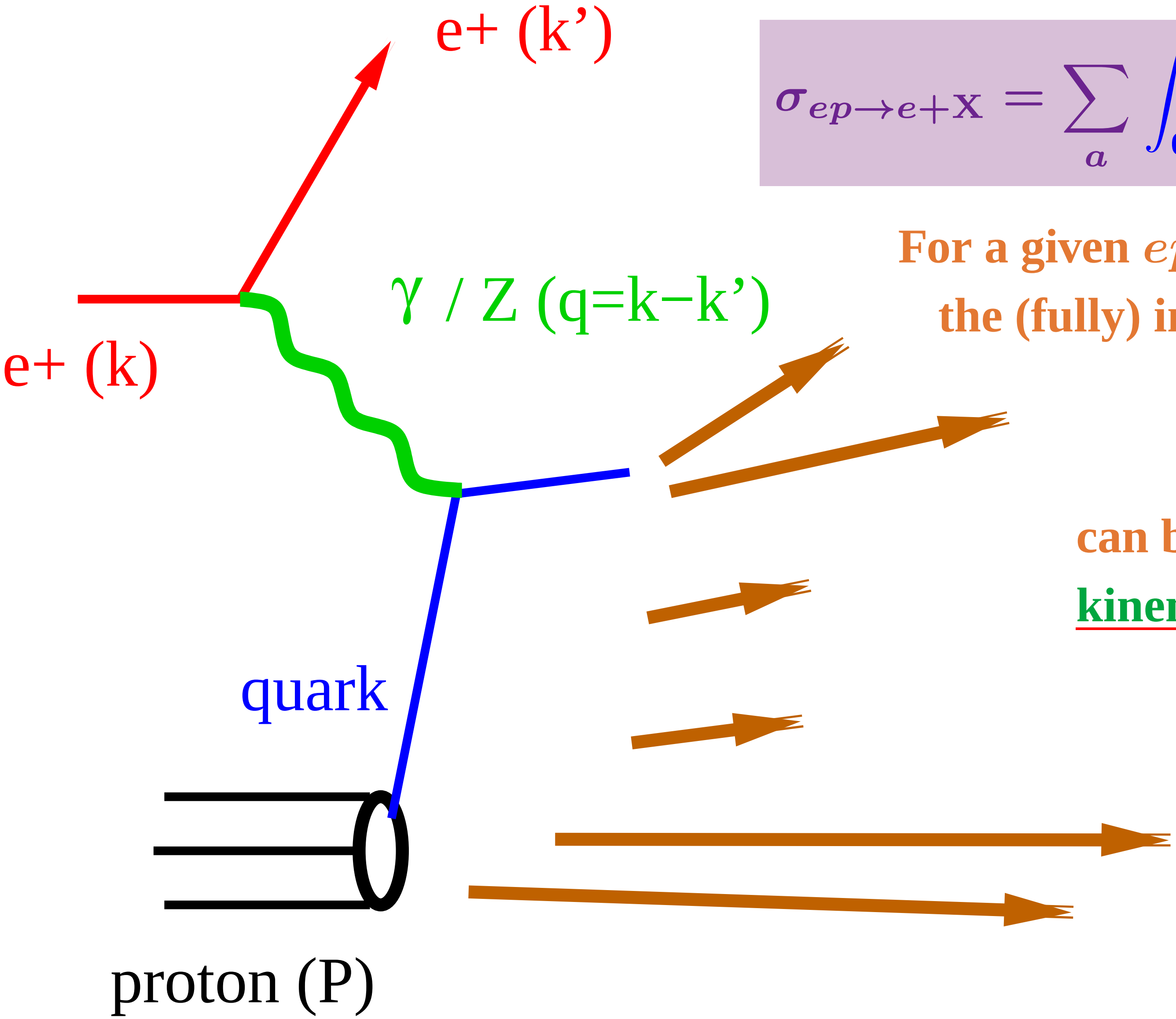

$$\sigma_{ep\to e+X} = \sum_a \int_0^1 dx_1\, f_{a/p}(x_1, \mu_F^2)\, \hat{\sigma}_{ea\to ea}$$

For a given *ep* centre-of-mass energy, $\sqrt{s}$, the (fully) inclusive cross section for

$$ep \to e + X$$

can be described by two independent kinematic variables, e.g.

$$Q^2 = -(k - k')^2$$

$$x_{Bj} = Q^2/(2P \cdot q)$$

Neutral Current Deep Inelastic Scattering

- **Neutral Current DIS event candidate**

  $Q^2 \sim 24000$ GeV^2 and $x_{Bj} \sim 0.5$

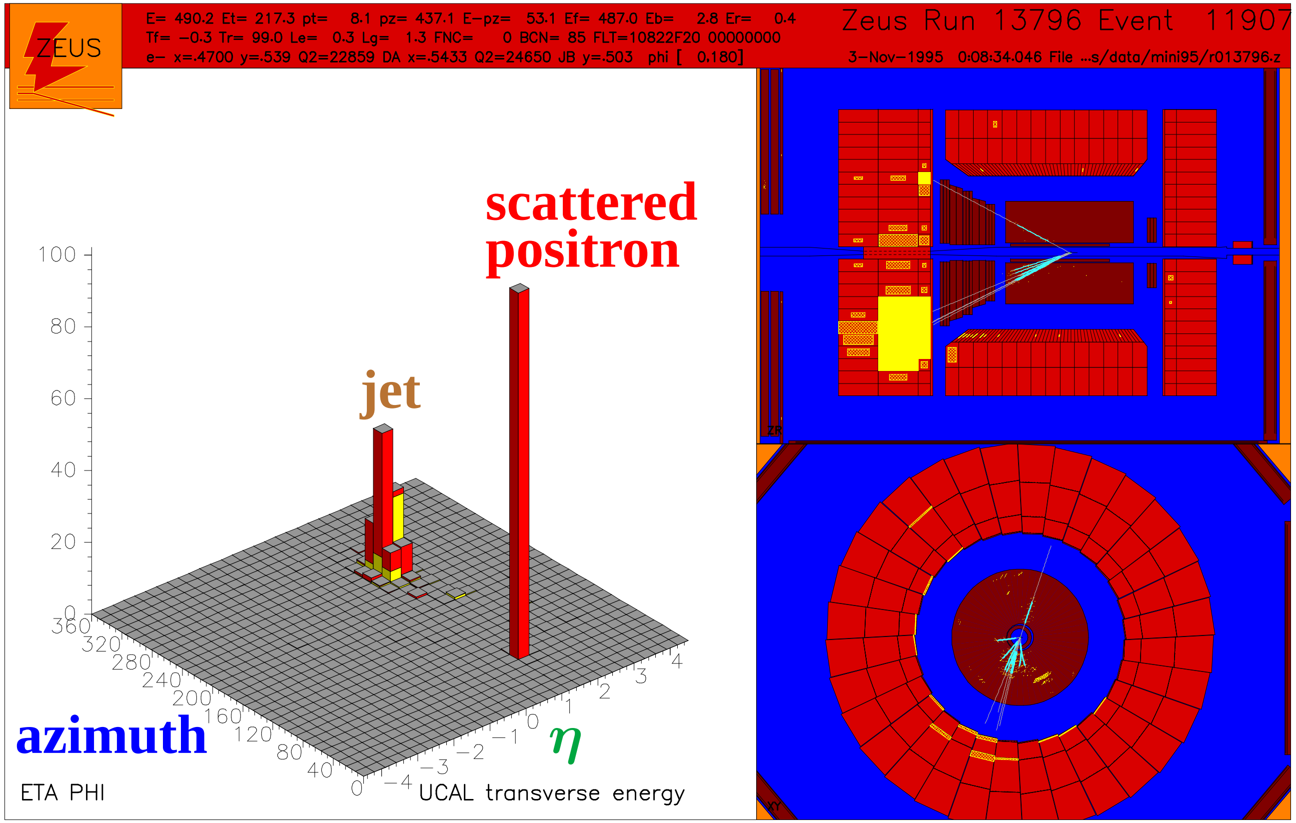

- **Coverage of kinematic plane (Q^2,x_{Bj})**

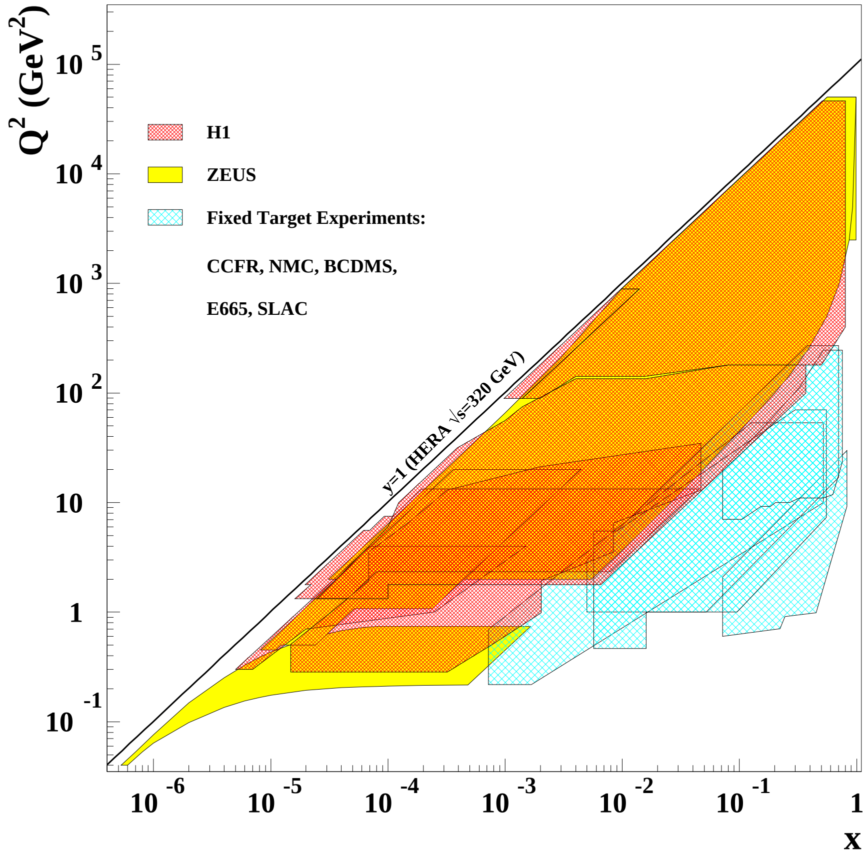

Neutral Current Deep Inelastic Scattering

- Inclusive process $e^{\pm}p \to e^{\pm} + \mathrm{X}$

$$\frac{d\sigma(e^{\pm}p)}{dxdQ^2} = \frac{2\pi\alpha^2}{xQ^4} \cdot \left(Y_+ \cdot F_2(x,Q^2) - y^2 \cdot F_L(x,Q^2) \mp Y_- \cdot xF_3(x,Q^2) \right)$$

Dominant — High y — High Q^2

where $Y_{\pm} = 1 \pm (1-y)^2$ and $y = Q^2/(sx)$ (inelasticity parameter)

- Structure functions of the proton (F_2, F_L, F_3) and QCD

$\to F_2 \sim x \sum_i e_i^2 \cdot (q_i(x,Q^2) + \bar{q}_i(x,Q^2))$ for $Q^2 \ll M_Z^2$

$\to$ the longitudinal structure function $F_L = 0$ in the quark-parton model

$\to$ parity-violating term F_3 is small for $Q^2 \ll M_Z^2$

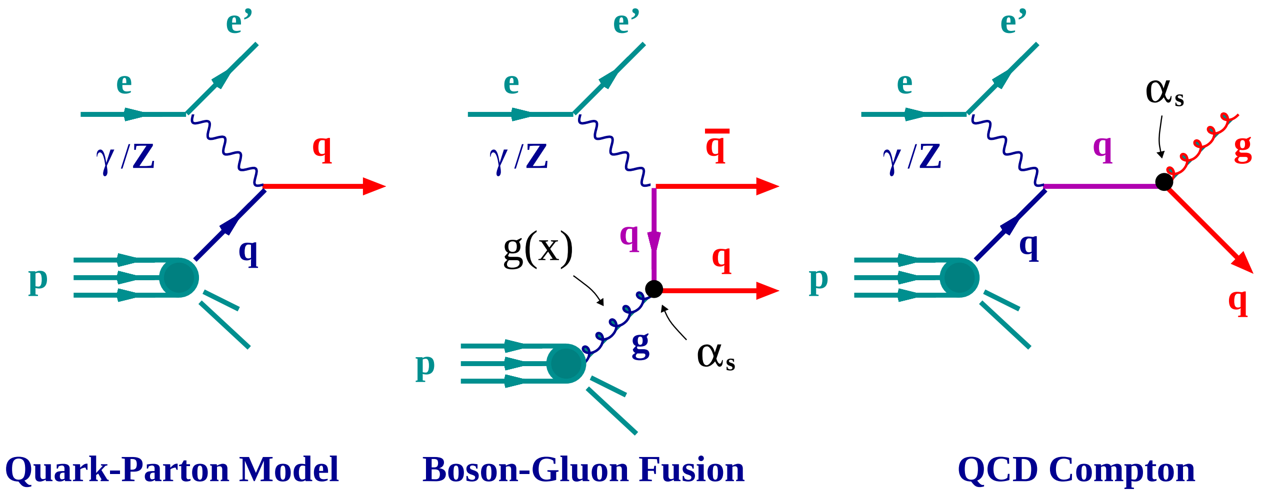

Clean probe of the Parton Distribution Functions in the Proton $q_i(x,Q^2), \bar{q}_i(x,Q^2)$ $g(x,Q^2)$

Determination of $F_2^{em}(x, Q^2)$

- Measurement of the doubly-differential cross section $d\sigma(e^+p)/dxdQ^2$ for the reaction $e^+p \to e^+ + X$ over a large range $2.7 < Q^2 < 30000$ GeV^2, $6 \cdot 10^{-5} < x < 0.65$
- Extraction of $F_2^{em}(x, Q^2)$ from the reduced cross section (corrected for QED effects):

$$\tilde{\sigma}(e^+p) = (2\pi\alpha^2 Y_+/xQ^4)^{-1} d\sigma_{\rm Born}/dxdQ^2$$

$$F_2 = F_2^{em} + F_2^{int} \cdot \eta_{\gamma Z} + F_2^{wk} \cdot \eta_{\gamma Z}^2$$
$$= F_2^{em}(1 + \Delta_{F_2})$$

where $\eta_{\gamma Z} = Q^2/(Q^2 + M_Z^2)$

$$\Rightarrow \tilde{\sigma}(e^+p) = F_2^{em}(1 + \Delta_{F_2} + \Delta_{F_3} + \Delta_{F_L})$$

- Typical precision 2-3%

$\to$ systematic uncertainties dominate $Q^2 < 800$ GeV^2

- Striking rise of F_2^{em} as x decreases

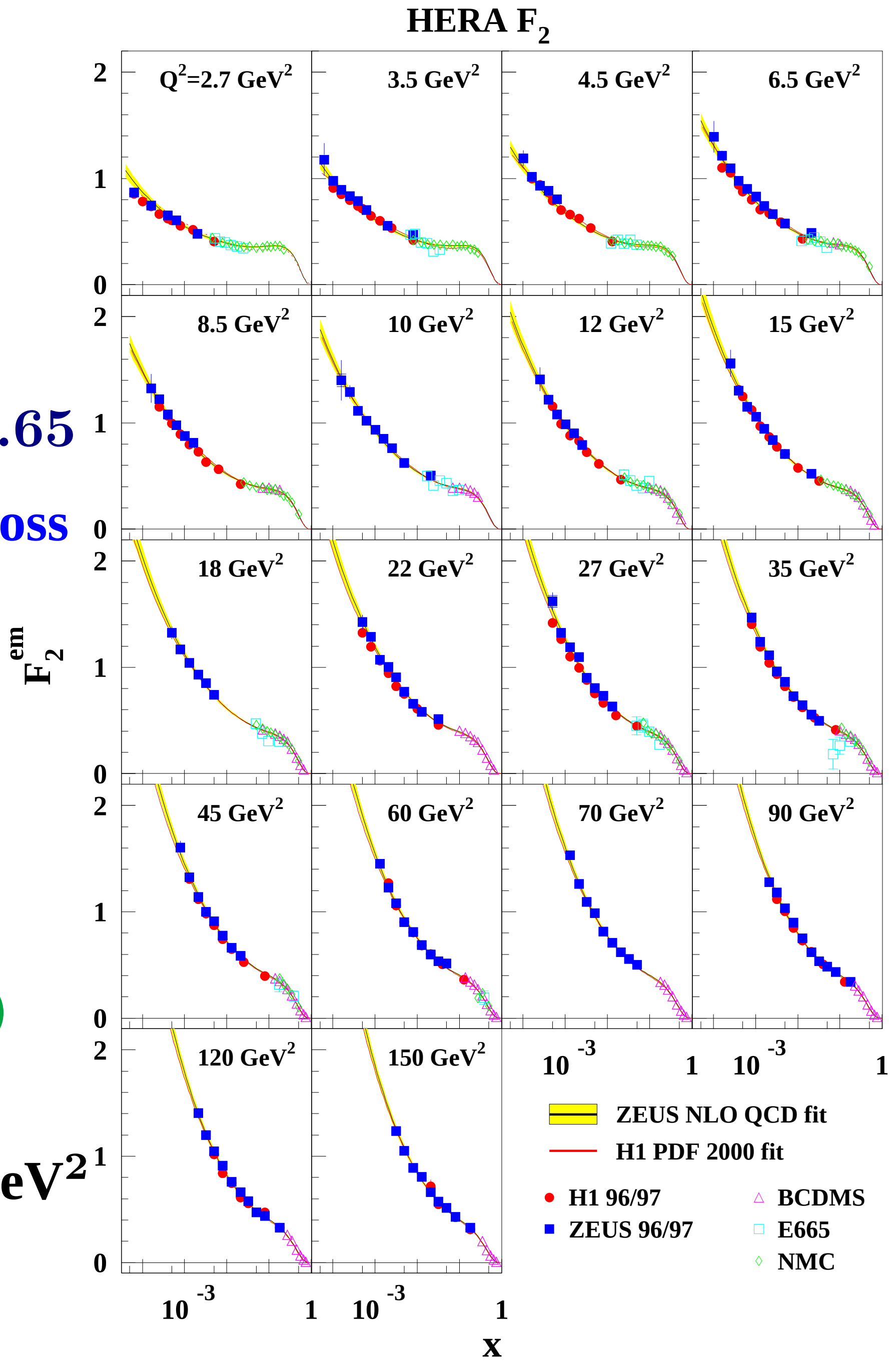

$F_2^{\rm em}(x,Q^2)$ provides...

$\rightarrow$ **direct information on quark densities**

$$F_2 \sim x \sum_i e_i^2 \cdot (q_i + \bar{q}_i)$$

$\rightarrow$ **indirect information on gluon density**

- **Large and positive scaling violations at low x**

dominance of BGF

$$\partial F_2 / \partial \ln Q^2 \sim \alpha_s \cdot xg$$

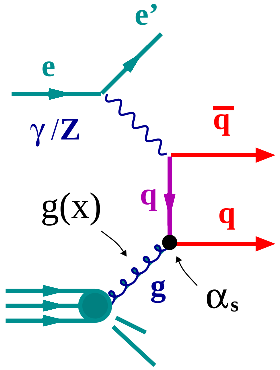

Boson−Gluon Fusion

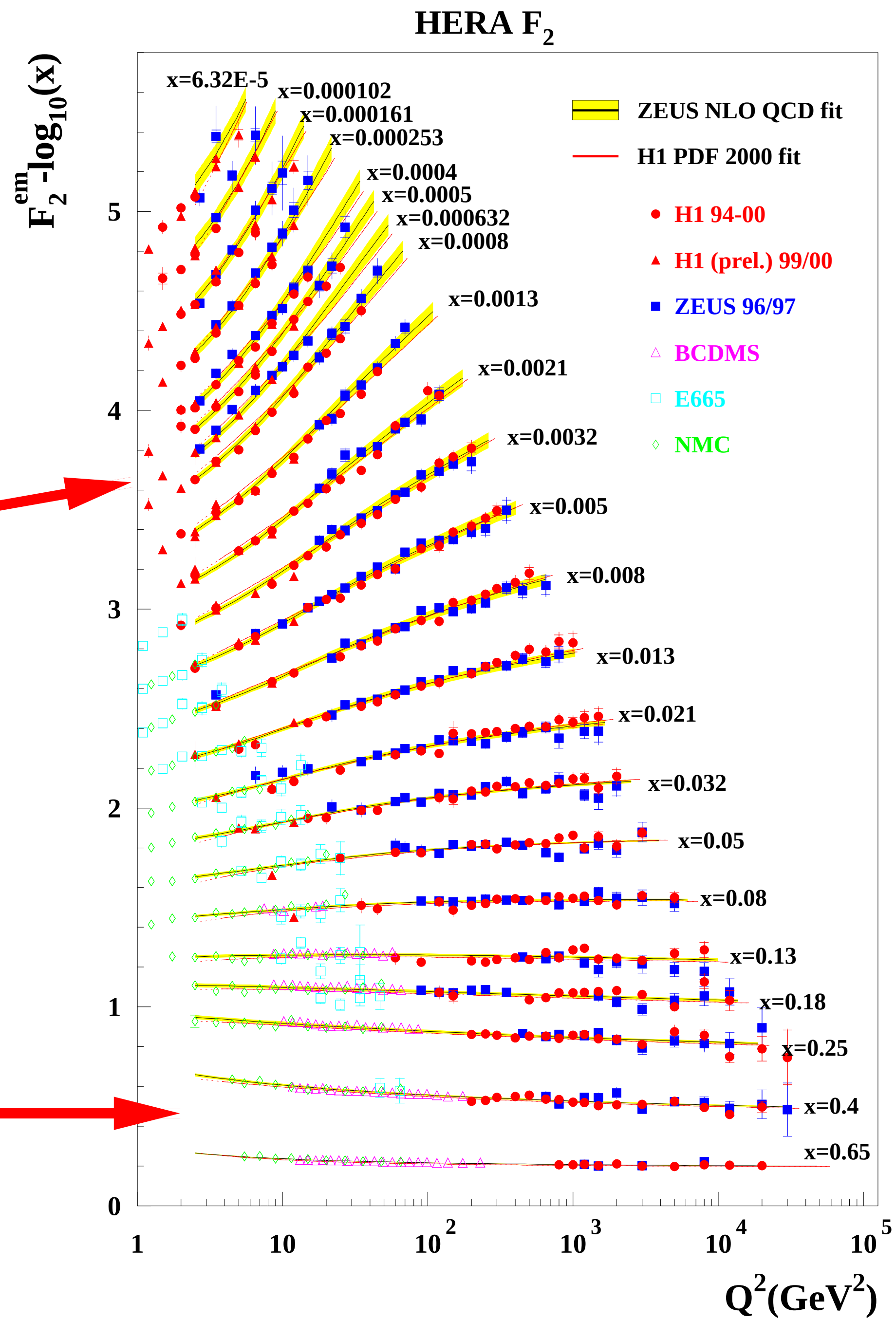

- **Aproximate scaling for $x \sim 0.1$**
- **Mild and negative scaling violations at high x**

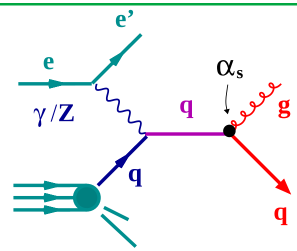

QCD Compton

Determination of the Parton Distribution Functions in the Proton

- In order to determine the proton PDFs additional experimental information is needed on
  - $\rightarrow$ quark densities at high x
  - $\rightarrow$ flavour composition of the sea
- Additional data sets
  - $\rightarrow$ F_2 data on μp scattering from BCDMS, NMC and E665 $\Rightarrow$ mid/high-x
  - $\rightarrow$ Deuterium-target data from NMC and E665 $\Rightarrow$ $\bar{u}$, $\bar{d}$
  - $\rightarrow$ NMC data on the ratio F_2^D/F_2^p $\Rightarrow$ high-x d/u
  - $\rightarrow$ xF_3 data from CCFR (ν-Fe interactions) $\Rightarrow$ high-x
- Global analysis using DGLAP evolution equations at next-to-leading order (NLO) in α_s

$$\frac{\partial q_i(x,\mu^2)}{\partial \ln \mu^2} = \frac{\alpha_s(\mu^2)}{2\pi} \int_x^1 \frac{dz}{z} \left(\sum_j P_{q_i q_j} \cdot q_j(x/z,\mu^2) + P_{q_i g} \cdot g(x/z,\mu^2) \right)$$

$$\frac{\partial g(x,\mu^2)}{\partial \ln \mu^2} = \frac{\alpha_s(\mu^2)}{2\pi} \int_x^1 \frac{dz}{z} \left(\sum_j P_{g q_j} \cdot q_j(x/z,\mu^2) + P_{gg} \cdot g(x/z,\mu^2) \right)$$

The DGLAP equations yield the proton PDFs at any value of Q^2 provided they are input as functions of x at some input scale Q_0^2

$\rightarrow$ number sum rules and the momentum sum rule are imposed

Determination of the Parton Distribution Functions in the Proton

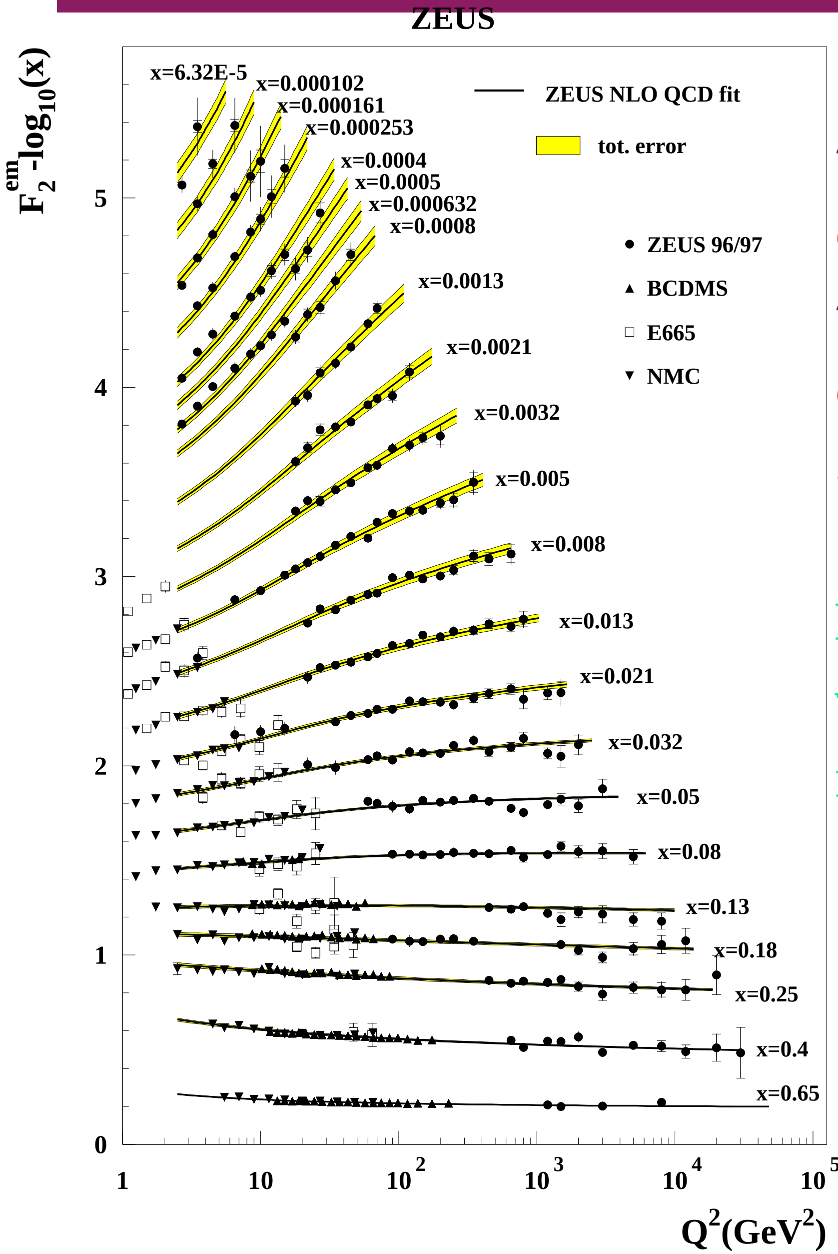

$u = u_V + u_{\rm sea}$

$d = d_V + d_{\rm sea}$

$\bar{u} = \bar{u}_{\rm sea}$

$\bar{d} = \bar{d}_{\rm sea}$

$s = s_{\rm sea} = \bar{s}_{\rm sea}$

S = total sea

Heavy quarks: variable-flavour-number scheme

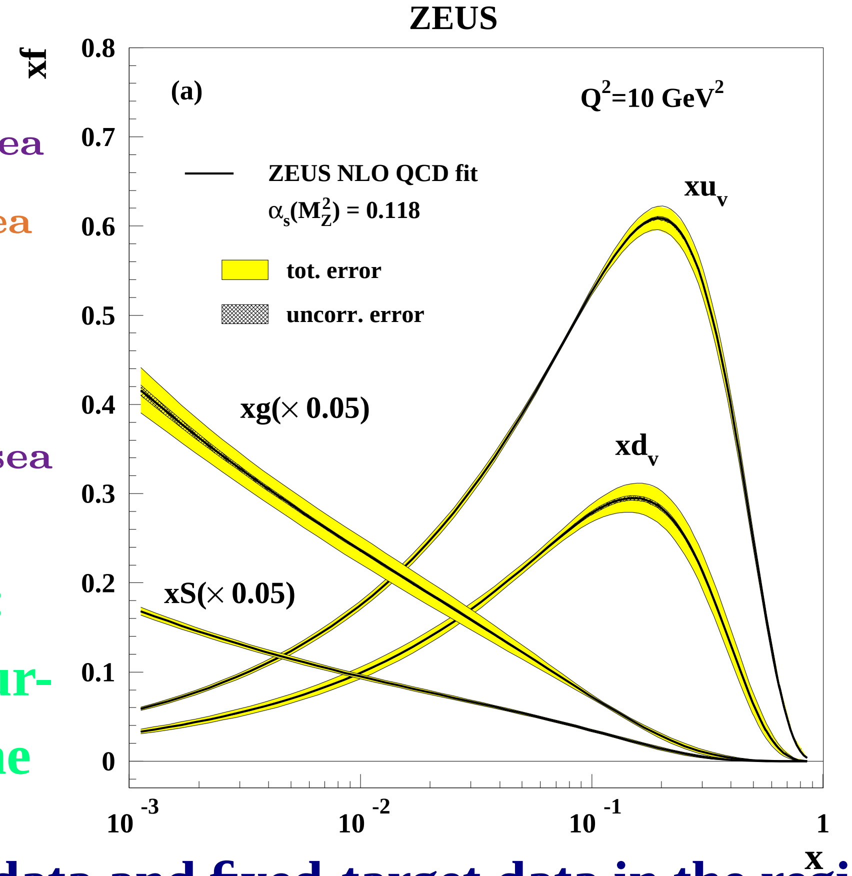

Fit of ZEUS data and fixed-target data in the region
$2.5 < Q^2 < 30000$ GeV^2, $6.3 \cdot 10^{-5} < x < 0.65$
and $W^2 > 20$ GeV^2 (1263 data points)

Full account of correlated exp. uncertainties

$\rightarrow$ **Good description of Struct. Func. data**

$\Rightarrow$ **Determination of proton PDFs**

Determination of the Sea Distribution

- The total sea distribution $xS(x,Q^2)$ as a function of x for different Q^2 values $\Rightarrow$
- Its uncertainty is below $\sim 5\%$ for $Q^2 > 2.5$ GeV^2 and $10^{-4} < x < 0.1$

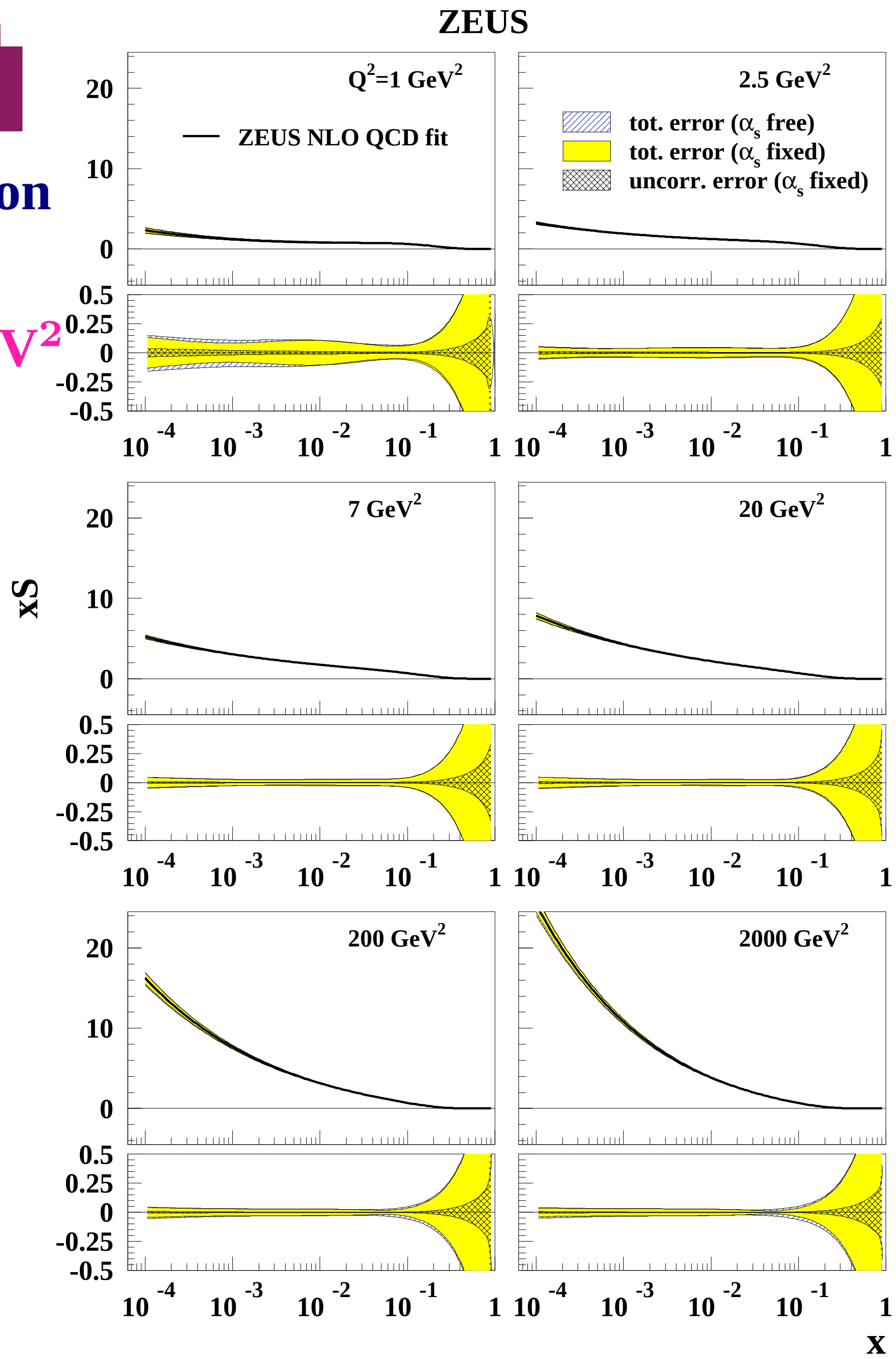

Determination of the Gluon Distribution

- The gluon distribution $xg(x, Q^2)$ as a function of x for different Q^2 values $\Rightarrow$
- Its uncertainty is $\sim$ 10% for $Q^2 \sim$ 20 GeV^2 and $10^{-4} < x < 0.1$
  $\rightarrow$ the uncertainty decreases as Q^2 increases

Determination of α_s

- Inclusion of low-x data allows a simultaneous (and precise) determination of PDFs and α_s:
  $\alpha_s(M_Z) = 0.1166 \pm 0.0008(\text{uncorr})$
  $\pm 0.0032(\text{corr}) \pm 0.0036(\text{norm})$
  $\pm 0.0018(\text{model}) \Rightarrow 0.1166 \pm 0.0052$

(+theor. unc. due to terms beyond NLO $\sim \pm 0.004$)

- Consistent with world average (Bethke, 2011):
  $\rightarrow \alpha_s(M_Z) = 0.1184 \pm 0.0007$

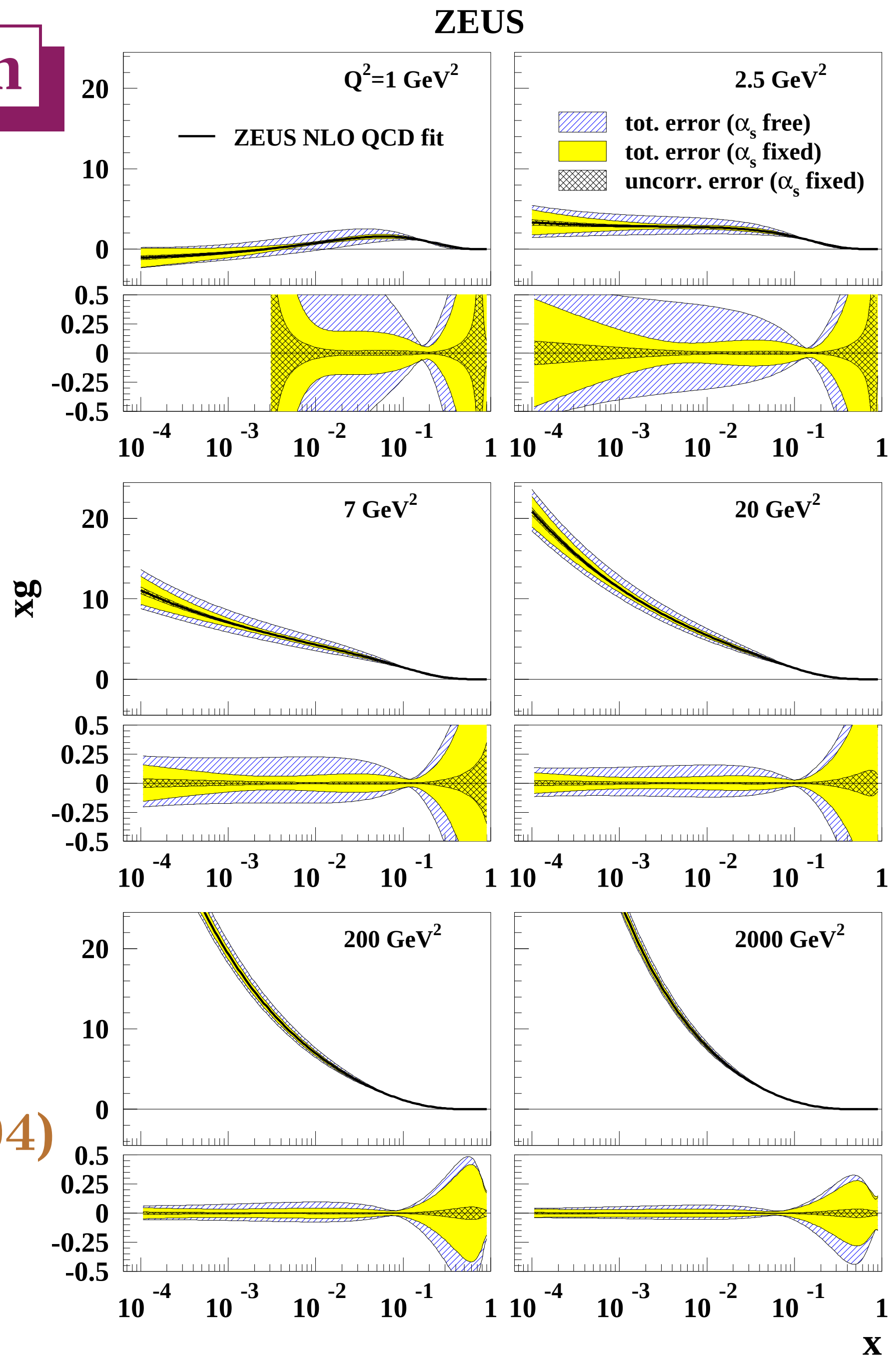

Universality (and usefulness) of Proton PDFs

$$\sigma_{pp\to H(W,Z,\dots)+X} = \sum_{a,b} \int_0^1 dx_1\, f_{a/p}(x_1,\mu_F^2) \int_0^1 dx_2\, f_{b/p}(x_2,\mu_F^2)\;\hat{\sigma}_{ab\to H(W,Z,\dots)}$$

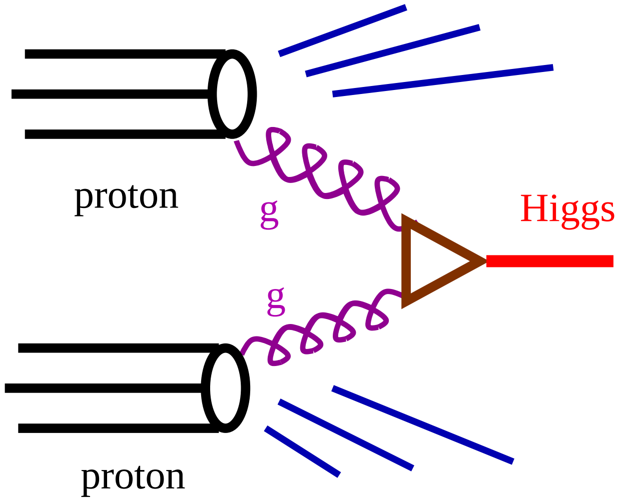

σ_H sensitive to gluon distribution at $x \sim \frac{M_H}{\sqrt{s}} \sim 8\cdot 10^{-3}$ **and** $\mu_F^2 \sim M_H^2 \sim$ ~ 13000 **GeV^2;** $\Delta\sigma_H^{PDF}/\sigma_H \sim \pm 3\%$ **(for $M_H = 115$ GeV)**

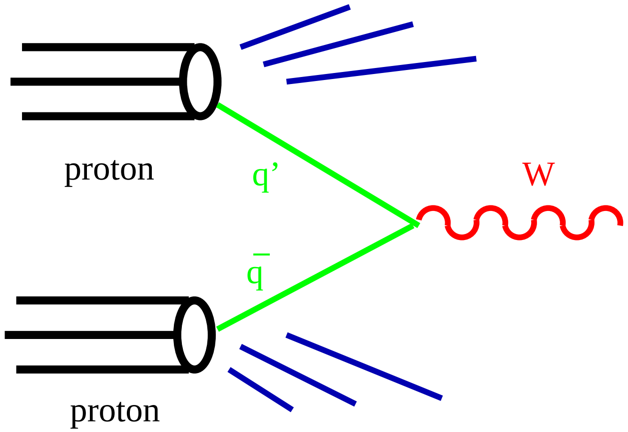

σ_W sensitive to sea distribution at $x \sim \frac{M_W}{\sqrt{s}} \sim 6\cdot 10^{-3}$

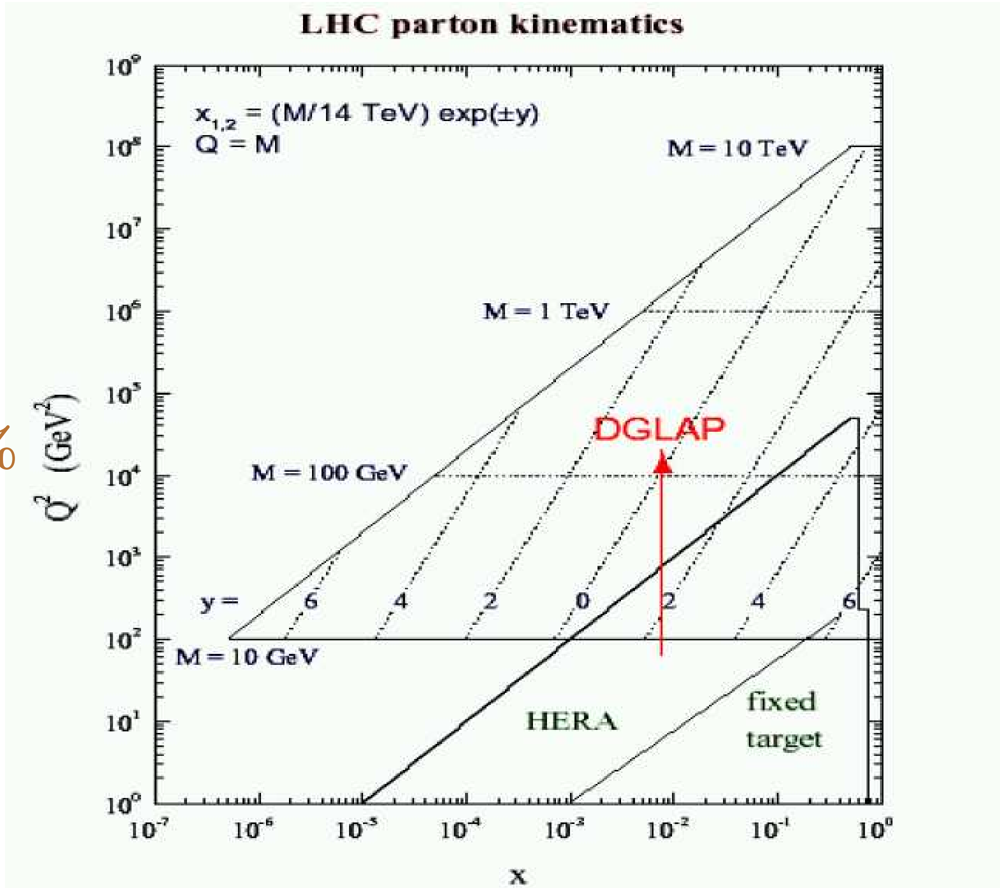

and $\mu_F^2 \sim M_W^2 \sim 6400$ **GeV^2;** $\Delta\sigma_W^{PDF}/\sigma_W \sim \pm 3\%$

Structure Functions (II)

Charged Current Deep Inelastic Scattering

- **Charged Current DIS event candidate**

  $Q^2 \sim 1200$ GeV^2 and $x_{Bj} \sim 0.06$

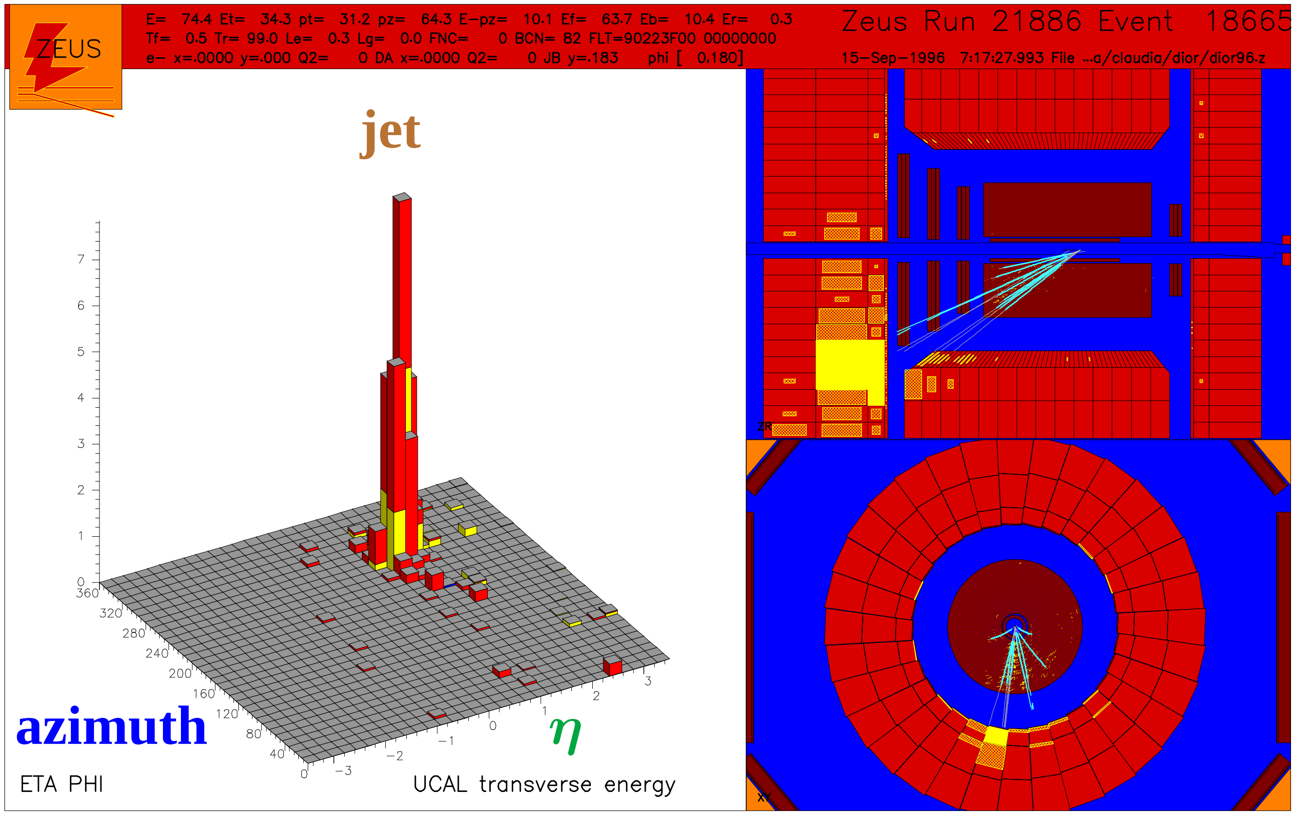

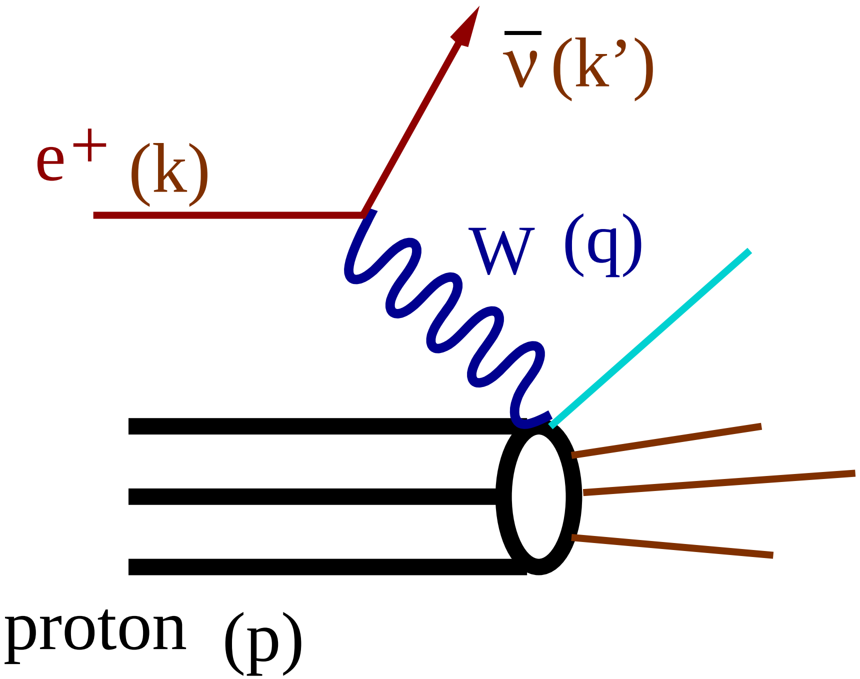

Charged Current Deep Inelastic Scattering

- **Measurements of the differential cross section** $d\sigma/dQ^2$ **in Charged Current DIS $e^{\pm}p$**

$$ep \rightarrow \nu + X$$

- **Cross-section formulae in LO QCD**

$$\frac{d\sigma(e^+p)}{dxdQ^2} = \frac{G_F^2}{2\pi}\eta_W^2 \cdot \sum_i(\bar{u}_i + (1-y)^2 d_i)$$

$$\frac{d\sigma(e^-p)}{dxdQ^2} = \frac{G_F^2}{2\pi}\eta_W^2 \cdot \sum_i(u_i + (1-y)^2 \bar{d}_i)$$

where $\eta_W = M_W^2/(Q^2 + M_W^2)$

$\Rightarrow$ **W-Propagator effects**

$\Rightarrow$ **flavour selection:**

d (u)-quark contributes only to e^+p (e^-p)

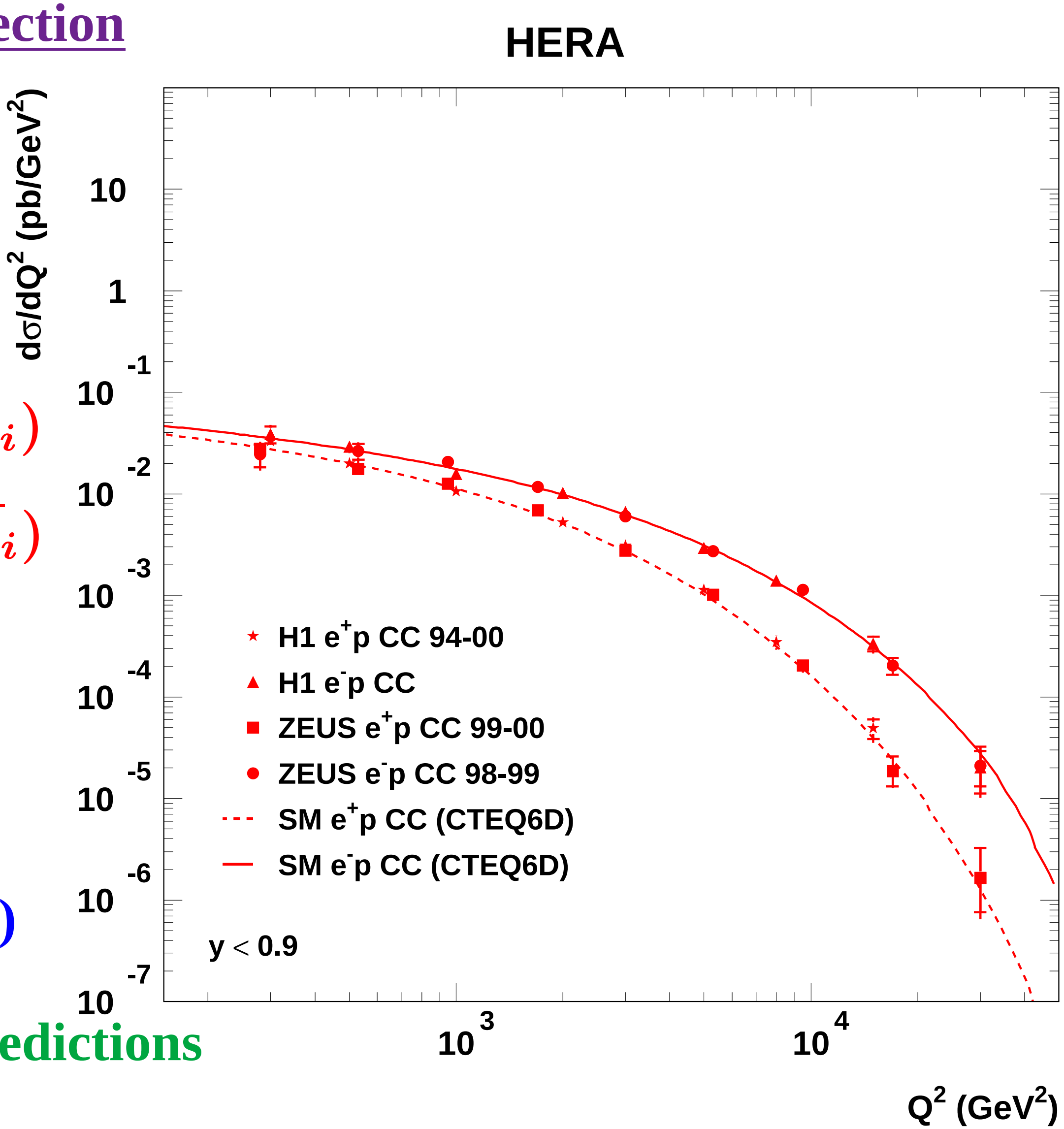

- **Good description by Standard Model Predictions up to the highest $Q^2 \sim 30000$ GeV^2**

Neutral Current Deep Inelastic Scattering

- **Measurements of the differential cross section $d\sigma/dQ^2$ in Neutral Current DIS $e^{\pm}p$**

$$ep \to e + X$$

- **Cross-section formulae in LO QCD**

$$\frac{d\sigma(e^{\pm}p)}{dxdQ^2} = \frac{2\pi\alpha^2}{xQ^4} \cdot (Y_+ \cdot F_2(x,Q^2) -$$

$$-y^2 \cdot F_L(x,Q^2) \mp Y_- \cdot xF_3(x,Q^2))$$

$$F_2 = F_2^{\mathrm{em}} + F_2^{\mathrm{int}} \cdot \eta_{\gamma Z} + F_2^{wk} \cdot \eta_{\gamma Z}^2$$

where $\eta_{\gamma Z} = Q^2/(Q^2 + M_Z^2)$

$\Rightarrow$ Z-Propagator effects

$\Rightarrow$ Parity-violating term (F_3) changes sign

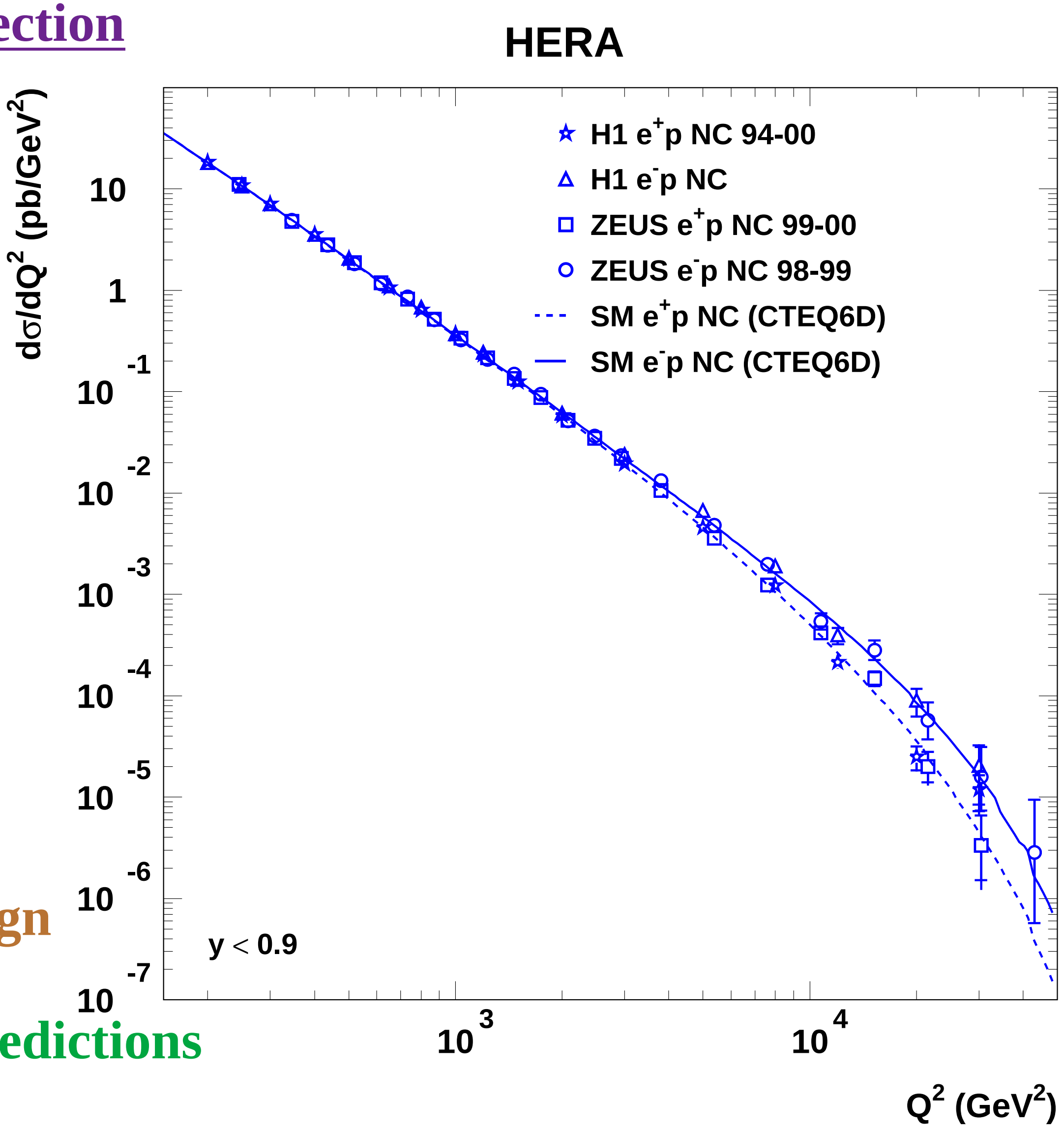

- **Good description by Standard Model Predictions up to the highest $Q^2 \sim 40000$ GeV^2**

Neutral vs Charged Current Deep Inelastic Scattering

- **Measurements of the differential cross section**

  $d\sigma/dQ^2$ in Neutral Current DIS $e^\pm p$

$$\frac{d\sigma(e^\pm p)}{dxdQ^2} = \frac{2\pi\alpha^2}{xQ^4} \cdot (Y_+ \cdot F_2(x,Q^2) - $$
$$-y^2 \cdot F_L(x,Q^2) \mp Y_- \cdot xF_3(x,Q^2))$$

$$F_2 = F_2^{\rm em} + F_2^{\rm int} \cdot \eta_{\gamma Z} + F_2^{wk} \cdot \eta_{\gamma Z}^2$$

where $\eta_{\gamma Z} = Q^2/(Q^2 + M_Z^2)$

and Charged Current DIS $e^\pm p$

$$\frac{d\sigma(e^+ p)}{dxdQ^2} = \frac{G_F^2}{2\pi}\eta_W^2 \cdot \sum_i (\bar{u}_i + (1-y)^2 d_i)$$

$$\frac{d\sigma(e^- p)}{dxdQ^2} = \frac{G_F^2}{2\pi}\eta_W^2 \cdot \sum_i (u_i + (1-y)^2 \bar{d}_i)$$

where $\eta_W = M_W^2/(Q^2 + M_W^2)$

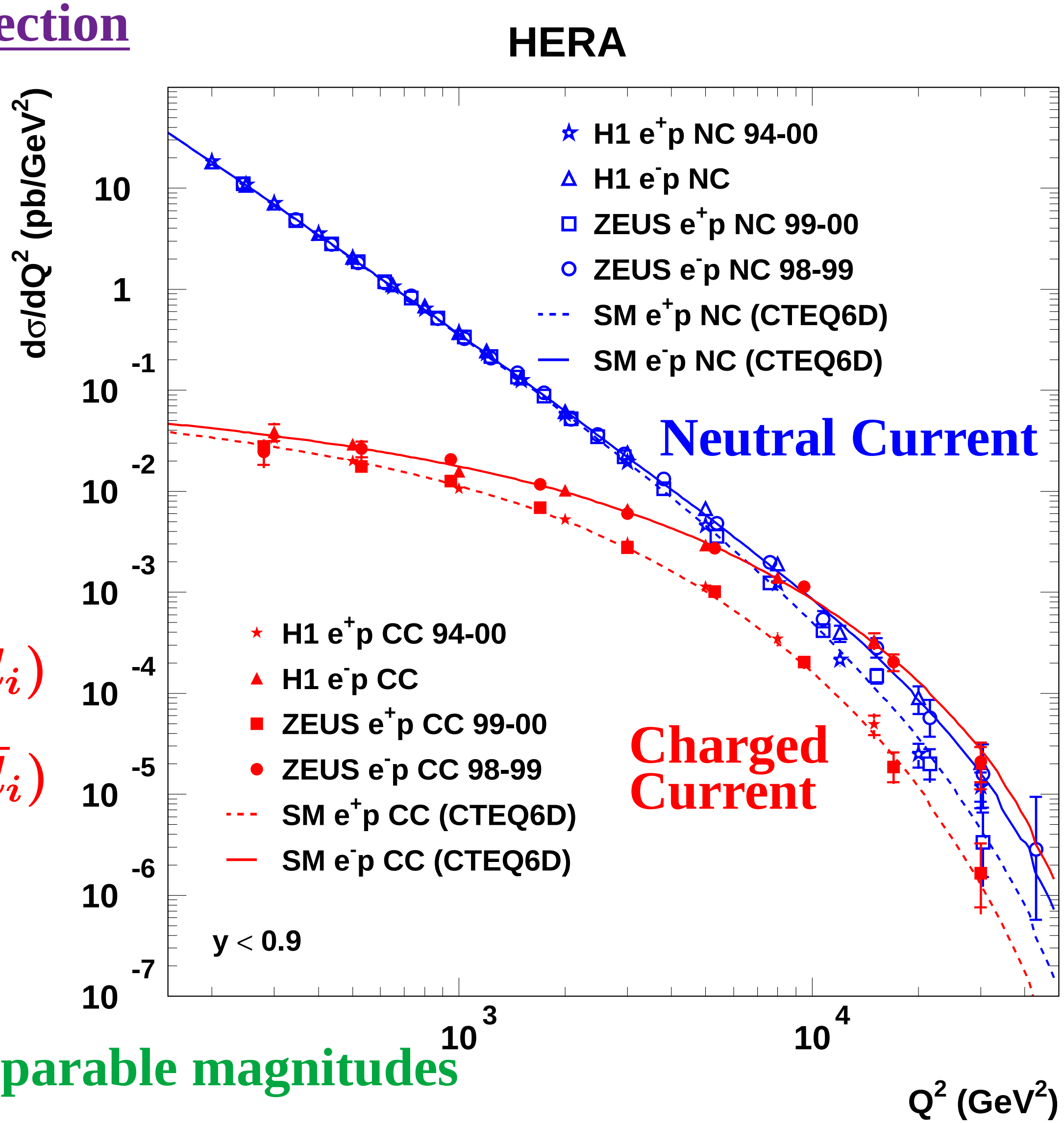

- **NC and CC DIS cross sections have comparable magnitudes at $Q^2 \sim M_W^2 \sim M_Z^2 \sim 10^4$ GeV² $\Rightarrow$ Direct observation of electroweak unification**

Charged Current Deep Inelastic e^+p Scattering

- **Measurement of the reduced cross section in CC DIS:**

$$\tilde{\sigma}(e^+p) = (G_F^2\eta_W^2/2\pi x)^{-1} d\sigma_{\mathrm{Born}}/dxdQ^2$$

$\rightarrow$ **Sensitivity to flavour composition**

$$\tilde{\sigma}(e^+p) = x(\bar{u} + \bar{c} + (1-y)^2(d+s))$$

$\rightarrow$ **Sensitivity to valence quarks**

$$\tilde{\sigma}(e^+p) \rightarrow x(1-y)^2 d_V \text{ (high-}x\text{)}$$

- **Good description by SM predictions based on CTEQ6 parametrizations of PDFs**

$\rightarrow$ **valence quarks and flavour composition determined from fixed-target data**

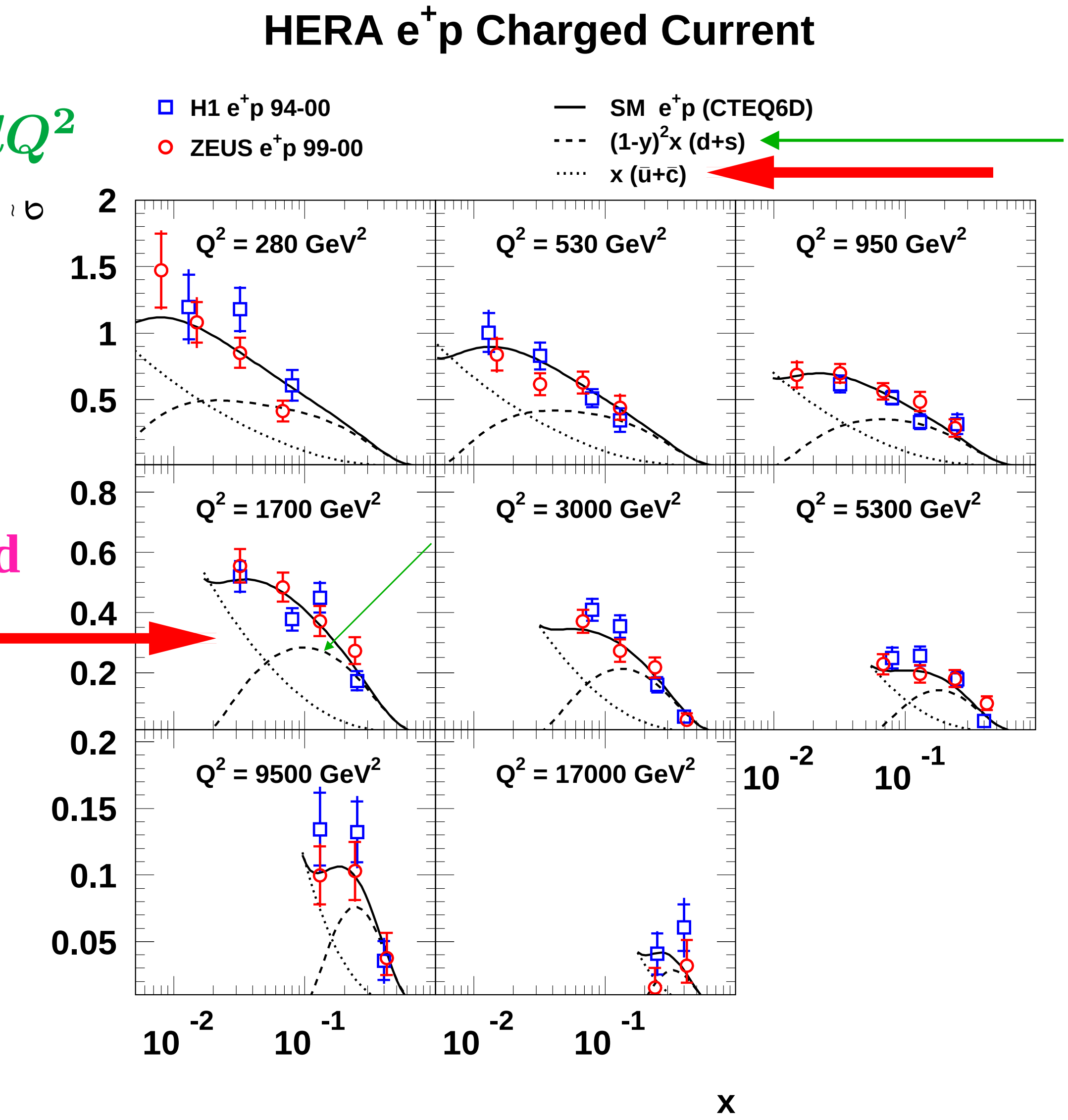

Charged Current Deep Inelastic $e^{-}p$ Scattering

- **Measurement of the reduced cross section in CC DIS:**

$$\tilde{\sigma}(e^{-}p) = (G_F^2 \eta_W^2 / 2\pi x)^{-1} d\sigma_{\rm Born}/dx dQ^2$$

$\rightarrow$ **Sensitivity to flavour composition**

$$\tilde{\sigma}(e^{-}p) = x(u + c + (1-y)^2(\bar{d} + \bar{s}))$$

$\rightarrow$ **Sensitivity to valence quarks**

$$\tilde{\sigma}(e^{-}p) \rightarrow x u_V \ \textbf{(high-}x\textbf{)}$$

- **Good description by SM predictions based on CTEQ6 parametrizations of PDFs**

$\rightarrow$ **valence quarks and flavour composition determined from fixed-target data**

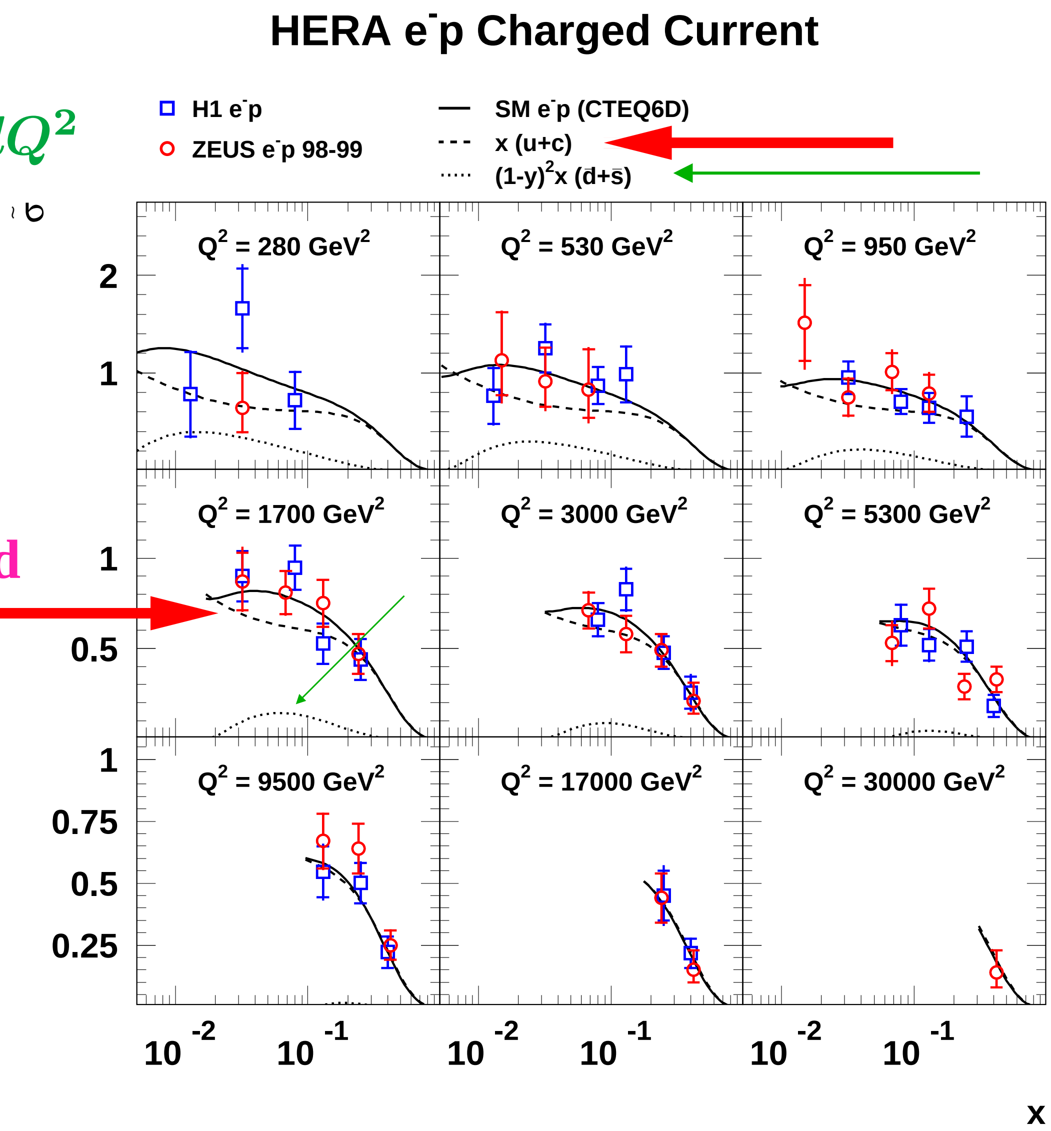

Determination of the Proton PDFs with ZEUS data alone

ZEUS NC DIS low Q^2

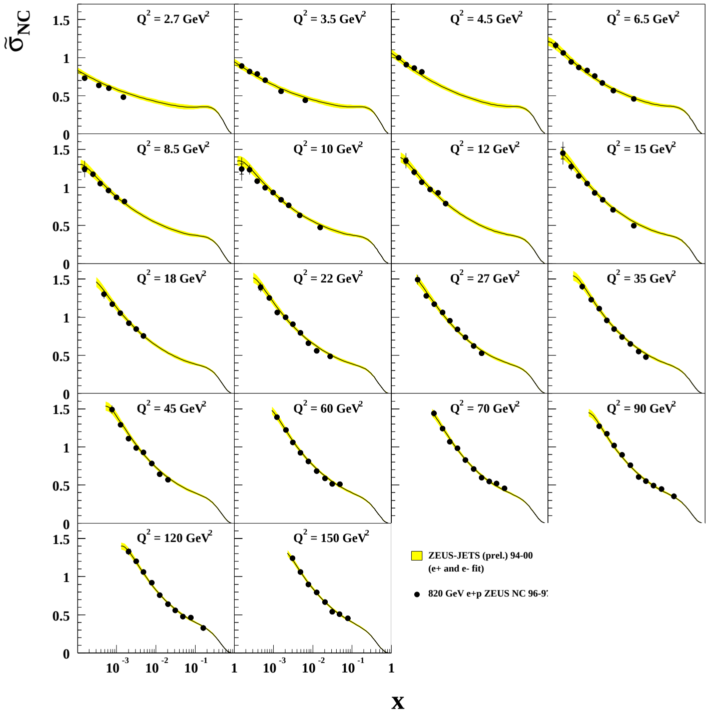

ZEUS NC DIS high Q^2

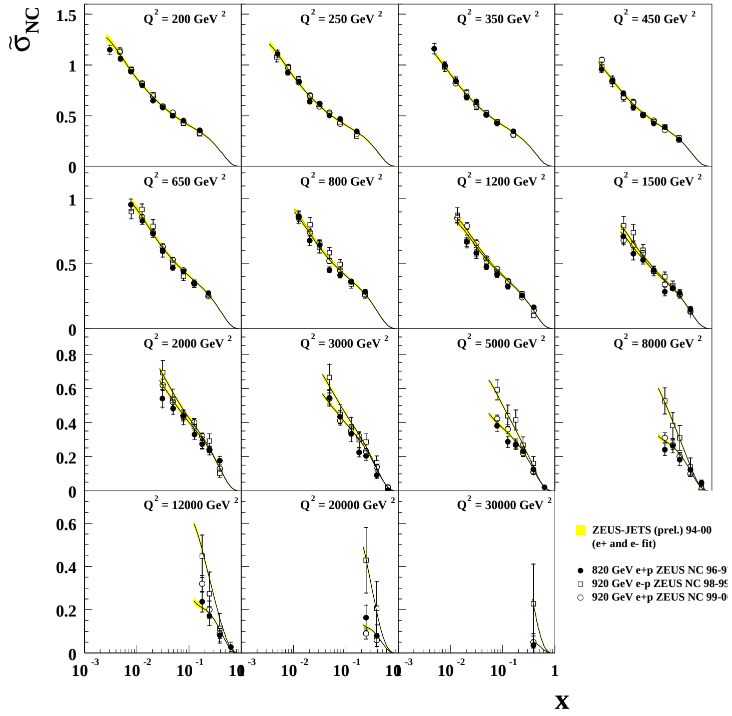

CC DIS high Q^2

ZEUS

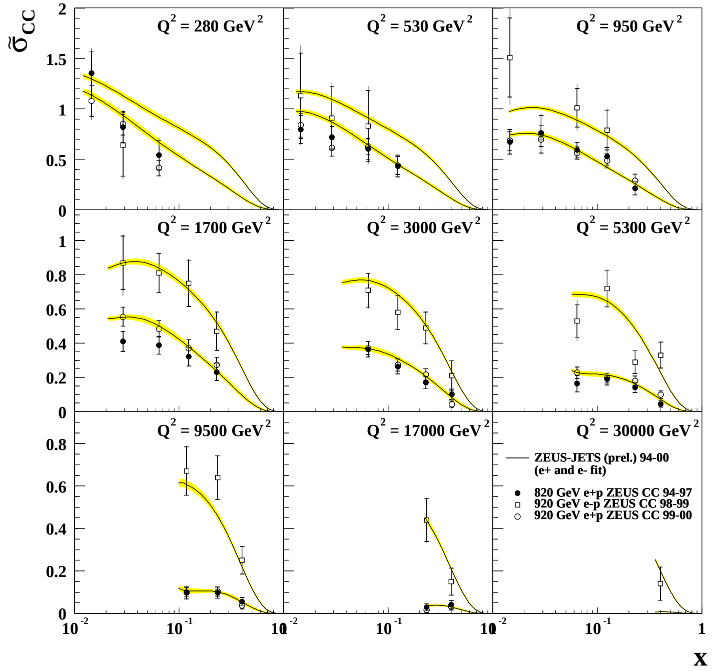

- Fit of ZEUS-only data: NC DIS $e^{\pm}p$ and CC DIS $e^{\pm}p$ in the region $2.5 < Q^2 < 30000$ GeV^2, $6.3 \cdot 10^{-5} < x < 0.65$ and $W^2 > 20$ GeV^2 using DGLAP evolution equations at NLO: $\rightarrow xu_V, xd_V, xS, xg$

  (no HERA information on flavour composition of the sea: flavour-averaged sea)

$\Rightarrow$ Good description of Structure Function data (577 data points)

Determination of the Proton PDFs with ZEUS data alone

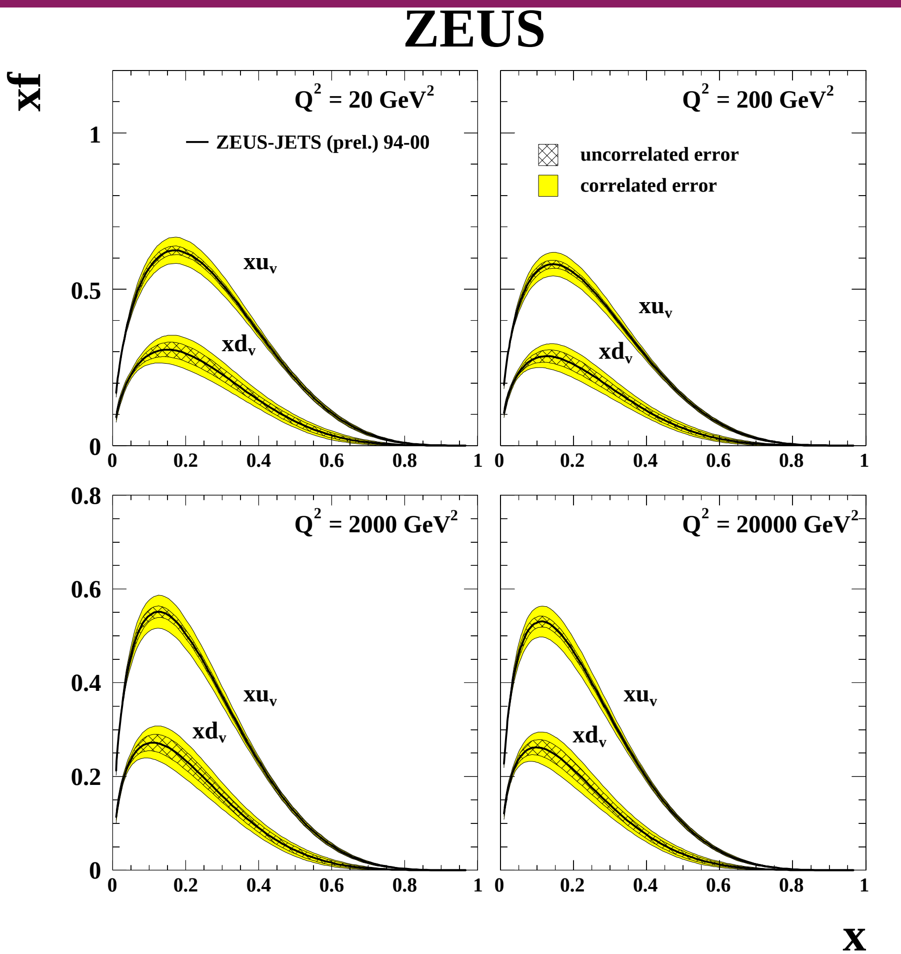

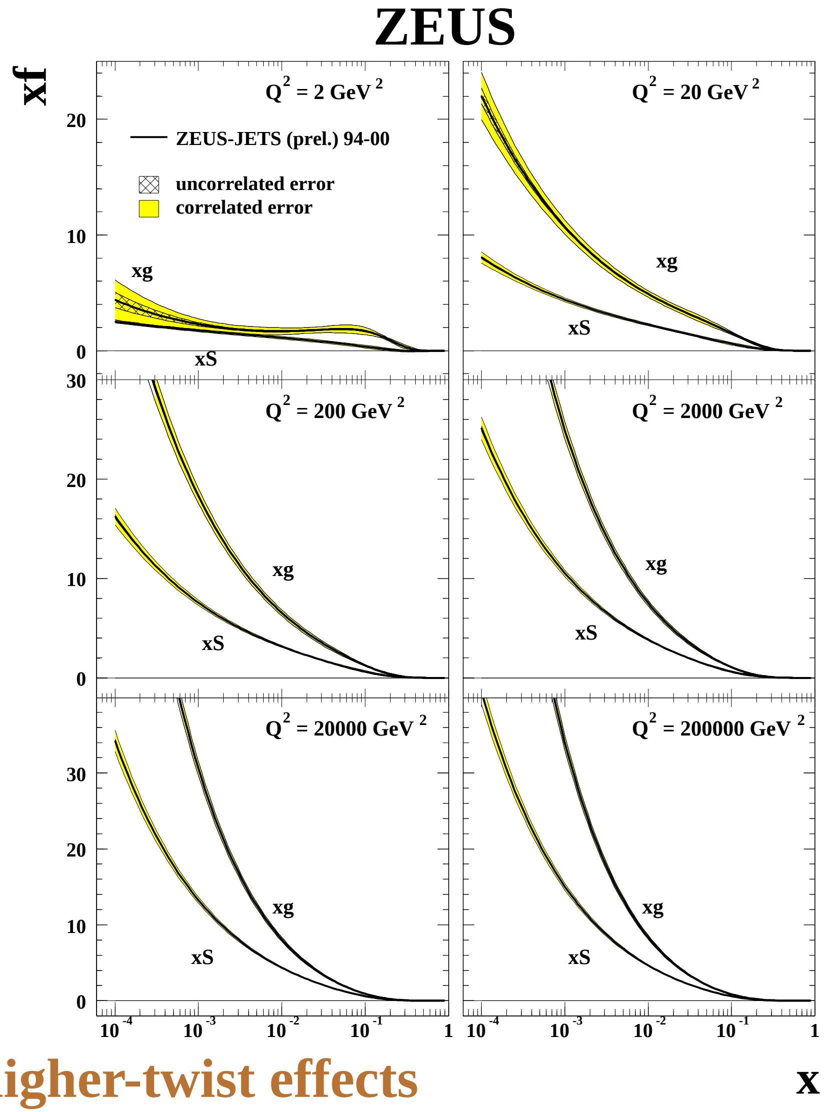

- xu_V, xd_V: precision competitive with global fits

$\longrightarrow$ free from uncert. due to nuclear corrections and higher-twist effects

- xS, xg: as precise as in global fits (HERA data are crucial)

Jets in NC DIS

Jet Production in Neutral Current Deep Inelastic Scattering

- Jet production in neutral current deep inelastic scattering up to $\mathcal{O}(\alpha_s)$:

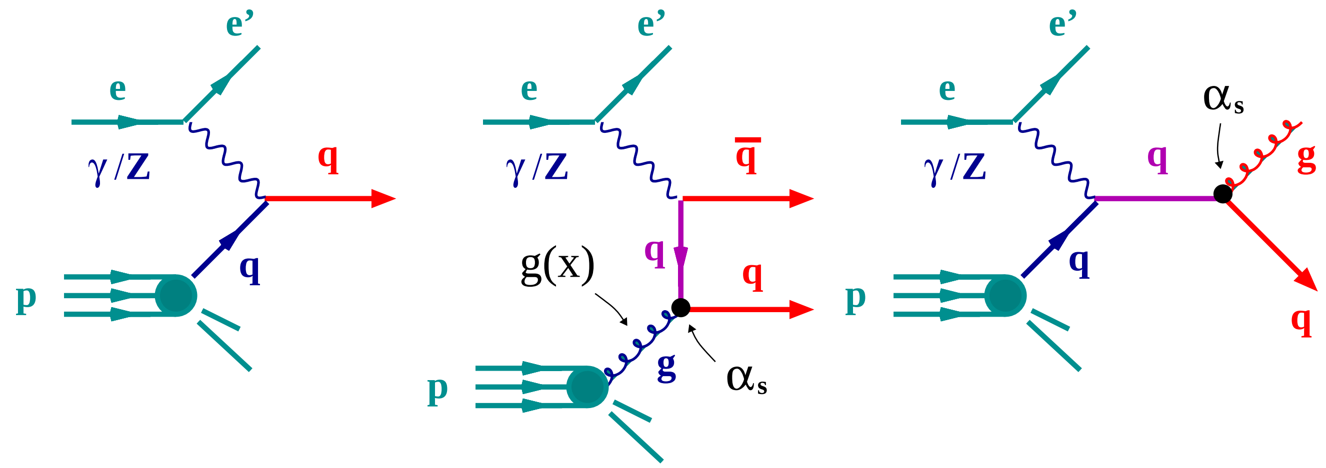

Quark-Parton Model Boson-Gluon Fusion QCD Compton

- Perturbative QCD calculations of jet cross sections:

$$\sigma_{jet} = \sum_{a=q,\bar{q},g} \int dx\, f_a(x,\mu_F^2)\, \hat{\sigma}_a(x,\alpha_s(\mu_R),\mu_R^2,\mu_F^2)$$

– f_a: parton a density in the proton, determined from experiment; long-distance structure of the target

– $\hat{\sigma}_a$: subprocess cross section, calculable in pQCD; short-distance structure of the interaction

Jet Production in Neutral Current Deep Inelastic Scattering

- In the region where the wealth of data from fixed-target and collider experiments has allowed an accurate determination of the proton PDFs, measurements of jet production in NC DIS provide
  - $\rightarrow$ a sensitive test of the pQCD predictions of the short-distance structure
  - $\rightarrow$ a determination of the strong coupling constant α_s
- To perform a stringent test of the pQCD predictions and a precise determination of α_s:
  - $*$ Observables for which the predictions are directly proportional to α_s
    - $\rightarrow$ Jet cross sections in the Breit frame
  - $*$ Small experimental uncertainties $\rightarrow$ Jets with relatively high transverse energy
  - $*$ Small theoretical uncertainties $\rightarrow$ NLO QCD calculations
  - $\rightarrow$ Jet algorithm: longitudinally invariant k_T cluster algorithm (Catani et al) (small parton-to-hadron effects, infrared safe, suppression of beam-remnant jet)
  - $\rightarrow$ Jet selection criteria

High-E_T Jet Production in the Breit Frame

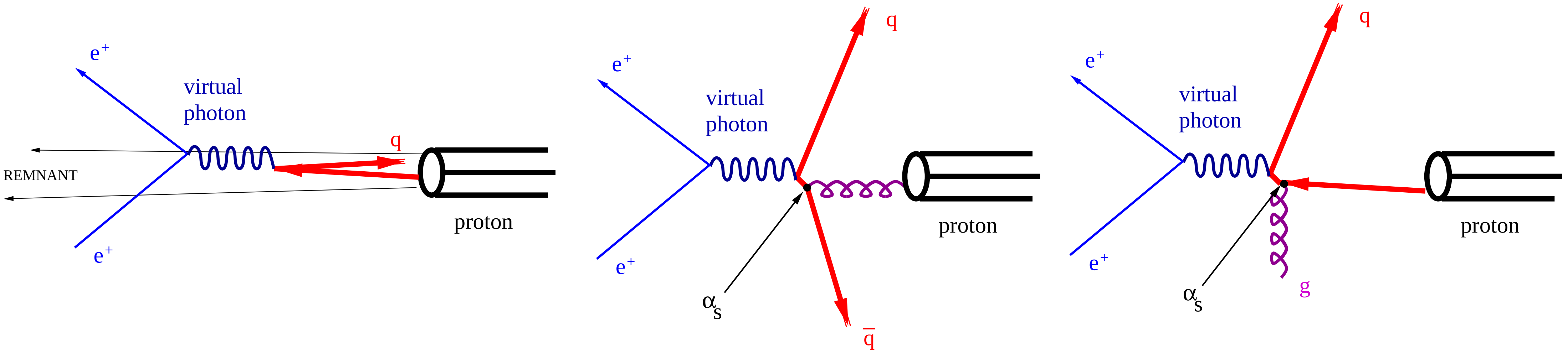

- In the Breit frame the virtual boson collides head-on with the proton
- High-E_T jet production in the Breit frame

  $\rightarrow$ suppression of the Born contribution (struck quark has zero E_T)

  $\rightarrow$ suppression of the beam-remnant jet (zero E_T)

  $\rightarrow$ lowest-order non-trivial contributions from $\gamma^* g \rightarrow q\bar{q}$ and $\gamma^* q \rightarrow qg$

  $\Rightarrow$ directly sensitive to hard QCD processes (α_s)

Variables for Jet Search in e^+e^- annihilations

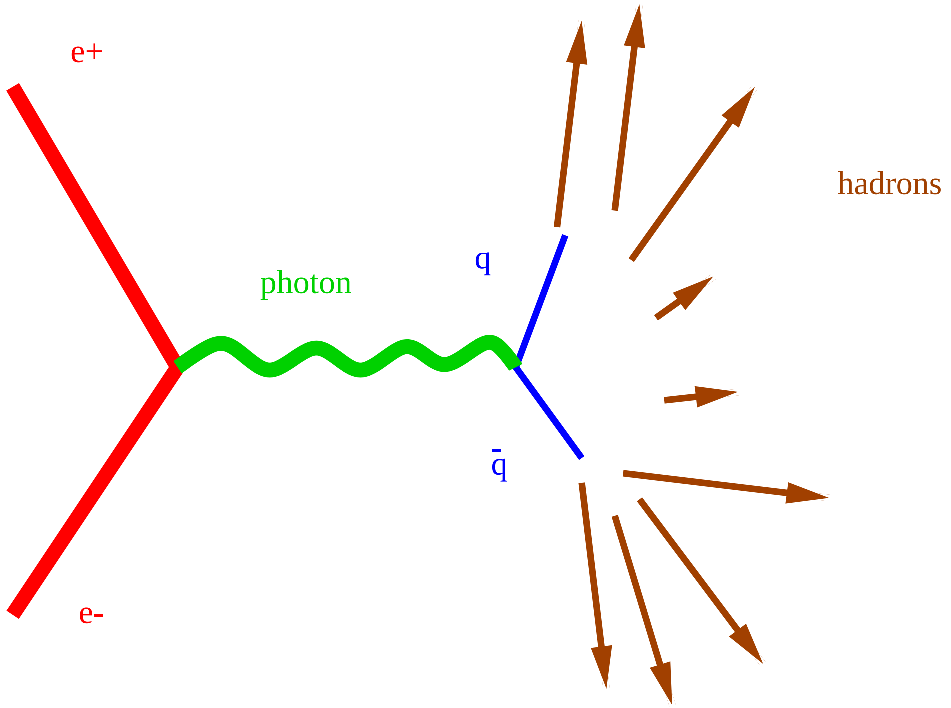

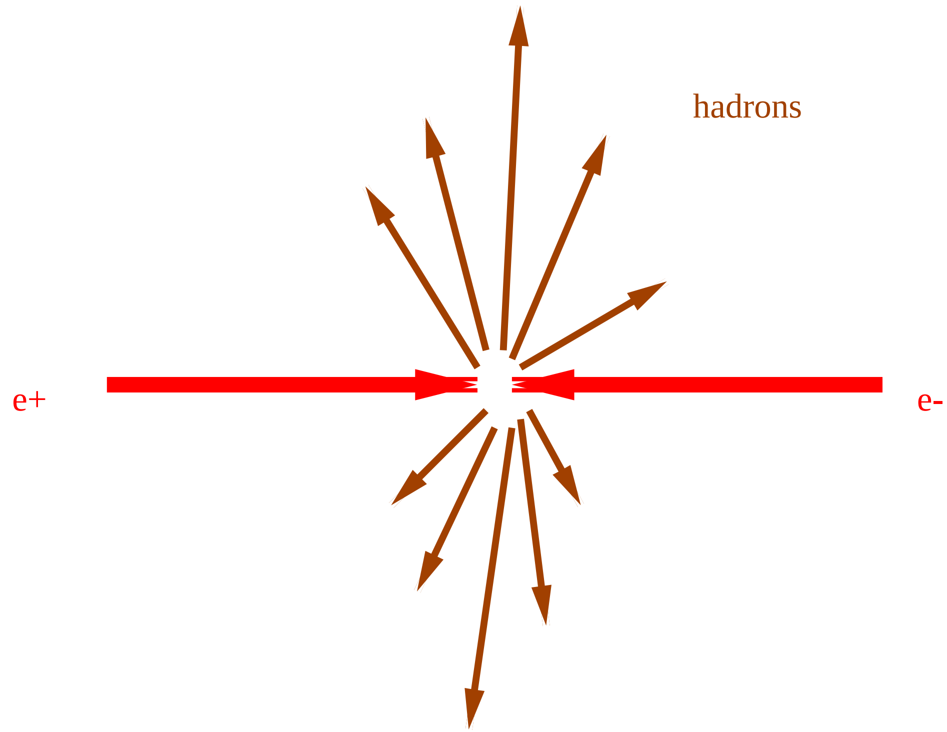

- e^+e^- **annihilations in the centre-of-mass system**
- **Invariance under rotations** $\Rightarrow$ **Energies and angles**

$\Rightarrow$ Input to the jet algorithm: $\boldsymbol{E_i}$, $\boldsymbol{\theta_i}$ and $\boldsymbol{\phi_i}$ for every hadron $\boldsymbol{i}$

$\Rightarrow$ "distance" between hadrons $\boldsymbol{i}$ and $\boldsymbol{j}$: their angular separation $\boldsymbol{\theta_{ij}}$

Variables for Jet Search in $p\bar{p}$ collisions

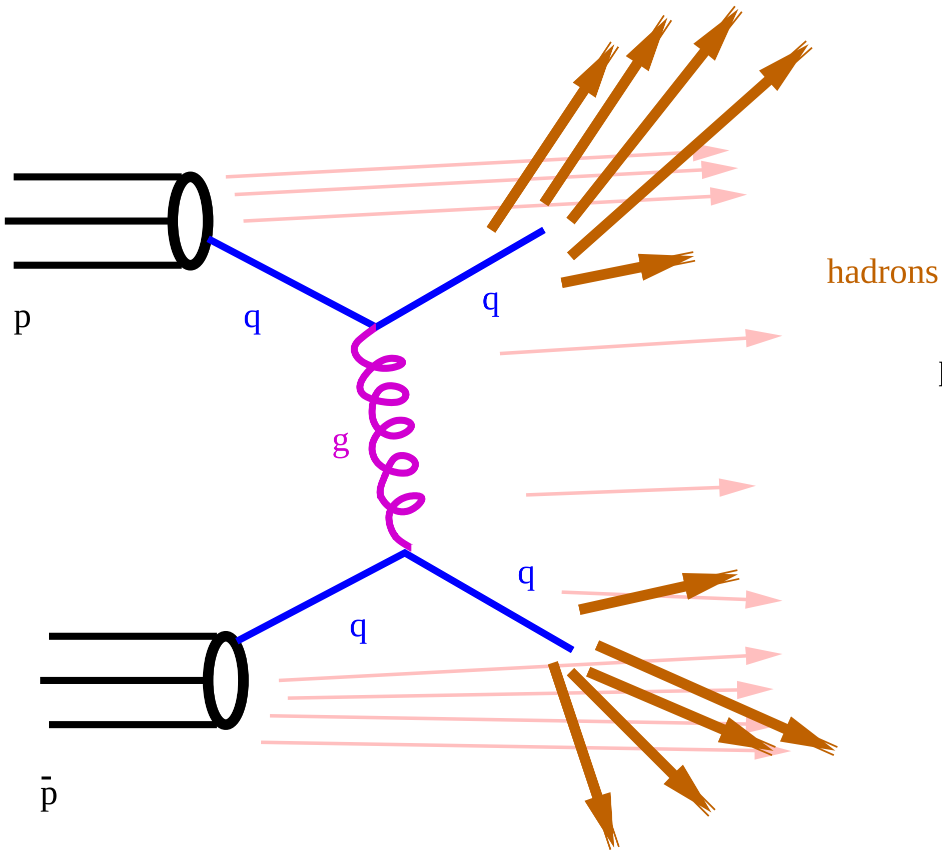

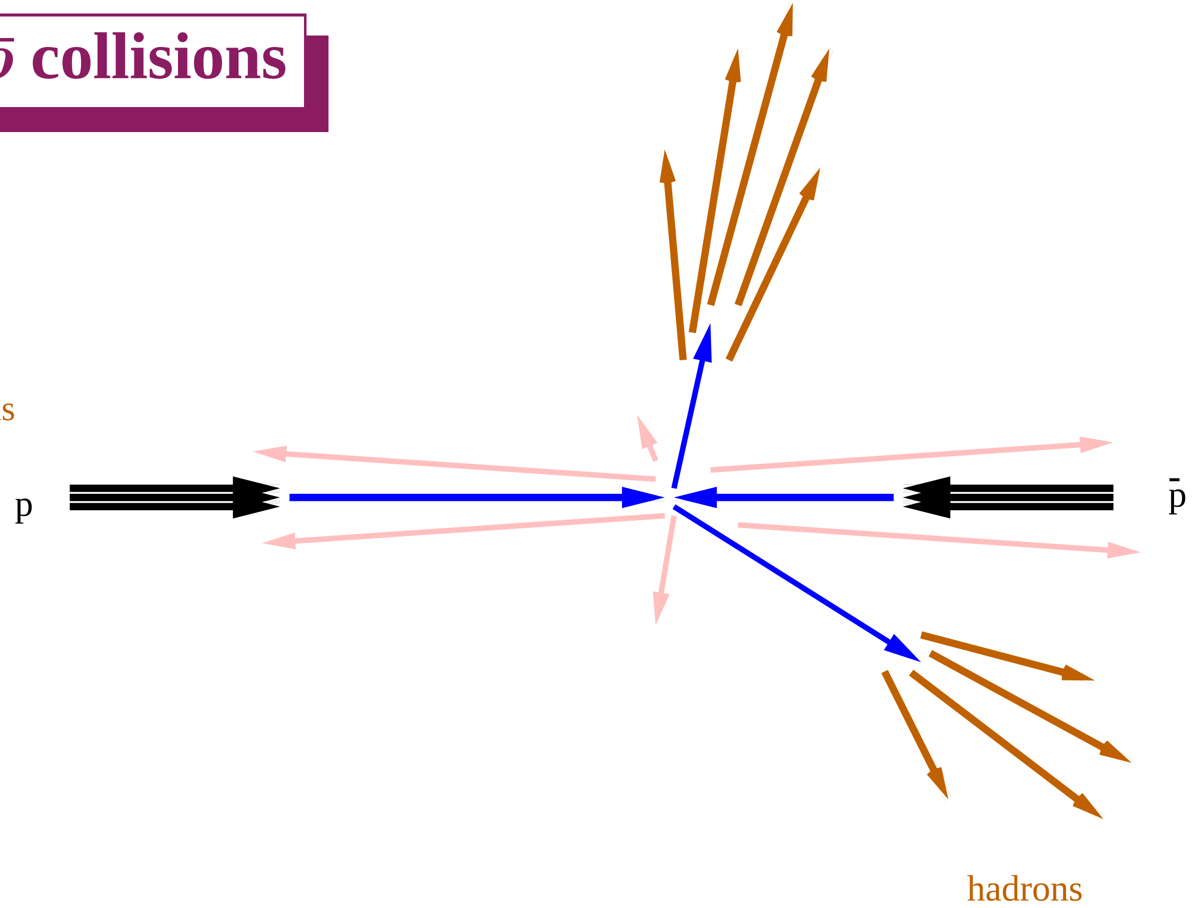

- $p\bar{p}$ collisions in the centre-of-mass system
- However the initial-state parton-parton system is NOT at rest!

depending upon the momentum fractions, x_p and $x_{\bar{p}}$, wrt the parent hadrons

$\Rightarrow$ the final-state partonic system is BOOSTED along the beam axis

Variables for Jet Search in $p\bar{p}$ collisions (II)

- **Angular separations are NOT invariant under boosts!**

⇒ a given set of hadrons will be appear more collimated depending upon the boost

- **To treat on equal footing all possible final-state hadronic systems**

invariance under longitudinal boosts ⇒ transverse energy, pseudorapidity* and azimuthal angle

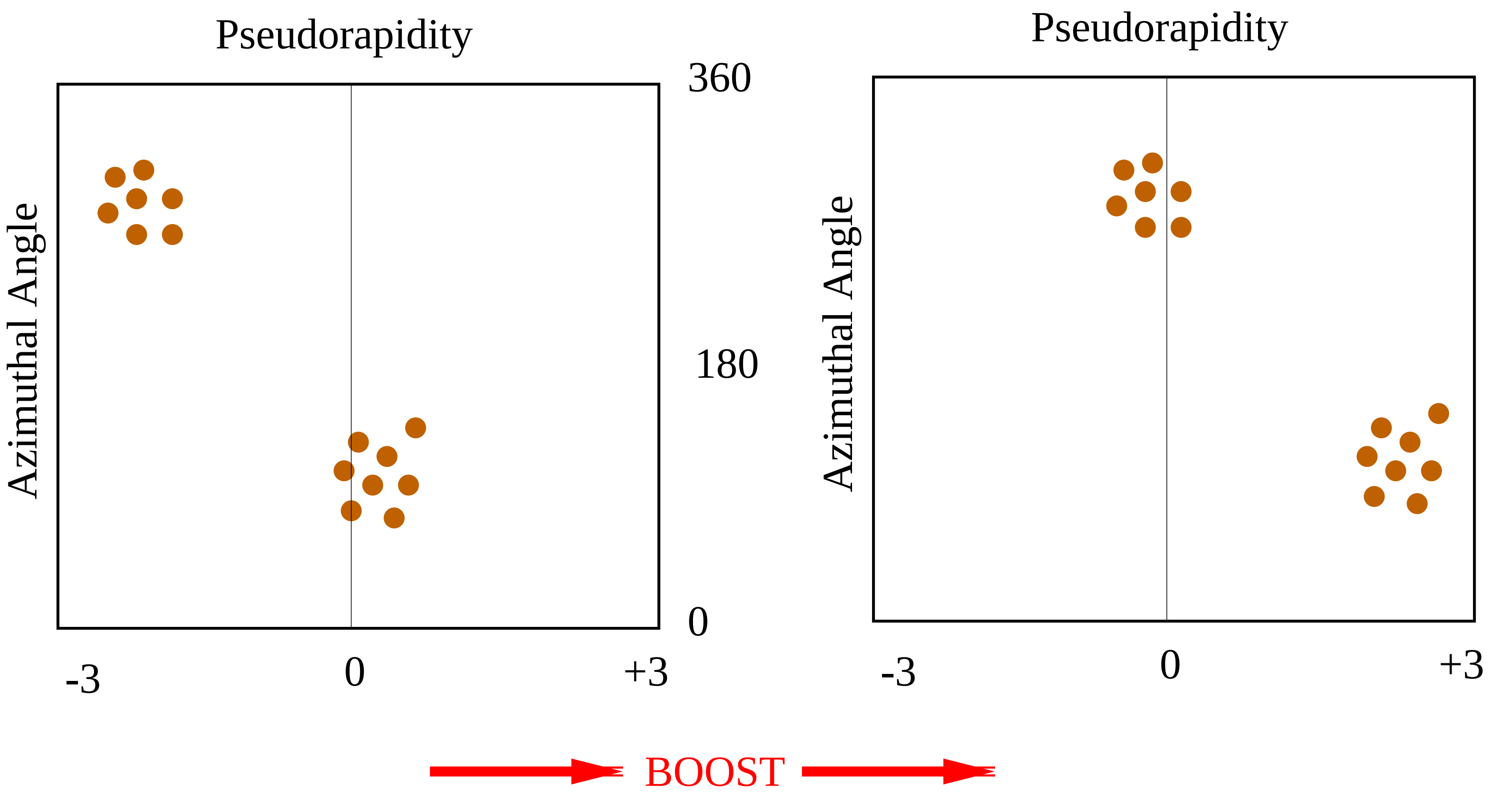

Under a boost:

$\eta' = \eta + f(x_p, x_{\bar{p}})$

⇒ the difference in η between hadrons i and j

$\Delta\eta_{ij}$ IS INVARIANT!

The "distance" defined as

$r \equiv \sqrt{\Delta\eta_{ij}^2 + \Delta\phi_{ij}^2}$

is INVARIANT!

Variables for Jet Search in $p\bar{p}$ collisions (III)

- **Advantage of using transverse energies:**

Large energy $\neq$ small distance (hard scattering!)

The beam remnant jets have huge energies, but they HAVE NOT undergone a hard scattering!

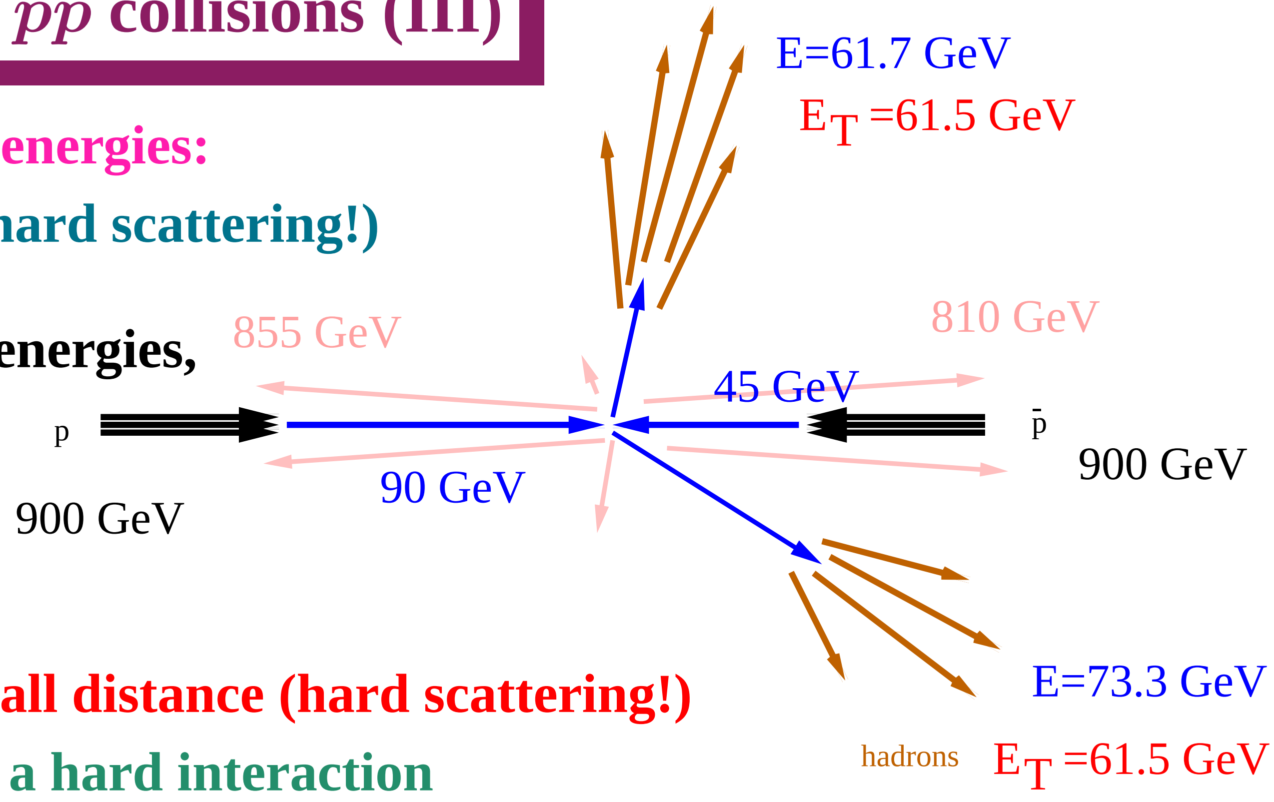

- **Large momentum transfer $\equiv$ small distance (hard scattering!)**

$\Rightarrow$ **large transverse energies signal a hard interaction**

- **The use of transverse energies helps to disentangle between the products of the hard interaction and the beam remnant jets (absent in e^+e^- annihilations)**

$\Rightarrow$ Input to the jet algorithm: $E_{T,i}$, η_i and ϕ_i for every hadron i

$\Rightarrow$ "distance" between hadrons i and j: $\sqrt{\Delta\eta_{ij}^2 + \Delta\phi_{ij}^2}$

Variables for Jet Search in ep collisions at high Q^2 (DIS)

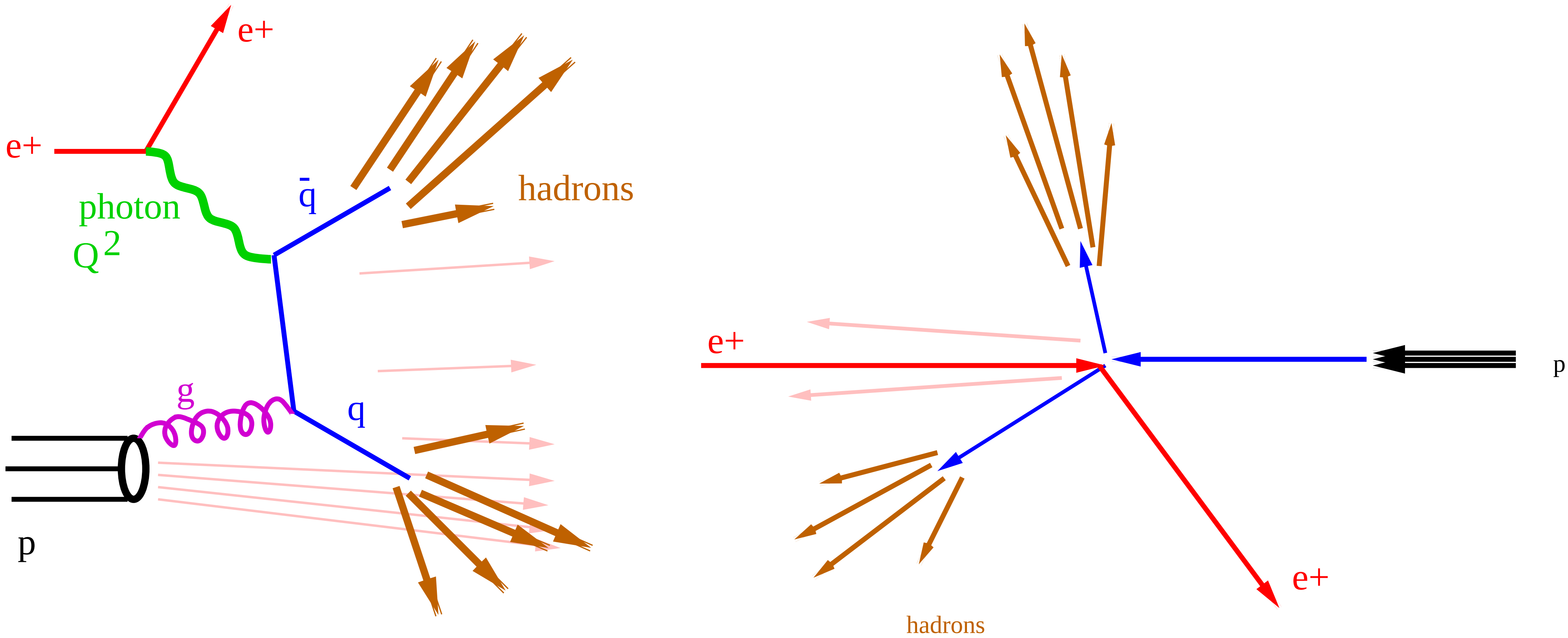

- **The kinematics of ep collisions at high Q^2 poses several challenges:**

→ Presence of beam remnant jet

→ the initial-state γ^*-parton system is boosted (the parton carries a fraction of the proton's momentum) and rotated (the γ^* carries P_T)

Variables for Jet Search in ep collisions at high Q^2 (II)

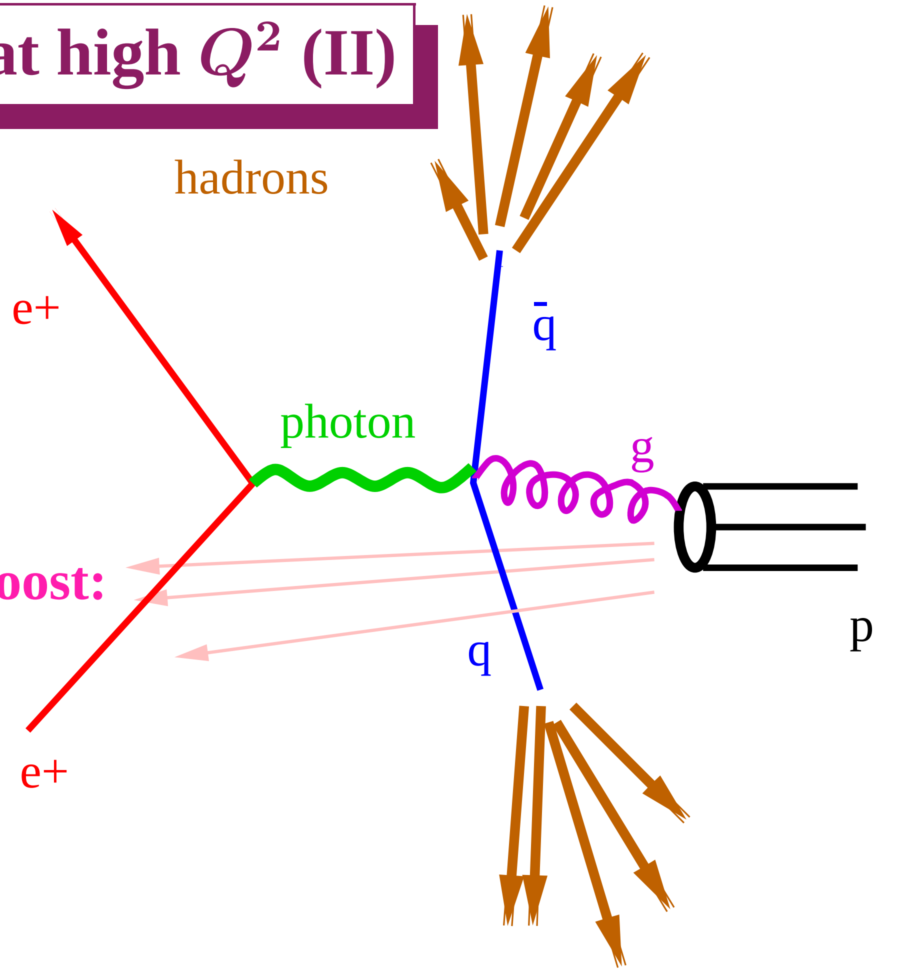

- The effect of the P_T carried by the γ^* is removed
  $\rightarrow$ by selecting a frame in which
  the γ^* collides head-on with the proton
  (the Breit frame is one example)

- The γ^*-parton system can still have a longitudinal boost:
  invariance under longitudinal boosts demands
  $\rightarrow$ the use of transverse energies, pseudorapidities*
  and azimuthal angles

- The use of transverse energies helps to suppress the effects of the beam remnant jet

$\Rightarrow$ Input to the jet algorithm: $E^B_{T,i}$, η^B_i and ϕ^B_i in the Breit frame for every hadron i

$\Rightarrow$ "distance" between hadrons i and j: $\sqrt{(\Delta\eta^B_{ij})^2 + (\Delta\phi^B_{ij})^2}$ in the Breit frame

The best choice for jet algorithm in ep collisions

- There is no best choice since, at the end, it is a question of having the smallest uncertainty for the given observable:
  - $\rightarrow$ the smallest theoretical uncertainties (higher-order contributions)
  - $\rightarrow$ the smallest hadronisation effects
  - $\rightarrow$ the smallest experimental uncertainties
- At present, the longitudinally invariant k_T algorithm is a good choice for accurate comparisons between data and perturbative QCD at HERA
  - $\rightarrow$ jet cross sections in neutral current DIS
  - $\rightarrow$ jet cross sections in photoproduction
- Performance of the longitudinally invariant k_T algorithm in ZEUS:
  - $\rightarrow$ small higher-order contributions (5%, $10-20\%$; varying μ_R by factors 0.5 and 2)
  - $\rightarrow$ small hadronisation corrections ($< 10\%$, $< 10\%$; comparing hadron/parton levels)
  - $\rightarrow$ small hadronisation uncertainties (1%, $2-3\%$; comparing two MC models)
  - $\rightarrow$ small experimental uncertainties (3%, 4%; comparing two MC models)

The longitudinally invariant k_T algorithm for ep collisions

- The clustering procedure is as follows:
  - → List of particles (or calorimeter cells, . . .)
  - → For every object k and for every pair of objects i, j the "distances" are evaluated

$$d_k^2 = E_{T,k}^2 \text{ (distance to the beam)}$$
$$d_{ij}^2 = \min(E_{T,i}^2, E_{T,j}^2) \cdot ((\eta_i - \eta_j)^2 + (\phi_i - \phi_j)^2)$$

  - → If, of all the values $\{d_k^2, d_{ij}^2\}$, d_{mn}^2 is the smallest, then objects m and n are combined into a single new object according to

$$E_{T,ij} = E_{T,i} + E_{T,j}, \quad \eta_{ij} = \frac{E_{T,i} \cdot \eta_i + E_{T,j} \cdot \eta_j}{E_{T,ij}}, \quad \phi_{ij} = \frac{E_{T,i} \cdot \phi_i + E_{T,j} \cdot \phi_j}{E_{T,ij}}$$

  - → If, however, d_k^2 is the smallest, then object k is considered a "protojet" and is removed from the list
  - → The procedure is iterated until the list of objects is empty
- From the list of "protojets" the jets are selected by imposing certain criteria:
  - → jet pseudorapidity in the range $C_L < \eta_{\rm jet} < C_U$
  - → jet transverse energy in the range $E_{T,\rm jet} > E_{T,0}$

⇒ the lower the $E_{T,0}$ is the larger the theoretical and experimental uncertainties are!

The longitudinally invariant k_T algorithm for NC DIS

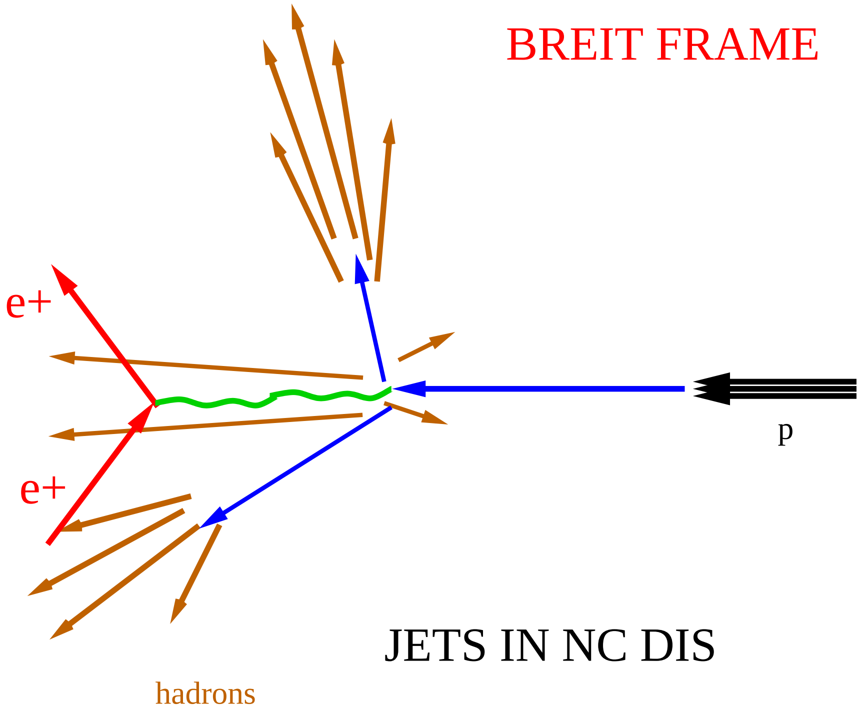

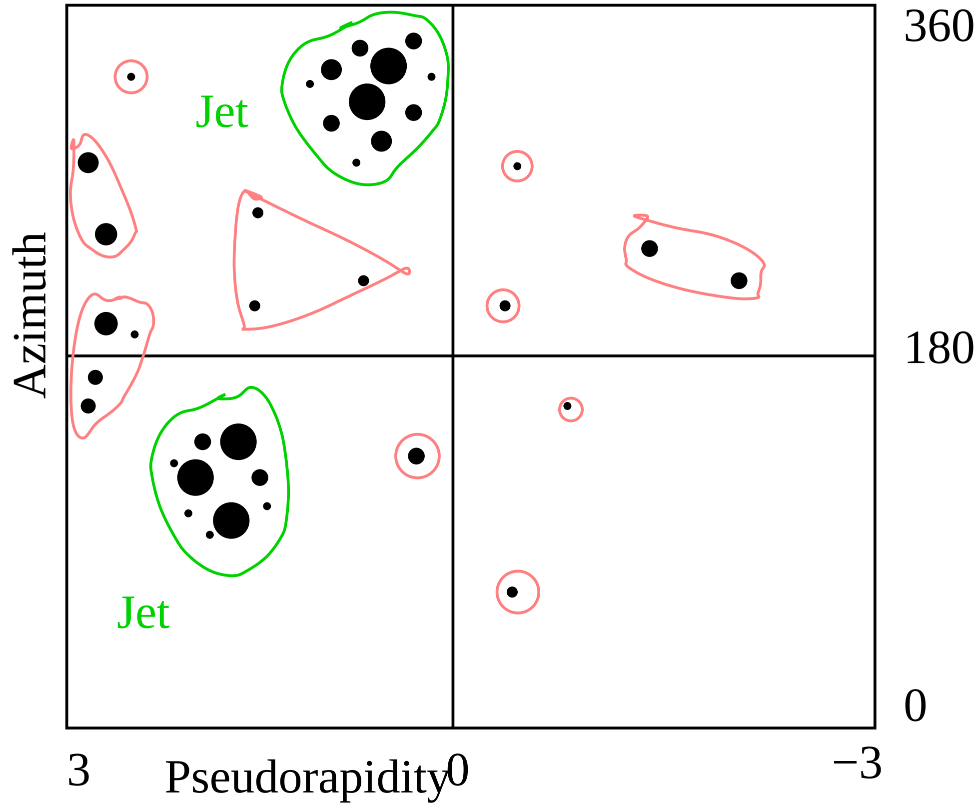

- **Infrared and collinear safe to all orders in perturbative QCD**
- **Invariant under longitudinal boosts (along the γ^*-proton axis)**
- **Suppression of beam remnant jet contributions through the use of transverse energies and by not forcing all the particles to be assigned to jets (nor requiring a certain jet shape)**
- **Small experimental and theoretical uncertainties**

Dijet Cross Sections in NC DIS ($5 < Q^2 < 15000$ GeV^2)

- Measurement of differential dijet cross sections over a wide range in $Q^2 \rightarrow 5 < Q^2 < 15000$ GeV^2 and $0.2 < y < 0.6$ for dijet production with
  - $E_T^{jet,1(2)}$(Breit)> 5 GeV
  - $E_T^{jet,1}$(Breit)$+E_T^{jet,2}$(Breit)> 17 GeV
  - $-1 < \eta^{jet,1(2)}$(Lab)< 2.5
- Detailed investigation of the jet algorithms:
  $\rightarrow$ Smallest parton-to-hadron effects: inclusive k_T
- Comparison with NLO QCD calculations:
  $\rightarrow \mu_R = \bar{E}_T, \mu_F = \sqrt{200}$ GeV
  $\rightarrow$ CTEQ5M1 parametrisations of proton PDFs
  $\rightarrow$ parton-to-hadron corrections applied
- NLO QCD gives a good description of the data over a wide range in Q^2 and E_T; the Q^2 dependence is observed to be reduced at high-E_T and described by NLO

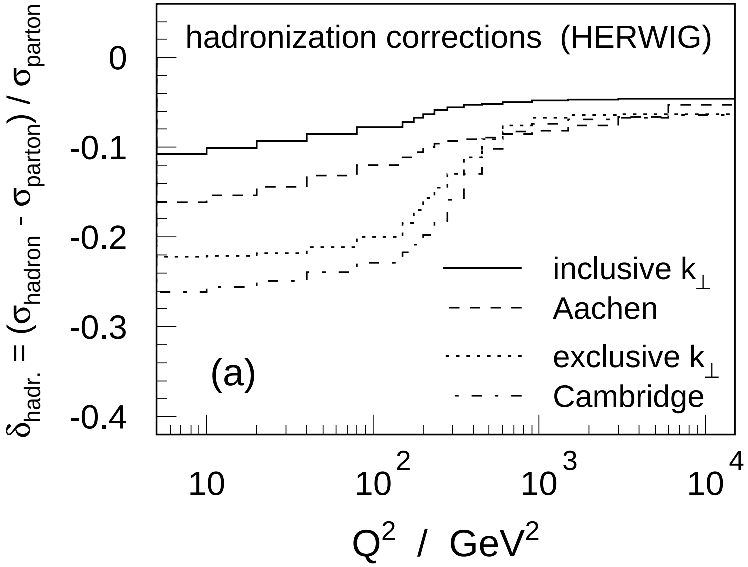

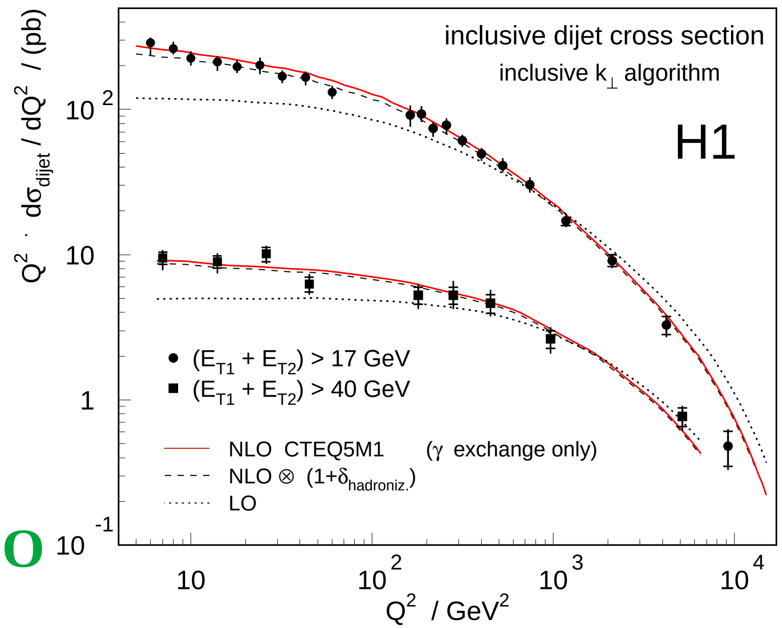

Dijet Cross Sections in NC DIS

- Measurement of double differential cross sections $d\sigma/dM_{JJ}dQ^2, d\sigma/d\bar{E}_T dQ^2$ over $5 < Q^2 < 5000$ GeV^2
- It is observed that the spectra get harder as Q^2 increases
- NLO QCD describes well the data over $15 < M_{JJ} < 95$ GeV and $8.5 < \bar{E}_T < 60$ GeV except at low Q^2, where the shape is ok but not the normalisation
- Overview: at high Q^2 (> 70 GeV^2) NLO describes the data well; as Q^2 decreases the theoretical uncertainties become large and NLO fails for $Q^2 < 10$ GeV^2

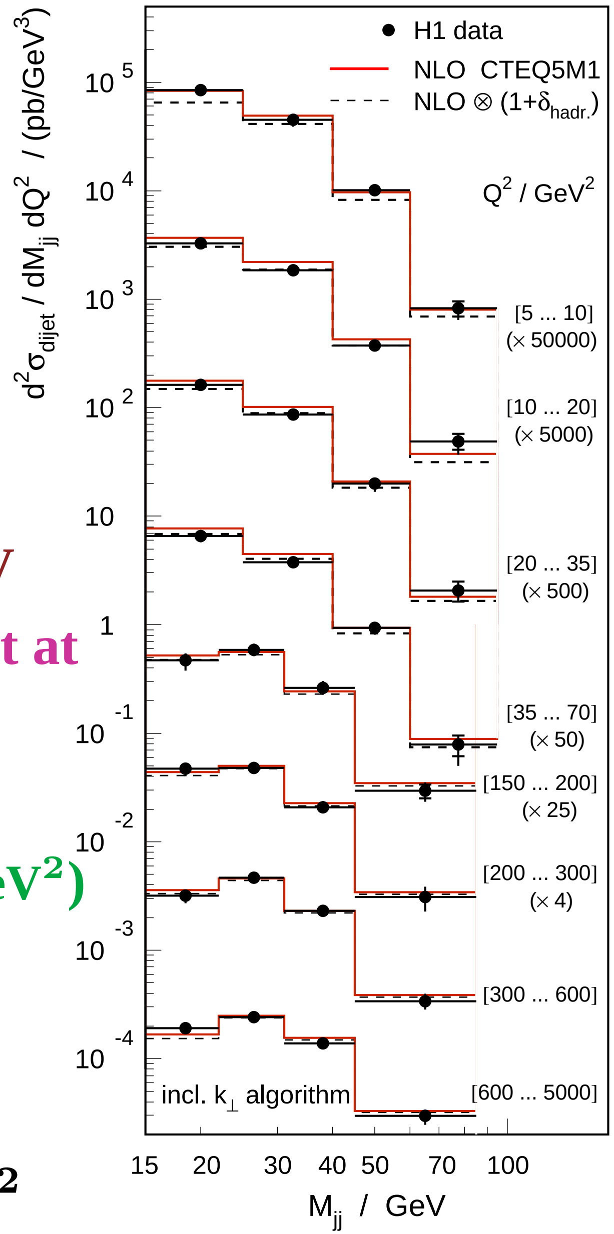

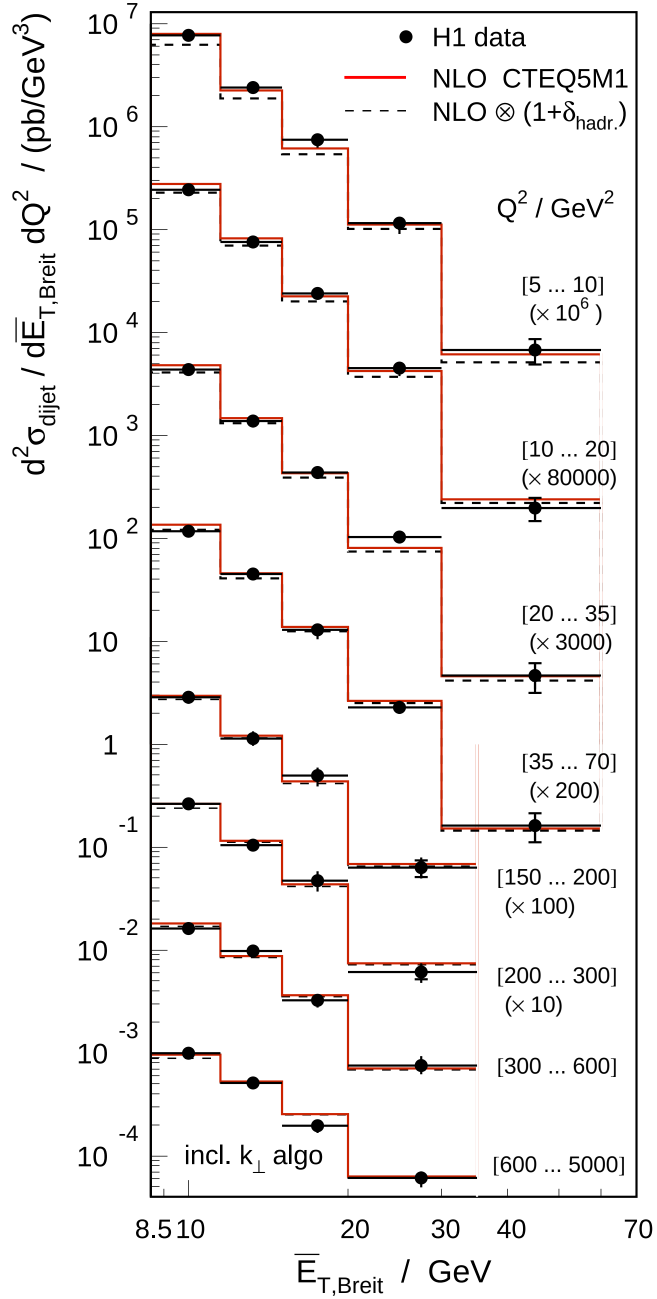

Dijet Cross Sections at $Q^2 > 470$ GeV^2 and extraction of α_s

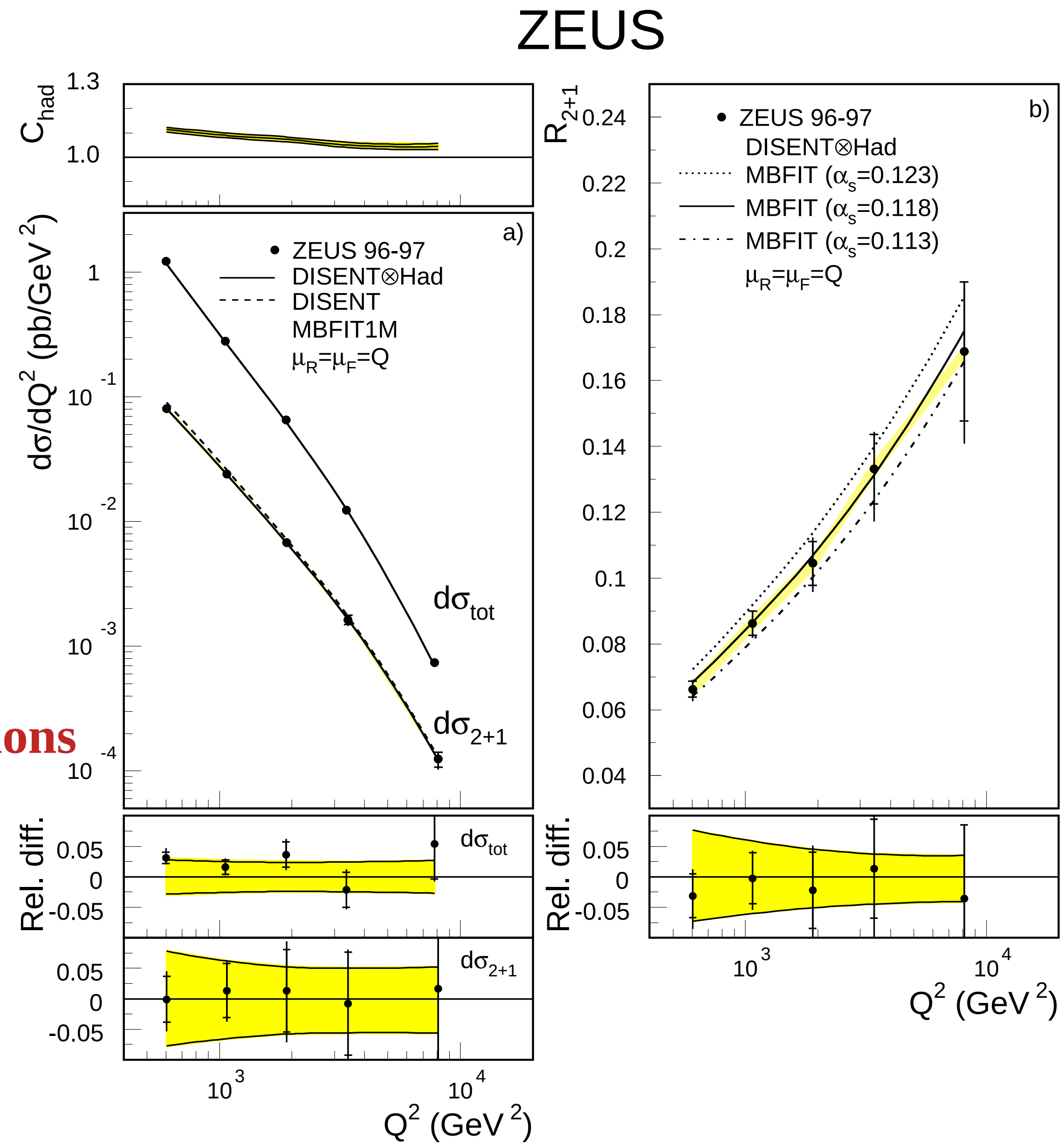

- Dijet cross section $d\sigma_{2+1}/dQ^2$ for
  $470 < Q^2 < 20000$ GeV^2
  $E_T^{jet,1}$(Breit)> 8 GeV
  $E_T^{jet,2}$(Breit)> 5 GeV
  $-1 < \eta^{jet,1(2)}$(Lab)< 2

$\rightarrow$ $\boxed{\text{Ratio } R_{2+1} \equiv \frac{d\sigma_{2+1}/dQ^2}{d\sigma_{tot}/dQ^2}}$

- Small experimental uncertainties.
- Comparison with NLO QCD calculations
- Small theoretical uncertainties:
  $\rightarrow$ uncertainties on the proton PDFs
  $\rightarrow$ hadronisation corrections
  $\rightarrow$ higher-order terms ($>$ NLO)

Uncertainties of the Proton PDFs: effects on jet cross sections

- Comparison of jet cross-section calculations using different parametrisations of the proton PDFs (e.g. MRST vs CTEQ) DOES NOT give a reliable estimation of the uncertainties due to the proton PDFs
- Several groups have developed methods to quantify these uncertainties by accounting (properly) for

$\rightarrow$ the statistical and correlated systematic uncertainties of each data set used in the determination of the PDFs

$\rightarrow$ the theoretical uncertainties affecting the extraction of the PDFs in the DGLAP fits

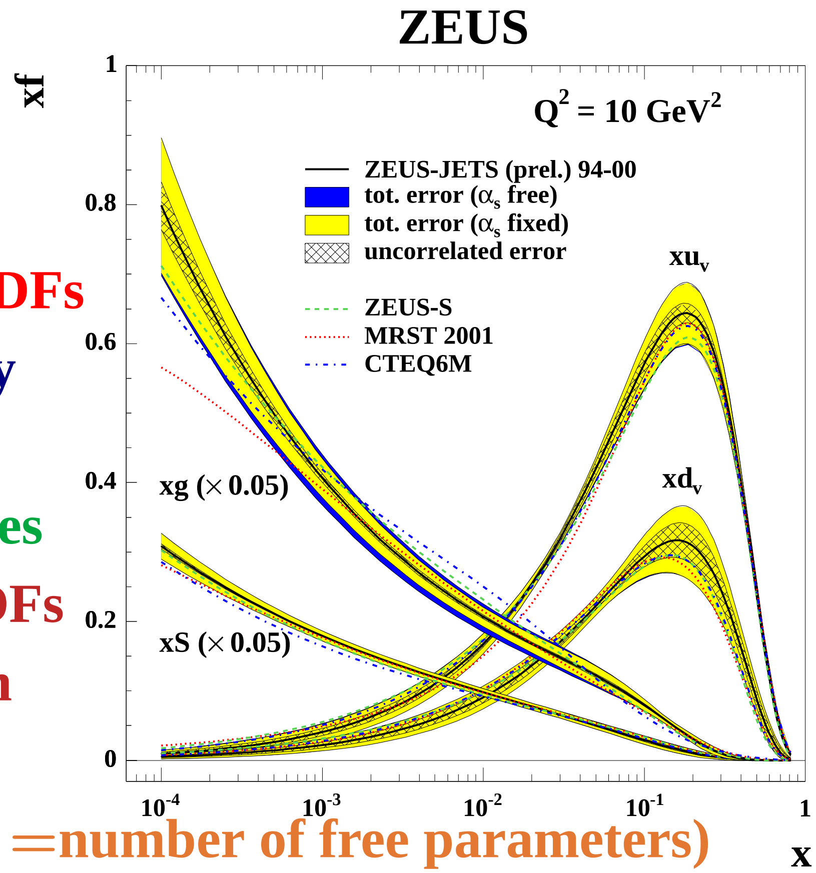

- CTEQ's analysis provides $2N_p + 1$ PDF sets (N_p =number of free parameters) consisting of the best fit S_0 and eigenvector basis sets in the plus and minus directions along each eigenvector, such that the best estimate and its uncertainty can be calculated $\Rightarrow$ for any function of the proton PDFs (e.g. σ_{jet})

$$\Delta\sigma_{jet} = \frac{1}{2}\left(\sum_{i=1,N_p}[\sigma_{jet}(S_i^+) - \sigma_{jet}(S_i^-)]^2\right)^{1/2}$$

Dijet Cross Sections at $Q^2 > 470$ GeV^2 and extraction of $\alpha_s(M_Z)$

- NLO QCD calculations of $d\sigma_{2+1}/dQ^2$ depend on $\alpha_s(M_Z)$ through

$\rightarrow$ Matrix Elements: $\hat{\sigma} \sim A \cdot \alpha_s + B \cdot \alpha_s^2$

$\rightarrow$ proton PDFs: α_s assumed in evolution

- To take into account the correlation the NLO QCD calculations are performed using various sets of proton PDFs which assume different values of α_s
- The resulting NLO QCD calculations are parametrised as a function of $\alpha_s(M_Z)$ in each region of Q^2 of the measurements
- From the measured value of R_{2+1} in each region of Q^2 the value of $\alpha_s(M_Z)$ and its uncertainty are extracted

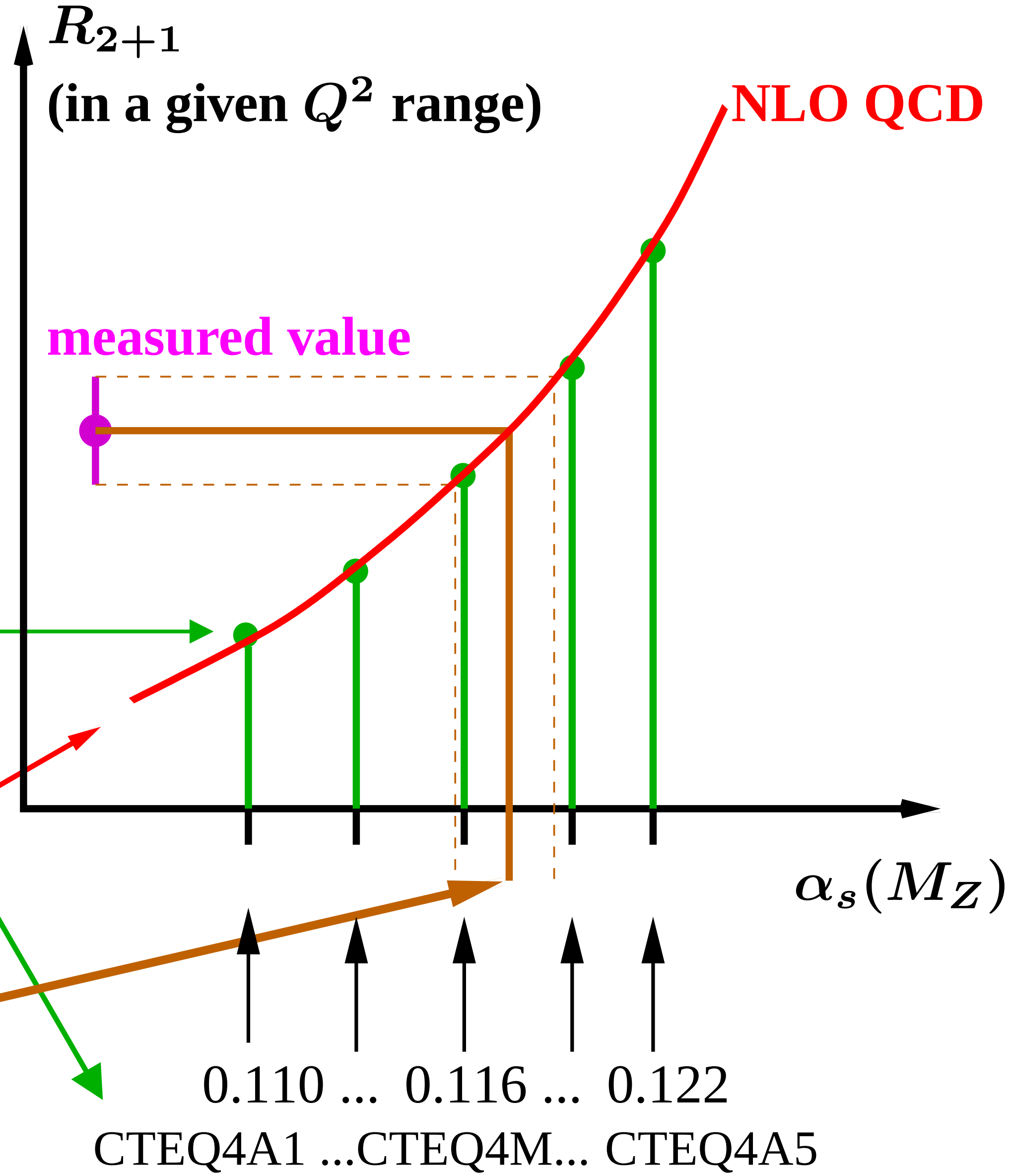

Dijet Cross Sections at $Q^2 > 470$ GeV^2 and extraction of α_s

- **Study of the scale dependence of $\alpha_s(Q)$:**
  from the measured $R_{2+1}(Q^2)$ in each Q^2 region
  $\rightarrow \alpha_s(< Q >)$ is extracted
  The measurements are consistent with
  the running of α_s predicted by perturbative QCD
- **A combined value of $\alpha_s(M_Z)$ has been extracted:**

$$\alpha_s(M_Z) = 0.1166 \pm 0.0019\ (\text{stat.})\ {}^{+0.0024}_{-0.0033}\ (\text{exp.})\ {}^{+0.0057}_{-0.0044}\ (\text{th.})$$

- **The theoretical uncertainty dominates:**

$\rightarrow$ terms beyond NLO $\Delta\alpha_s(M_Z) = {}^{+0.0055}_{-0.0042}$

$\rightarrow$ uncertainties proton PDFs $\Delta\alpha_s(M_Z) = {}^{+0.0012}_{-0.0011}$

$\rightarrow$ hadronisation corrections $\Delta\alpha_s(M_Z) = \pm 0.0005$

Improvements depend upon further Theoretical Work

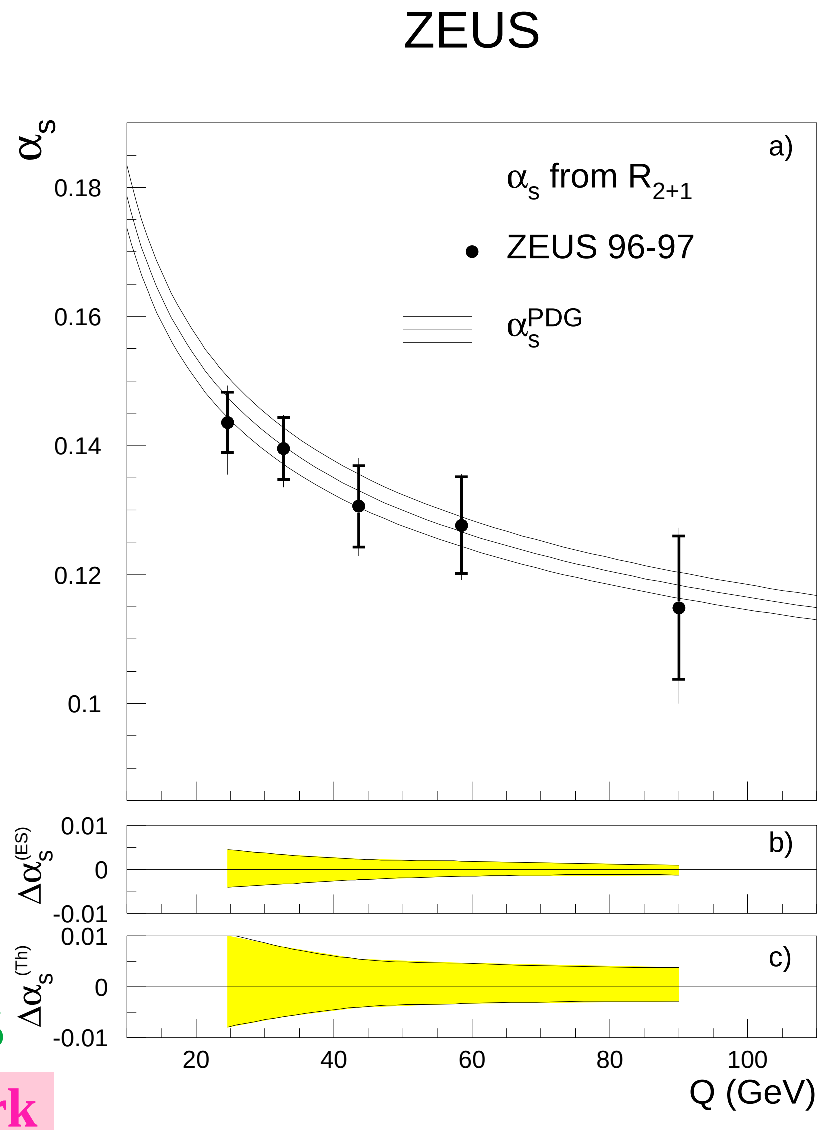

Inclusive Jet Cross Sections in NC DIS at $Q^2 > 125$ GeV^2

$ep \to e + \text{jet} + \text{X}$: inclusive jets at high Q^2

- Jets searched using the k_T cluster algorithm in Breit frame
- Kinematic region: $Q^2 > 125$ GeV^2 and $|\cos\gamma_h| < 0.65$
- At least one jet with $E_{T,\mathrm{B}}^{\mathrm{jet}} > 8$ GeV and $-2 < \eta_{\mathrm{B}}^{\mathrm{jet}} < 1.5$

$\mathcal{L} = 300$ pb^{-1}

- **Small experimental uncertainties**
  - $\to$ uncorrelated: $\sim \pm 3\ (7)\%$ at low (high) $Q^2/E_{T,\mathrm{B}}^{\mathrm{jet}}$
  - $\to$ correlated: $\sim \pm 5\ (2)\%$ at low (high) $Q^2/E_{T,\mathrm{B}}^{\mathrm{jet}}$
- **Small theoretical uncertainties**
  - $\to$ higher orders (below $\pm 5\%$ for $Q^2 > 250$ GeV^2)
  - $\to$ proton PDFs (below $\pm 3\%$)
  - $\to$ $\alpha_s(M_Z)$ (below $\pm 1\ (2)\%$ at low (high) $Q^2/E_{T,\mathrm{B}}^{\mathrm{jet}}$)
  - $\to$ parton-to-hadron corrections (below $\pm 2\%$)

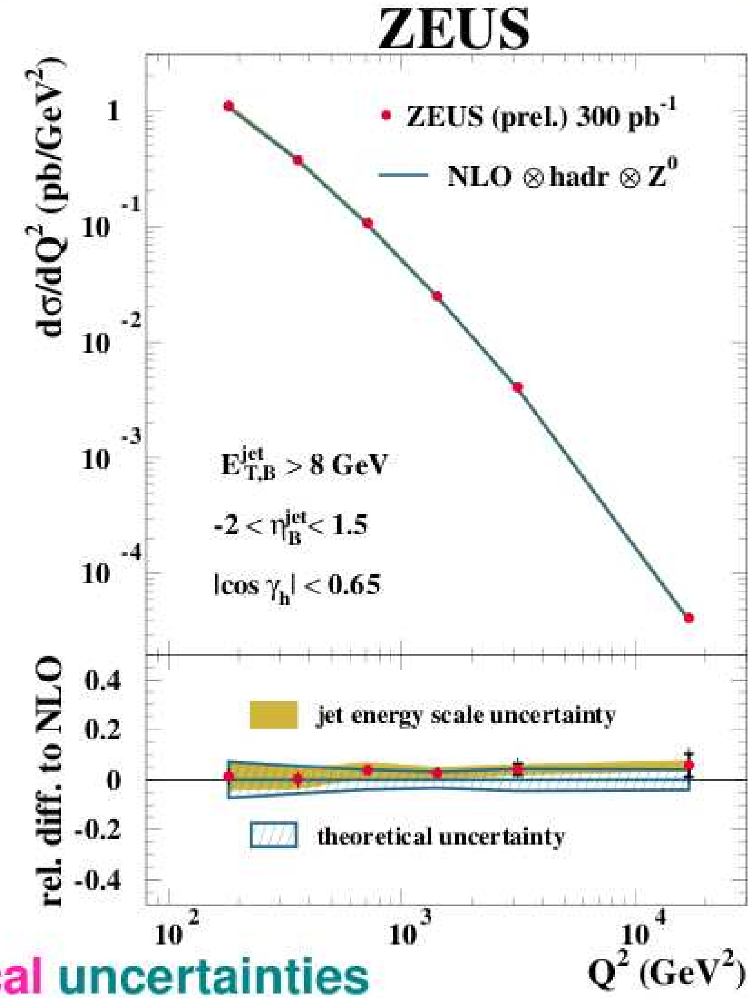

$\longrightarrow$ **Good description of data by NLO prediction**

$\longrightarrow$ validity of the description of the dynamics of jet production at $\mathcal{O}(\alpha_s^2)$

$\longrightarrow$ Measurements provide direct sensitivity to $\alpha_s(M_Z)$ with small experimental and theoretical uncertainties

Inclusive Jet Cross Sections and extraction of α_s

- The energy-scale dependence of the coupling was determined by extracting α_s from the measured $d\sigma/dE^{\rm jet}_{T,\rm B}$ at different $E^{\rm jet}_{T,\rm B}$ values:

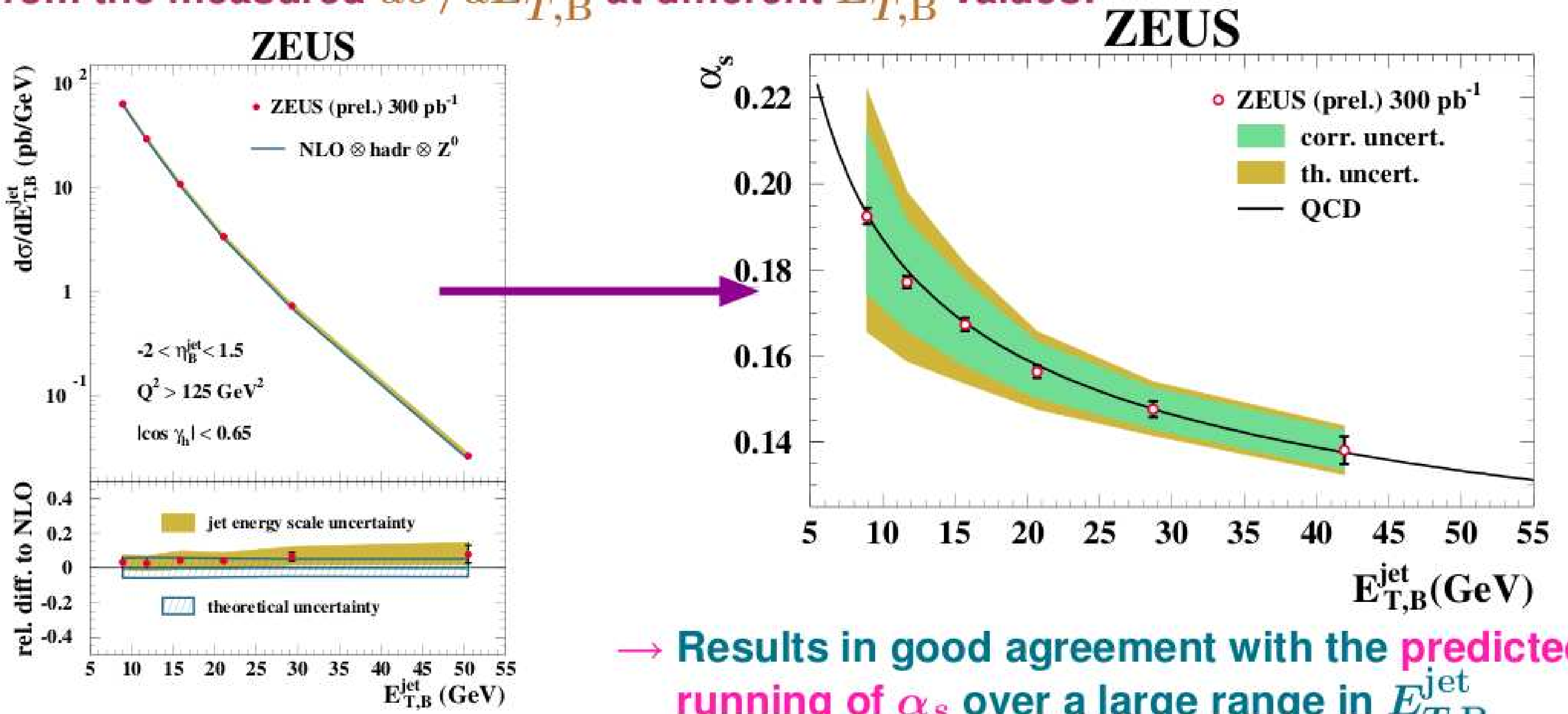

→ Results in good agreement with the predicted running of α_s over a large range in $E^{\rm jet}_{T,\rm B}$

- A value of $\alpha_s(M_Z)$ was determined from $Q^2 > 500$ GeV^2:

$$\alpha_s(M_Z) = 0.1208^{+0.0037}_{-0.0032}\,(\text{exp.})\;^{+0.0022}_{-0.0022}\,(\text{th.})$$

experimental uncertainty: $^{+3.1}_{-2.6}\%$
theoretical uncertainty: $\pm 1.9\%$

Three-jet cross sections in NC DIS

- Three-jet cross sections test QCD beyond LO directly $\rightarrow \sigma_{3jet} \propto \alpha_s^2$
- At least three jets with E_T^{jet}(Breit)$>$ 5 GeV and $-1 < \eta^{jet}$(Lab)< 2.5, $M_{3jets} > 25$ GeV

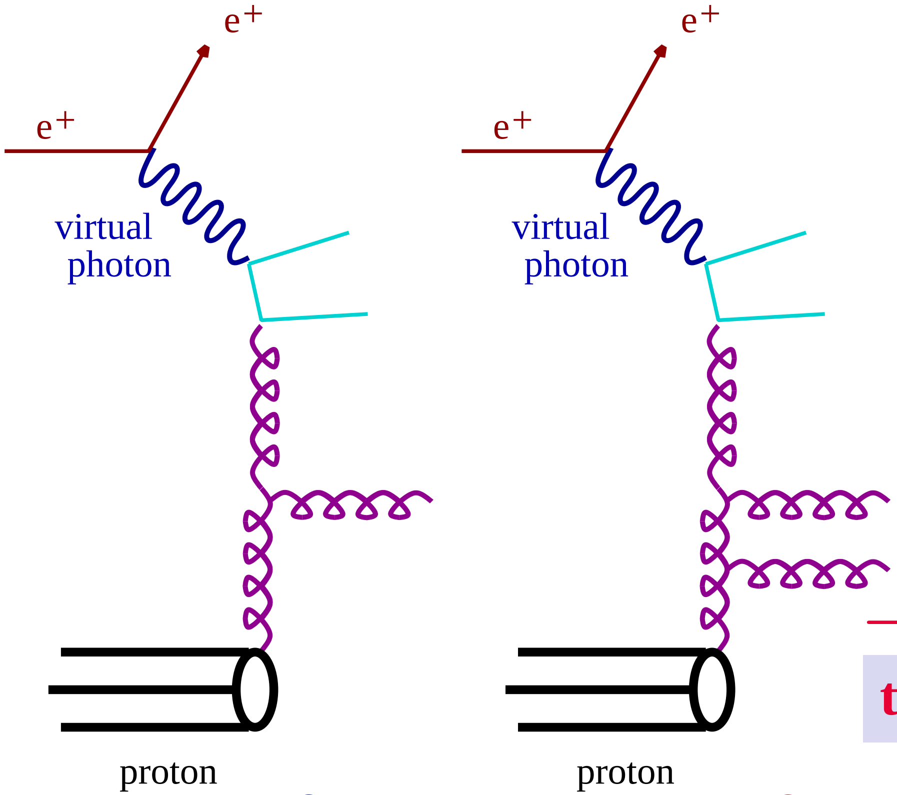

LO $\mathcal{O}(\alpha_s^2)$ **NLO** $\mathcal{O}(\alpha_s^3)$

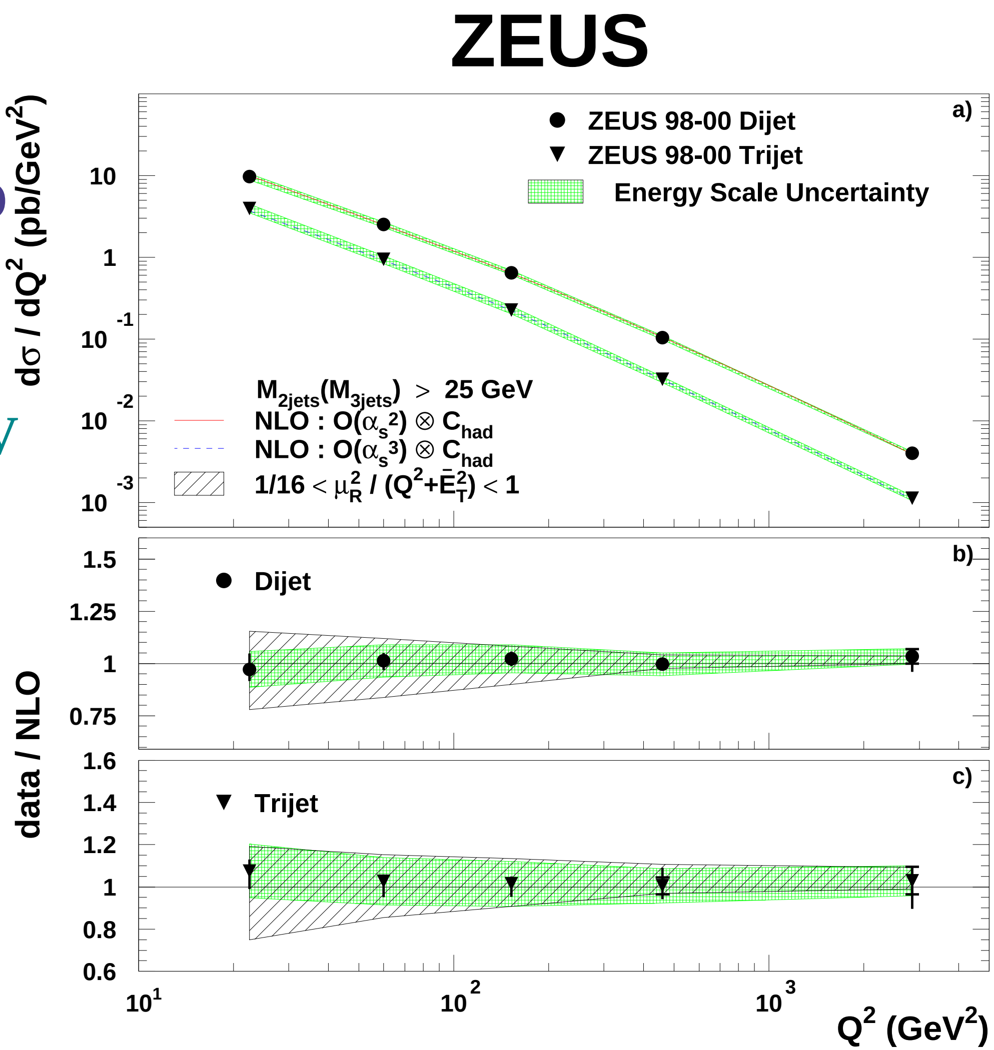

→ NLO calculations ($\mathcal{O}(\alpha_s^3)$): good description of the data over the whole range $10 < Q^2 < 5000$ GeV^2

→ $\alpha_s(M_Z) = 0.1179 \pm 0.0013\ (\text{stat.})^{+0.0028}_{-0.0046}\ (\text{exp.})^{+0.0064}_{-0.0046}\ (\text{th.})$

Jets in photoproduction

Photoproduction of Jets

- **Production of jets in γp collisions has been measured via ep scattering at $Q^2 \approx 0$**

- **At lowest order QCD, two hard scattering processes contribute to jet production $\Rightarrow$**

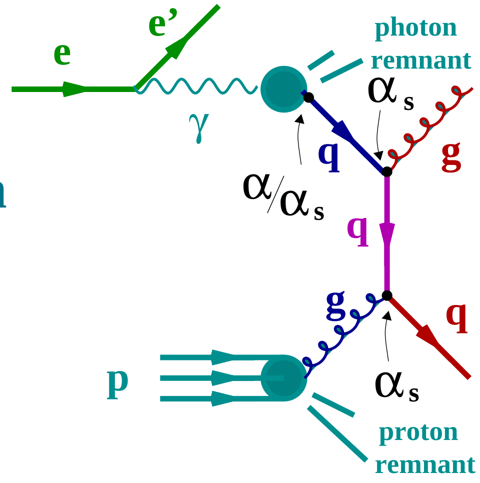

Resolved process

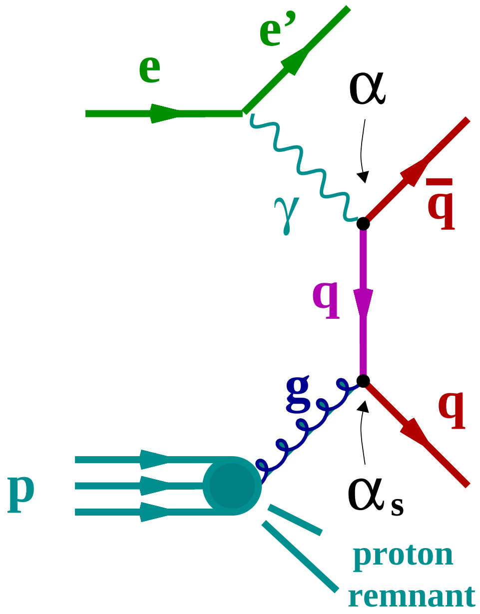

Direct process

- **pQCD calculations of jet cross sections**

$$\sigma_{jet} = \sum_{a,b} \int_0^1 dy\, f_{\gamma/e}(y) \int_0^1 dx_\gamma\, f_{a/\gamma}(x_\gamma, \mu_{F\gamma}^2) \int_0^1 dx_p\, f_{b/p}(x_p, \mu_{Fp}^2)\; \hat{\sigma}_{ab \to jj}$$

longitudinal momentum fraction of γ/e^+ (y), parton a/γ (x_γ), parton b/proton (x_p)

$\rightarrow f_{\gamma/e}(y) =$ **flux of photons in the positron (WW approximation)**

$\rightarrow f_{a/\gamma}(x_\gamma, \mu_{F\gamma}^2) =$ **parton densities in the photon (for direct processes $\delta(1 - x_\gamma)$)**

$\rightarrow f_{b/p}(x_p, \mu_{Fp}^2) =$ **parton densities in the proton**

$\rightarrow \sigma_{ab \to jj}$ **subprocess cross section; short-distance structure of the interaction**

Photoproduction of Jets

- Measurements of jet photoproduction provide

$\to$ Test of NLO QCD predictions based on current parametrisations of the proton and photon PDFs

$\to$ Dynamics of resolved and direct processes

$\to$ Photon structure: information on quark densities from F_2^γ in e^+e^-; gluon density poorly constrained. Jet cross sections in photoproduction are sensitive to both the quark and gluon densities in the photon at larger scales $\mu_{F\gamma}^2 \sim E_{T,jet}^2$ $(200 - 10^4\ \text{GeV}^2)$

$\to$ Proton structure: well constrained by DIS except for the gluon density at high x. Jet cross sections in γp are sensitive to parton densities at x_p up to ~ 0.6

- Observable to separate the contributions: the fraction of the photon's energy participating in the production of the dijet system $\boxed{x_\gamma^{OBS} = \frac{1}{2E_\gamma} \sum_{i=1}^{2} E_T^{jet_i} e^{-\eta^{jet_i}}}$

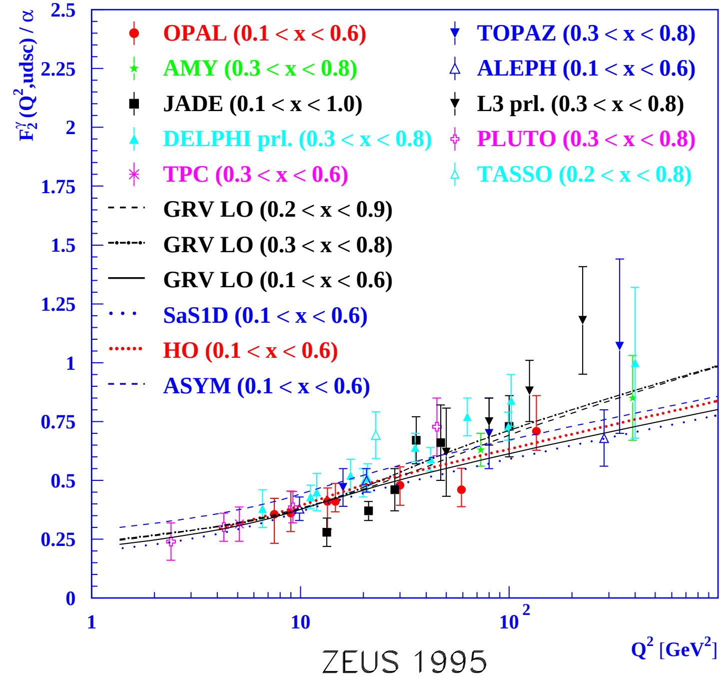

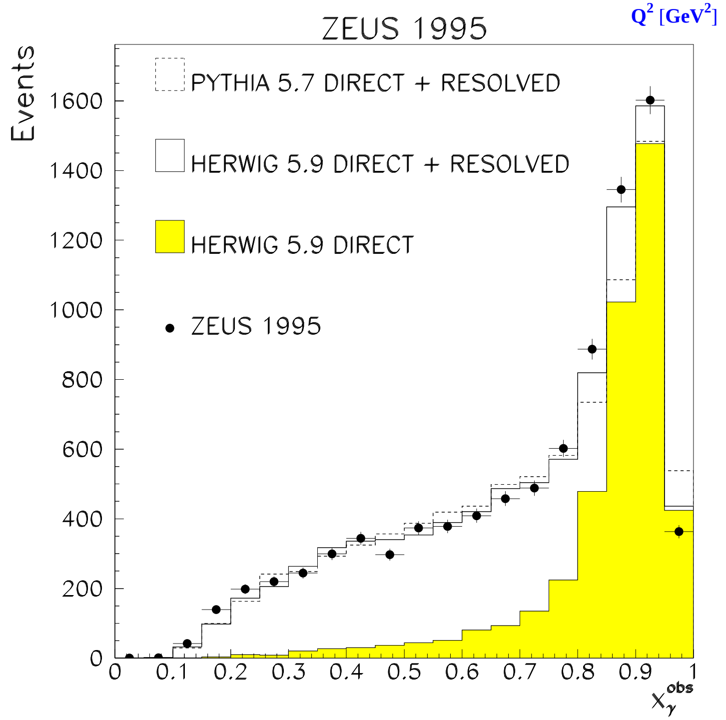

Variables for Jet Search in ep collisions at low Q^2 (Photoproduction)

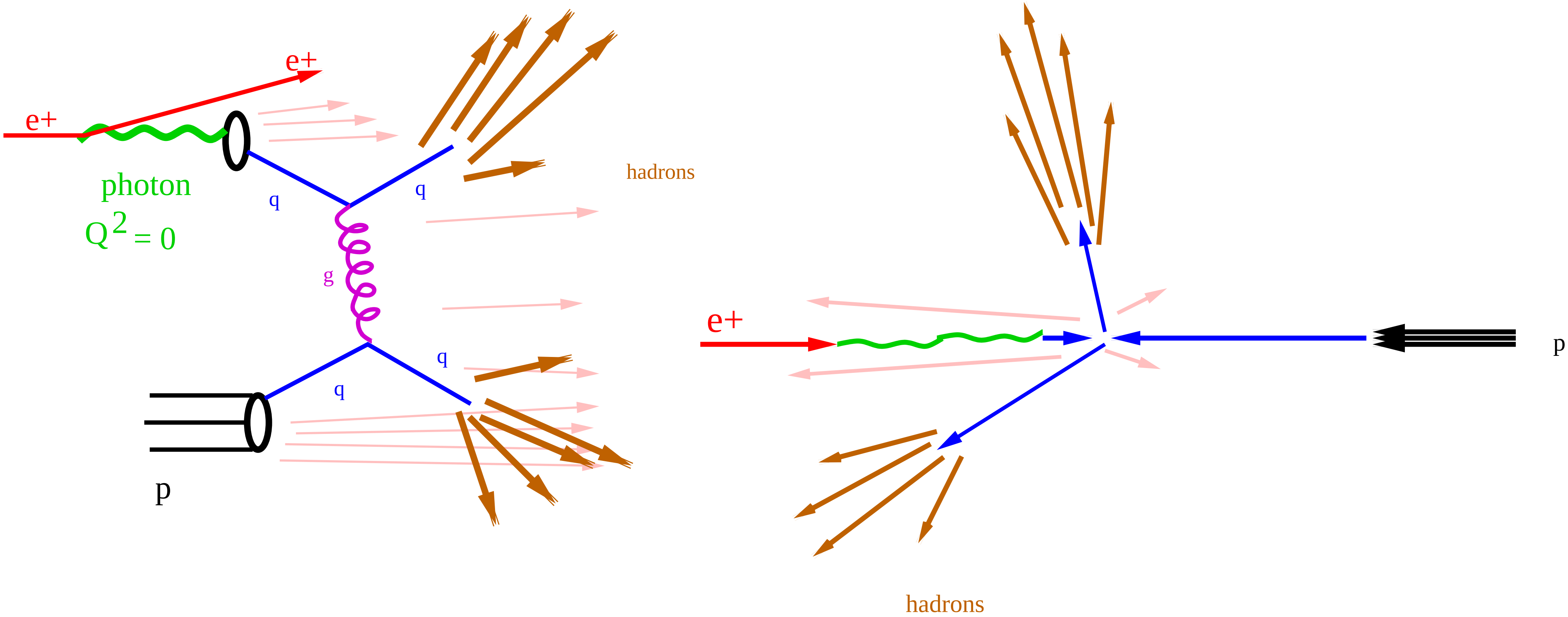

- The kinematics of ep collisions at low Q^2 is similar to that of $p\bar{p}$ collisions

$\Rightarrow$ Input to the jet algorithm: $E_{T,i}$, η_i and ϕ_i for every hadron i

$\Rightarrow$ "distance" between hadrons i and j: $\sqrt{\Delta\eta_{ij}^2 + \Delta\phi_{ij}^2}$

The longitudinally invariant k_T algorithm for photoproduction

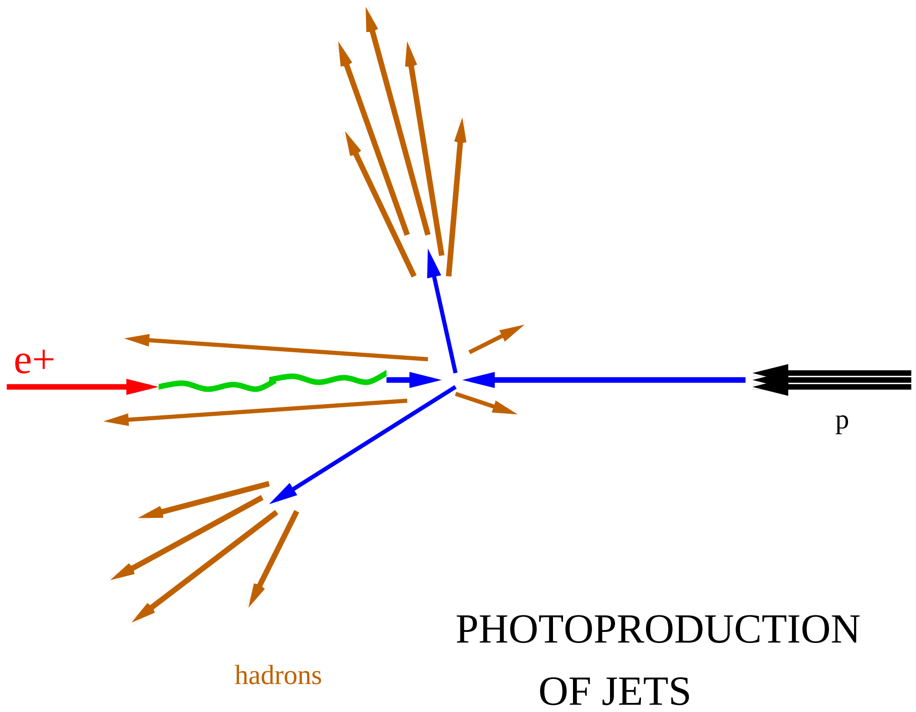

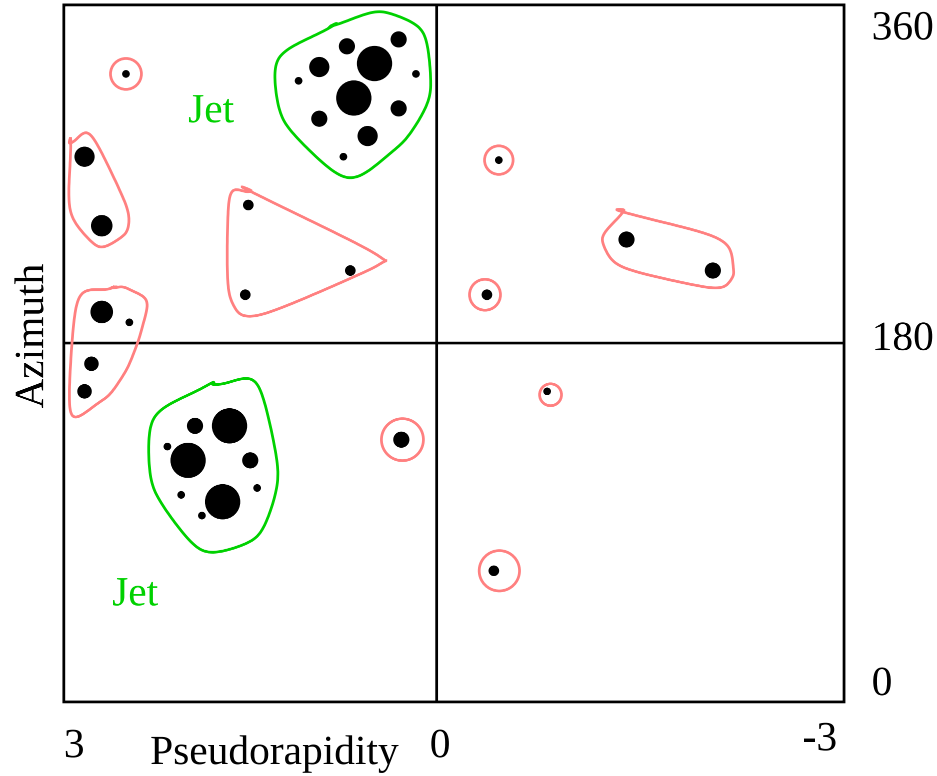

- **Infrared and collinear safe to all orders in perturbative QCD**
- **Invariant under longitudinal boosts (along the beam axis)**
- **Suppression of beam remnant jet contributions through the use of transverse energies and by not forcing all the particles to be assigned to jets (nor requiring a certain jet shape)**
- **Small experimental and theoretical uncertainties**

Dijet Photoproduction: the dynamics of resolved and direct processes

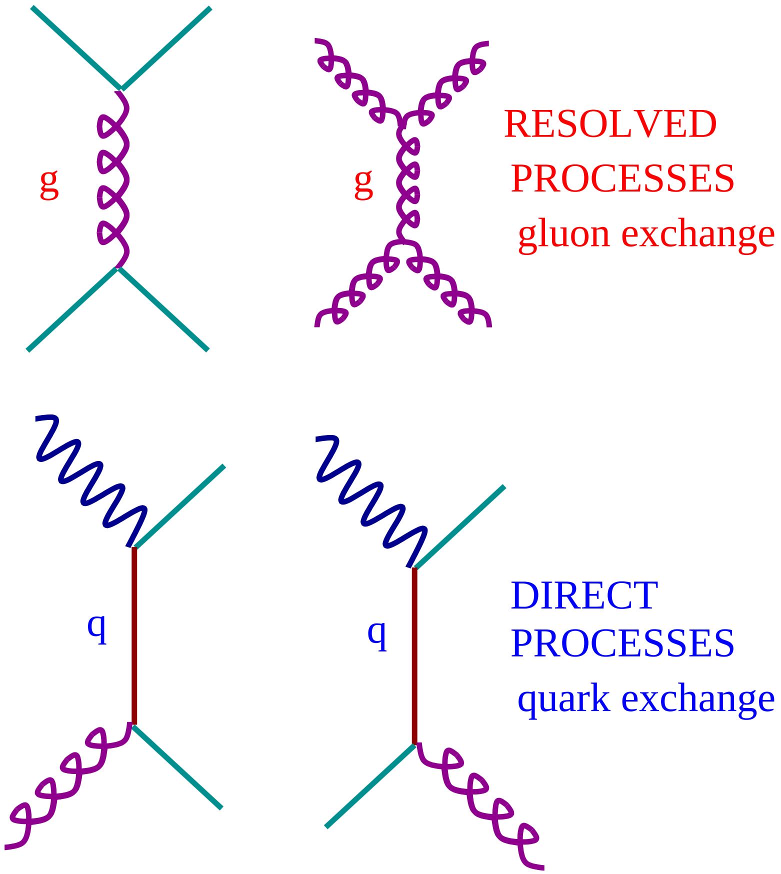

- **The dynamics of dijet production has been investigated by studying the variable:**

$$\cos\theta^* \equiv tanh(\tfrac{1}{2}(\eta^{jet,1} - \eta^{jet,2}))$$

$\longrightarrow$ for two-to-two parton scattering θ^* coincides with the scattering angle in the dijet CMS

- **QCD predicts different dijet angular distributions for resolved and direct:**

$\longrightarrow$ **Resolved (gluon-exchange dominated)**

$$d\sigma/d|\cos\theta^*| \sim \frac{1}{(1-|\cos\theta^*|)^2}$$

$\longrightarrow$ **Direct (quark-exchange only)**

$$d\sigma/d|\cos\theta^*| \sim \frac{1}{(1-|\cos\theta^*|)^1}$$

- **The dijet angular distribution $d\sigma/d|\cos\theta^*|$ for $x_\gamma^{OBS} < 0.75$ ("resolved") should be steeper than that of $x_\gamma^{OBS} > 0.75$ ("direct") as $|\cos\theta^*| \rightarrow 1$**

Dijet Photoproduction: the dynamics of resolved and direct processes

- Measurement of the dijet differential cross section $d\sigma/d|\cos\theta^*|$ for dijet events with
  $E_T^{jet,1} > 14$ GeV, $E_T^{jet,2} > 11$ GeV
  $-1 < \eta^{jet} < 2.4$ (both jets)
  in the kinematic region
  $Q^2 < 1$ GeV^2 and $134 < W_{\gamma p} < 277$ GeV
- Phase-space region:
  $|\cos\theta^*| < 0.8$, $M_{JJ} > 42$ GeV
  $0.1 < \frac{1}{2}(\eta^{jet,1} + \eta^{jet,2}) < 1.3$
- Comparison with NLO QCD calculations:
  $\rightarrow$ High-x_γ^{OBS} ("direct"): NLO describes the shape and normalisation of the data
  $\rightarrow$ Low-x_γ^{OBS} ("resolved"): NLO describes the shape and (reasonably) the normalisation of the data
- The dijet angular distribution of the "resolved" sample is steeper than that of "direct"

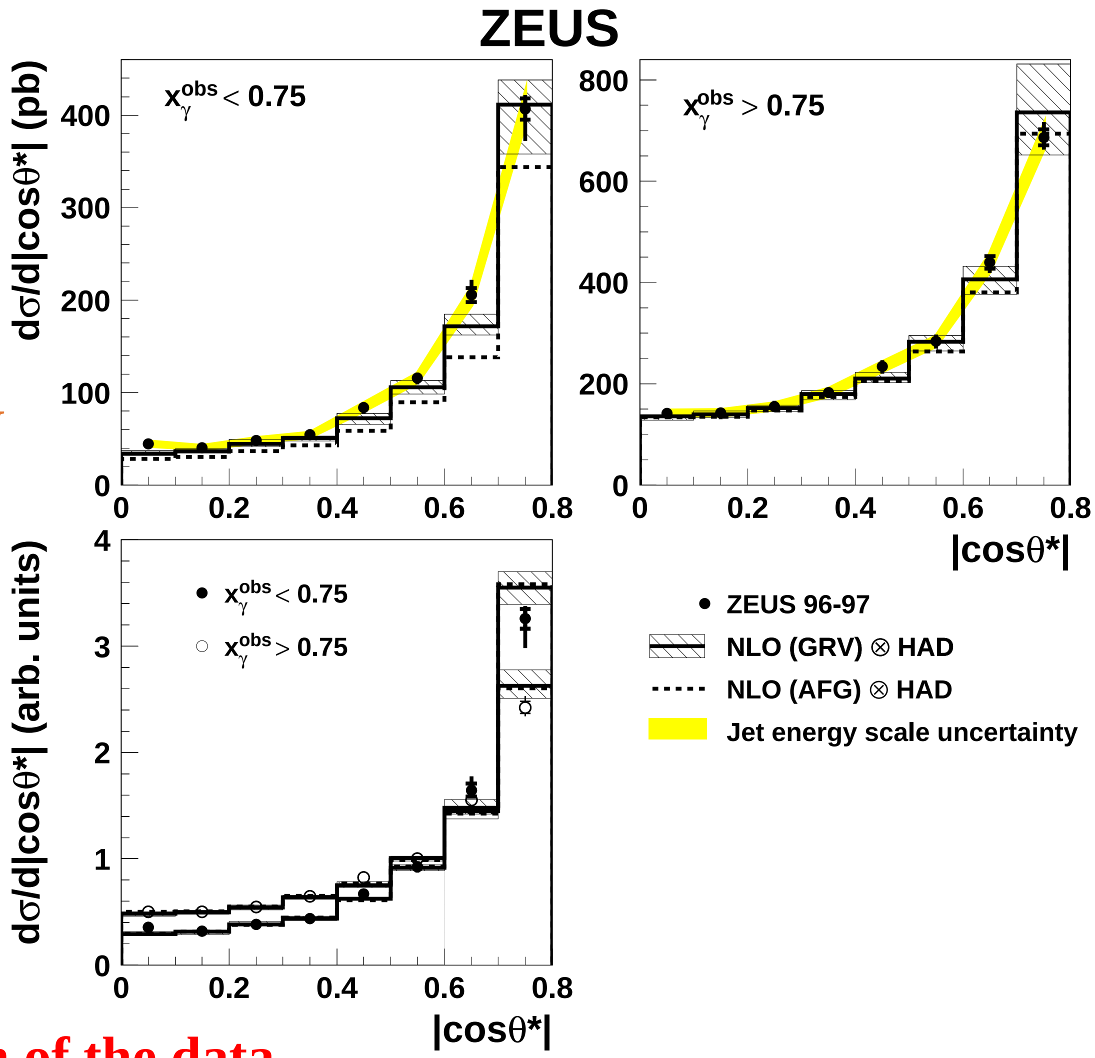

High-M_{JJ} Dijet Photoproduction

- Measurement of the dijet differential cross section $d\sigma/dM_{JJ}$ in the range $47 < M_{JJ} < 160$ GeV for dijet events with $E_T^{jet} > 14$ GeV, $-1 < \eta^{jet} < 2.5$ and $|\cos\theta^*| < 0.8$
- Small experimental uncertainties:

$\rightarrow$ jet energy scale known to 1% $\Rightarrow$ 5% on $d\sigma/dM_{JJ}$

- Small theoretical uncertainties:

$\rightarrow$ higher-order terms (varying μ_R) below 15%

$\rightarrow$ γ PDFs (GRV-HO,AFG-HO) below 10%

$\rightarrow$ resolved processes suppressed at high M_{JJ}

$\rightarrow$ small hadronisation corrections, below 5%

- NLO QCD calculations describe the shape and normalisation of the measurements well

$\rightarrow$ Validity of the pQCD description of the dynamics of parton-parton and γ-parton interactions in photoproduction

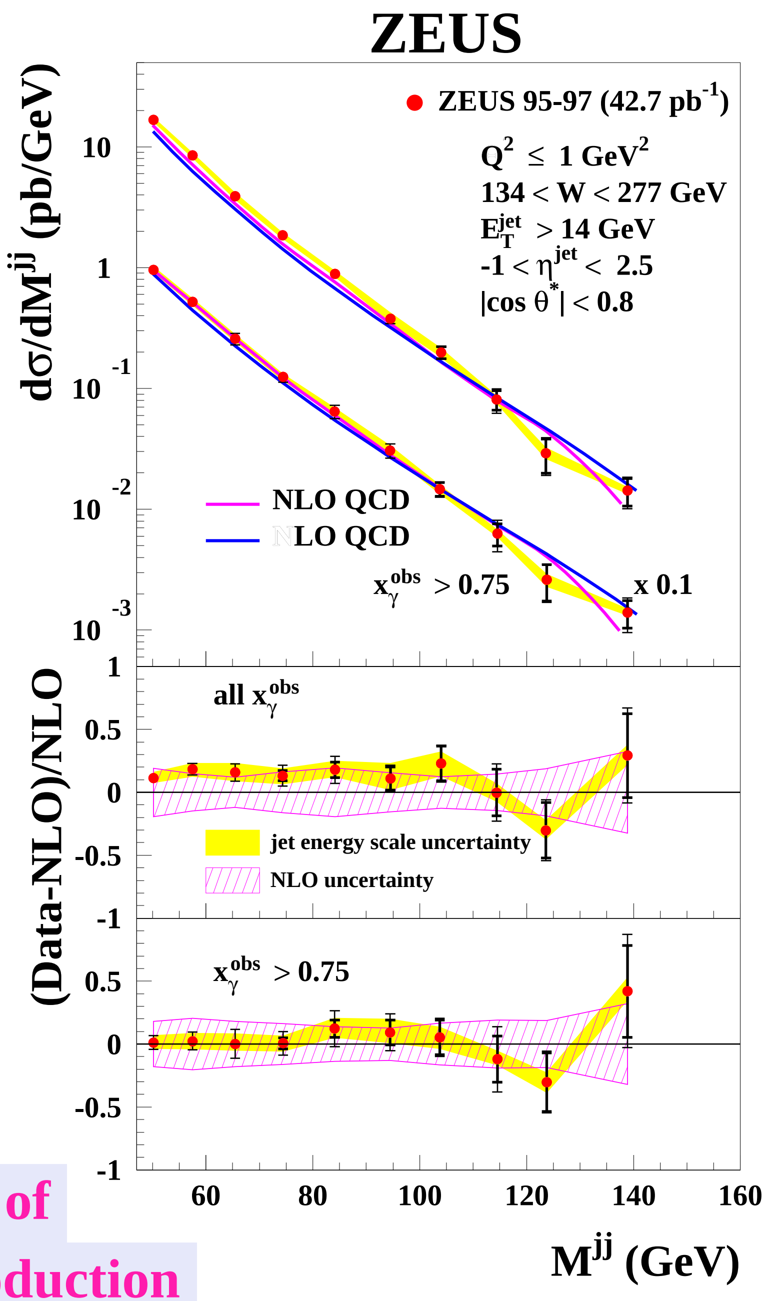

New jet algorithms

- Tests of pQCD with jets require infrared- and collinear-safe jet algorithms:
  - $\longrightarrow$ performance of k_T cluster algorithm in longitudinally invariant inclusive mode (S Catani, S Ellis & D Soper) tested extensively at HERA:
  - $\longrightarrow$ stringent tests of pQCD: good description of data for different jet radii
  - $\longrightarrow$ good performance of algorithm: small theoretical uncertainties / hadronisation corrections
  - $\longrightarrow$ new measurements in photoproduction presented here
- New infrared- and collinear-safe jet algorithms:
  - $\longrightarrow$ anti-k_T (M Cacciari, G Salam & G Soyez) provides $\approx$ circular jets
    - $\star$ experimentally desirable
  - $\longrightarrow$ SIScone (G Salam & G Soyez) seedless cone algorithm provides infrared- and collinear-safe calculations
    - $\star$ theoretically necessary
- New studies at HERA:
  - $\longrightarrow$ test performance of anti-k_T and SIScone in well-understood hadron-induced reaction:
    - $*$ comparison to measurements based on k_T
    - $*$ comparison of measurements and NLO QCD calculations
    - $*$ study of theoretical uncertainties and hadronisation corrections

New jet algorithms

- New infrared- and collinear-safe jet algorithms:
  $\longrightarrow$ anti-k_T (M Cacciari, G Salam & G Soyez) and SIScone (G Salam & G Soyez)
- Cluster algorithms:
  $\longrightarrow$ $d_{ij} = \min[(E^i_{T,\mathrm{B}})^{2p}, (E^j_{T,\mathrm{B}})^{2p}] \cdot \Delta R^2/R^2$ with $p = 1$ (-1) for k_T (anti-k_T)
  $\longrightarrow$ anti-k_T keeps infrared and collinear safety and provides $\approx$ circular jets (experimentally desirable)
- Cone algorithms:
  $\longrightarrow$ seedless cone algorithm produces also jets with well-defined area and is infrared and collinear safe (theoretically necessary)

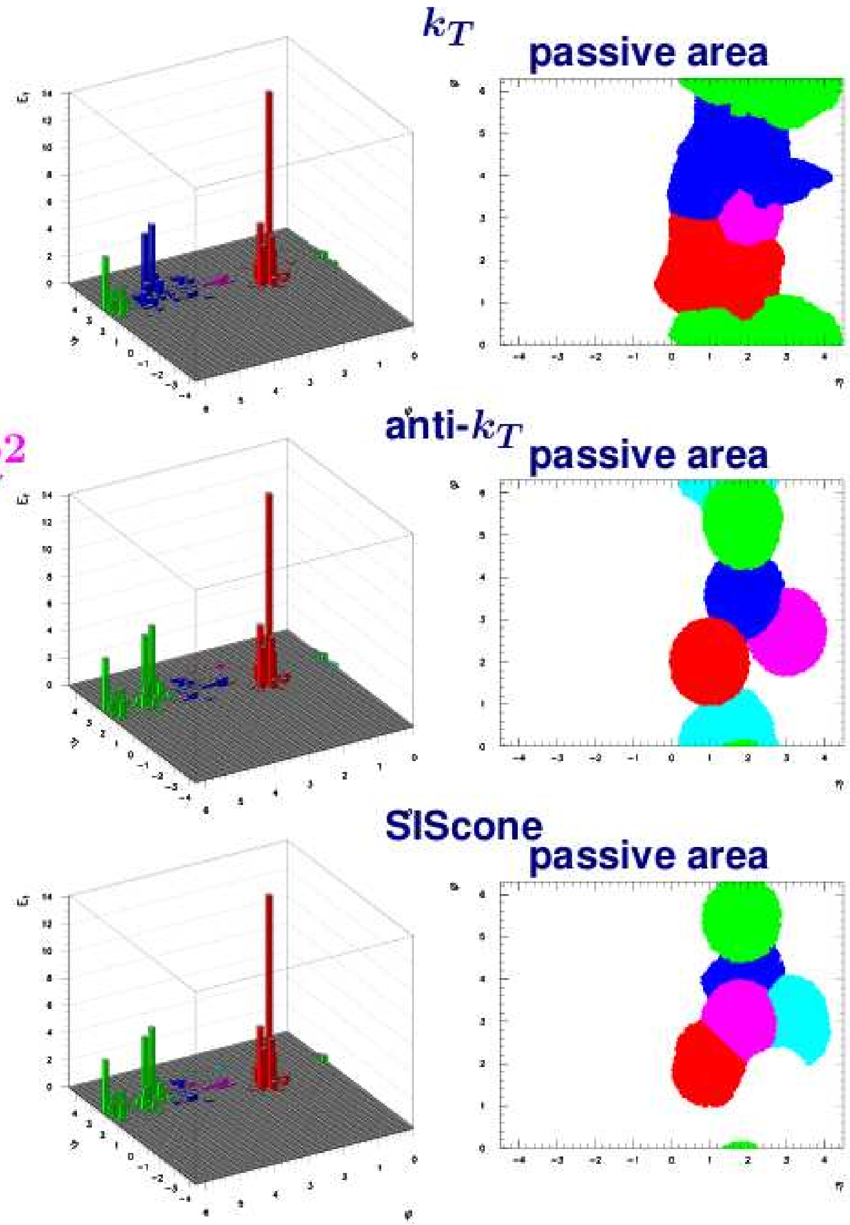

Benefits of the new jet algorithms

- Anti-k_t and SISCONE jet algorithms provide jets with better control on the shape ($\approx$ circular) and area (dictated by the jet radius R) than with the k_t jet algorithm

- Essential to control and suppress the energy contributions from particles that fall into the jet but originate from

$\rightarrow$ the "underlying event" (hadrons from the same proton-proton collision but unrelated to the hard interaction (a proton is an extended object)

$\rightarrow$ additional soft proton-proton interactions overlaid with the interesting one (pile-up)

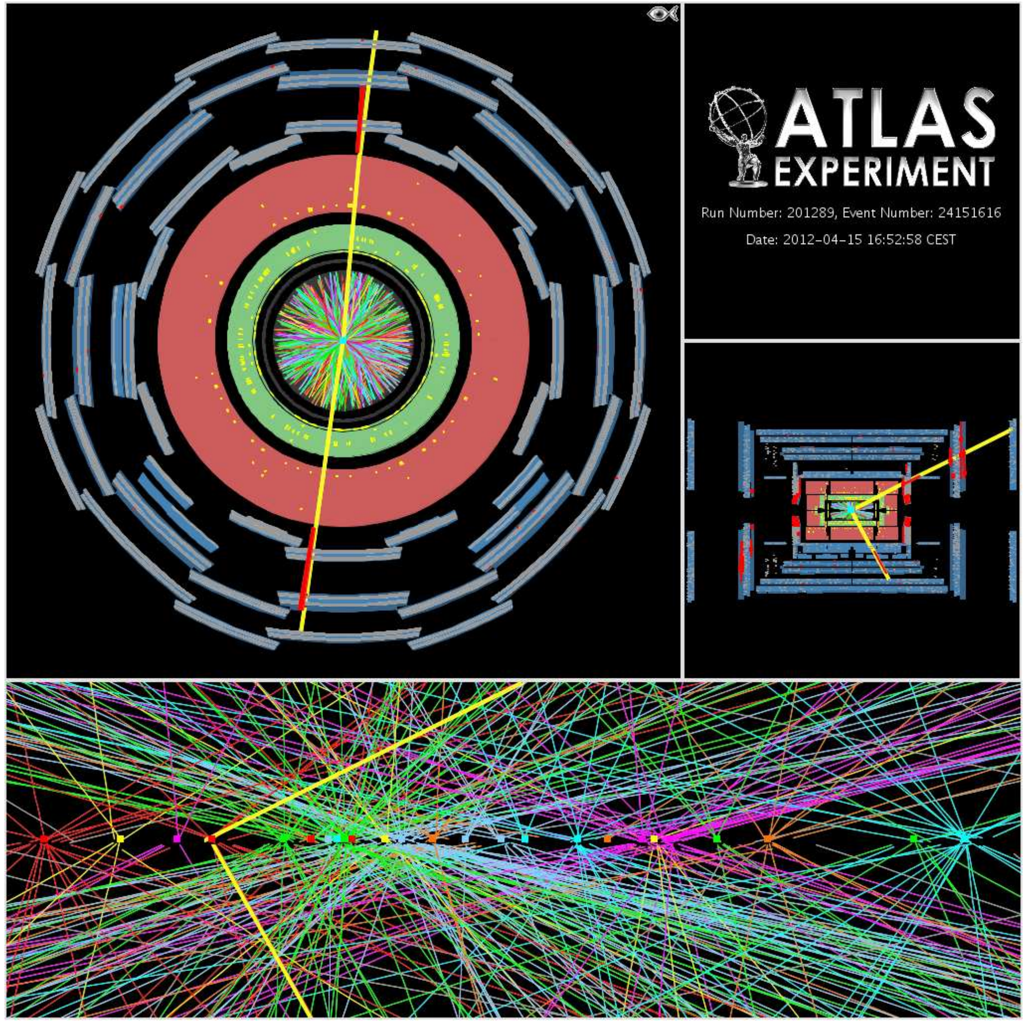

$Z \rightarrow \mu^+\mu^-$ event candidate
with 25 (!!) reconstructed vertices
High pile-up environment in 2012

Inclusive Jet Photoproduction

$ep \to e + \text{jet} + X$: inclusive-jet cross sections

- Kinematic region: $Q^2 < 1$ GeV^2 and $0.2 < y < 0.85$
- Jet search: k_T, anti-k_T and SIScone in laboratory frame
- At least one jet with $E_T^{\rm jet} > 17$ GeV and $-1 < \eta^{\rm jet} < 2.5$

$\mathcal{L} = 0.3$ fb^{-1}

- Experimental uncertainties:
  - $\rightarrow$ systematic: typically below $\pm5\%$
  - $\rightarrow$ energy scale $\pm1\%$ (!): $\sim \pm5$ $(10)\%$ at low (high) $E_T^{\rm jet}$
- Comparison to NLO predictions (Klasen et al):
  - $\rightarrow$ good description of data by NLO prediction
    - $\rightarrow$ validity of the description of the dynamics of jet photoproduction at $\mathcal{O}(\alpha_s^2)$
- Theoretical uncertainties:
  - $\rightarrow$ higher orders: ±10 $(4)\%$ at low (high) $E_T^{\rm jet}$ (k_T/anti-k_T)
    ±14 $(7)\%$ at low (high) $E_T^{\rm jet}$ (SIScone)
  - $\rightarrow$ proton PDFs: ±1 $(5)\%$ at low (high) $E_T^{\rm jet}$
  - $\rightarrow$ hadronisation: $< \pm3\%$; $\alpha_s(M_Z)$: $< \pm2\%$
  - $\rightarrow$ photon PDFs: $\pm9 - 10$ $(1-3)\%$ at low (high) $E_T^{\rm jet}$

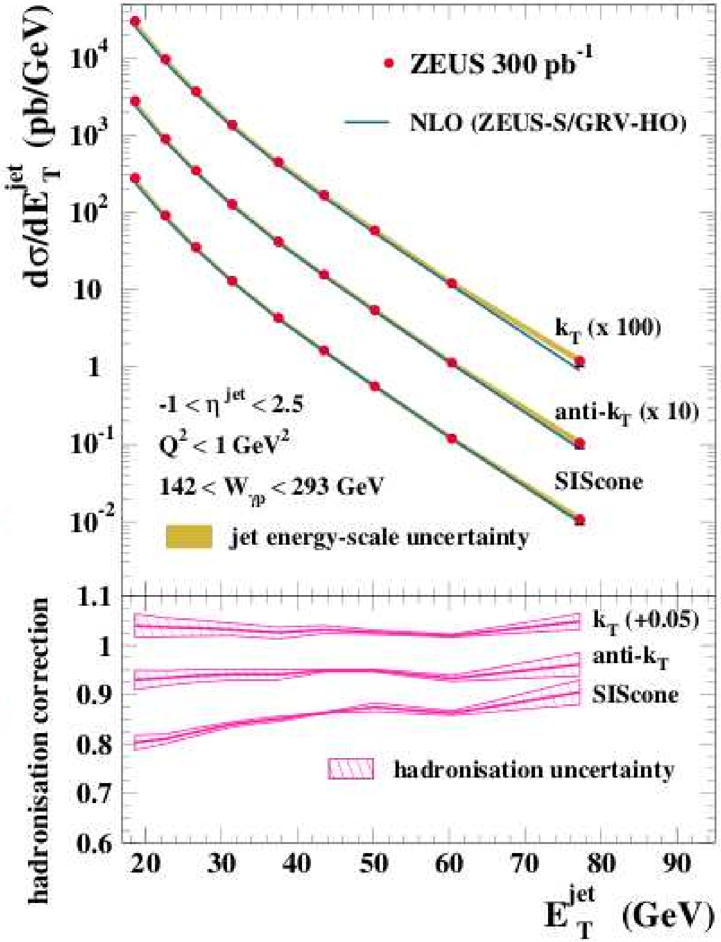

$\rightarrow$ Measurements provide direct sensitivity to α_s and gluon density with small experimental and theoretical uncertainties

ZEUS Collab, DESY-12-045

Inclusive Jet Photoproduction and Determination of α_s

- The energy-scale dependence of the coupling was determined from the data $\longrightarrow$ results in good agreement with predicted running of α_s over a wide range in $E_T^{\rm jet}$
- Values of $\alpha_s(M_Z)$ were extracted from the measured cross sections for $21 < E_T^{\rm jet} < 71$ GeV:

anti-k_T:

$$\alpha_s(M_Z) = 0.1198^{+0.0023}_{-0.0022}\,(\text{exp})^{+0.0041}_{-0.0034}\,(\text{th})$$

uncert: $^{+1.9}_{-1.8}\%$ (exp), $\pm1.0\%$ (pPDFs), $\pm0.4\%$ (hadr), $^{+2.3}_{-2.4}\%$ (HO), $^{+2.2}_{-0.9}\%$ (γPDFs), $^{+3.9}_{-3.4}\%$ (total)

SIScone:

$$\alpha_s(M_Z) = 0.1196^{+0.0022}_{-0.0021}\,(\text{exp})^{+0.0046}_{-0.0043}\,(\text{th})$$

uncert: $\pm1.8\%$ (exp), $\pm1.0\%$ (pPDFs), $\pm0.2\%$ (hadr), $^{+3.2}_{-3.3}\%$ (HO), $^{+1.9}_{-0.9}\%$ (γPDFs), $^{+4.3}_{-4.0}\%$ (total)

k_T:

$$\alpha_s(M_Z) = 0.1206^{+0.0023}_{-0.0022}\,(\text{exp})^{+0.0042}_{-0.0035}\,(\text{th})$$

uncert: $^{+1.9}_{-1.8}\%$ (exp), $\pm1.0\%$ (pPDFs), $\pm0.4\%$ (hadr), $^{+2.4}_{-2.5}\%$ (HO), $^{+2.3}_{-0.9}\%$ (γPDFs), $^{+4.0}_{-3.4}\%$ (total)

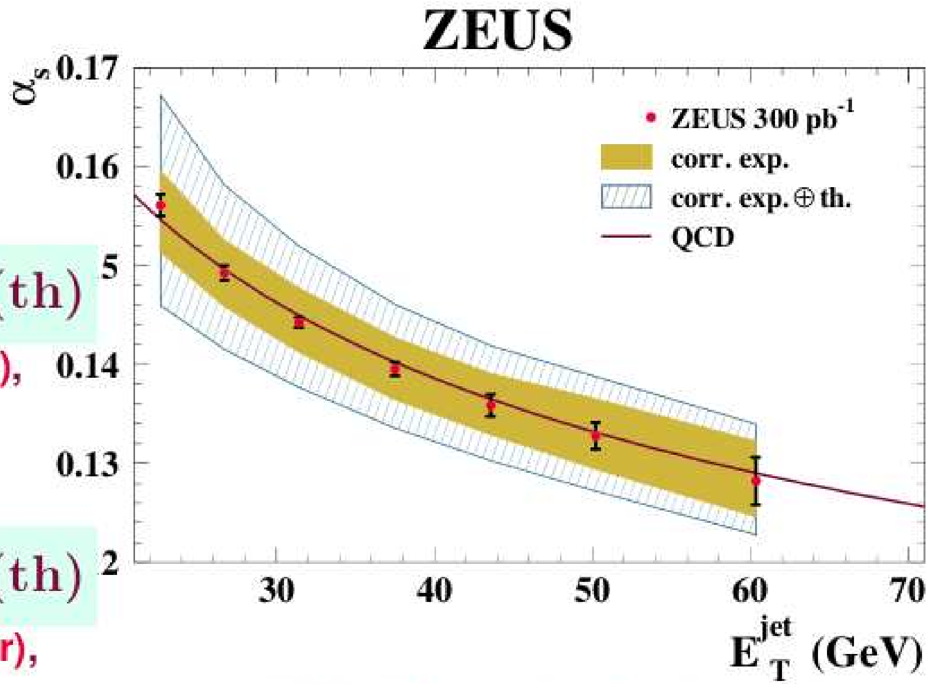

$\longrightarrow$ $\alpha_s(M_Z)$ from inclusive-jet cross sections in PHP with different jet algorithms are consistent with each other and have similar precision

ZEUS Collab, DESY-12-045

Not yet the end

- The “jet” saga continues tomorrow morning

  → jets in hadron-hadron colliders → by Caterina Doglioni